POLITECNICO DI MILANO

Facoltà di Ingegneria dei Processi Industriali

Corso di Laurea Magistrale in Ingegneria Elettrica

UHV AND HVDC TRANSFORMERS BUSHINGS, ANALYSIS OF TEMPERATURE RISE TESTS RESULTS AND DEFINITION OF A SIMPLIFIED METHODOLOGY FOR THE CALCULATION AND PREDICTION OF THE THERMAL BEHAVIOR

Relatore: Prof. Antonino Claudio DI GERLANDO

Correlatore: Ing. Giovanni TESTIN

Tesi di Laurea Magistrale di:
Alessio Pirovano
Matr. 755510

Anno Accademico 2012-2013

Main Index

List of Figures

List of Tables

ABSTRACT

This thesis has been written as the conclusion of a 6 months stage for the company Alstom Grid, in the Passoni&Villa division (RPV) in Milan. The specialization of this division is the designation and the fabrication of the bushing insulators.

The main aspect of the bushings treated during these months of internship is about the evaluation of the thermal behavior in the product, in particular for what concerns the prediction of the maximum temperature reached in a bushing in service.

In this thesis are discussed the several problems to face for obtaining a correct thermal behavior evaluation, with the mandatory test arrangements and requirements, and through the analysis of the data obtained are made some consideration about the validity of the reference Standard for this type of test.

Are viewed some alternative methods existent to predict the temperature rise, focusing specially on the thermal simulations.

Afterwards, is proposed an alternative analytic method to can calculate in a simple way the maximum temperature in a specific family of bushing, the PNO (Passante Normale OIP) type, through an equivalent thermal circuit and an associate calculation program.

Chapter 1 is an introductive chapter where a general overview about bushings is make, with a description of their working principles and the main differences between the various types.

Chapter 2 reports the Standards IEC 60137 and IEC 62199, focusing on the temperature rise test: indications to make it correctly, how is their effective realization in the test chamber and analysis of the critical point of the process.

Chapter 3 contains an analysis about the results obtained by several test in the last years, and furthermore a discussion about the validity of the indications given by the Standards IEC.

Chapter 4 describes the making process of a bushing thermomagnetic simulation and also quickly describes some alternative methods to estimate the thermal behavior.

Chapter 5 shows the development process of the alternative method proposed: the starting model definition and the theoretical informations used to get the bushing equivalent thermal circuit.

Chapter 6 reports the entire calculation program created to can resolve the equivalent thermal circuit giving directly the temperature values on the bushing.

Chapter 7 presents a comparison among the circuital calculation results with the ones given by tests and simulations, with an analysis of the reliability of the alternative method proposed, its critical points and possible future improvements.

ABSTRACT

Questa tesi è stata scritta a conclusione di un tirocinio della durata di 6 mesi svolto presso la divisione Passoni&Villa (RPV) dell'azienda Alstom Grid S.p.A. Il principale ambito di lavoro di questa divisione riguarda la progettazione e fabbricazioni di isolatori passanti.

L'aspetto su cui si focalizza questo lavoro di tesi è la valutazione del comportamento termico degli isolatori passanti, in particolare per ciò che concerne la previsione della massima temperatura raggiunta nel componente in servizio.

Dopo una rapida panoramica per introdurre in generale gli isolatori passanti, vengono riportati i procedimenti e i requisiti da soddisfare per realizzare la prova di sovratemperatura così come indicato negli Standard di riferimento per i passanti IEC 60137 e IEC 62199. Sono quindi esposti sia i metodi di prova, con le relative problematiche da affrontare per riuscire ad avere una corretta valutazione, sia i risultati raccolti in questi ultimi anni.

L'analisi dello storico dati permette di fare alcune considerazioni sul metodo proposto dagli Standard IEC stessi, evidenziando come le indicazioni riportate stiano iniziando a perdere di affidabilità a fronte delle nuove tecnologie e soluzioni applicate nella costruzioni di isolatori passanti.

Sono poi analizzati metodi alternativi con cui valutare il comportamento termico di un passante, con particolare attenzione allo sviluppo di simulazioni magnetotermiche tramite l'uso di programmi di analisi ad elementi finiti.

Viene infine proposto un metodo di alternativo di valutazione della sovratemperatura basato sullo sviluppo di un circuito termico equivalente del passante, associato a un programma di calcolo che permette di ottenere la temperatura massima con l'inserimento di poche variabili e in tempi rapidi. Al momento della fine del tirocinio non si è riuscito a sviluppare questo metodo per un'applicazione generale su tutti gli isolatori passanti, ma solo per una famiglia specifica: i PNO (Passanti Normali OIP) dove l'isolamento principale è formato da carta impregnata d'olio.

Nei vari capitoli che compongono la tesi troviamo:

Capitolo 1 è un introduzione generale sugli isolatori passanti, con una descrizione dei principi di funzionamento e le differenza fra le varie tipologie esistenti.

Capitolo 2 riporta gli Standard IEC 60137 e IEC 62199, concentrandosi in particolare sulla prova di sovratemperatura: indicazioni su come eseguirla correttamente, la sua effettiva realizzazione in camera di test a un analisi dei punti critici del procedimento.

Capitolo 3 contiene un'analisi sui risultati ottenuti dalle prove fatte negli ultimi anni, e una discussione sulla validità delle indicazioni fornite dagli Standard IEC stessi.

Capitolo 4 riporta il processo di realizzazione di una simulazione termomagnetica e, inoltre, contiene un veloce descrizione di altri metodi alternativi visti per valutare il comportamento termico di un passante.

Capitolo 5 mostra lo sviluppo del metodo circuitale proposto: la definizione del modello di partenza e le nozioni teoriche usate per costruire il circuito termico equivalente del passante.

Capitolo 6 contiene l'intero programma di calcolo che consente di risolvere il circuito termico equivalente, restituendo direttamente le temperature nei vari punti del passante.

Capitolo 7 riporta un confronto fra i risultati ottenuti col metodo circuitale e quelli ottenuti con test e simulazioni, con un analisi sull'affidabilità del metodo proposto, i suoi punti deboli e i possibili futuri sviluppi e miglioramenti apportabili.

INTRODUCTION

The main focus of this dissertation is about the evaluation of the thermal behavior of a bushing, in particular for what concerns the definition of a methodology to can predict the highest temperature reached in the powered bushing.

In the last years, the arrangements given by the bushings reference Standard IEC 60137 and IEC 62199 to realize the temperature rise test are beginning to show several limitations, since some obtained results have strange values or even no physical sense at all.

Therefore, after an introductive chapter where are presented the bushings in general and a quickly overview about the reference Standards, the first argument treated in this thesis is trying to understand under which conditions the Standard IEC indications maintain their validity through an analysis of the tests results, individuating also the possible reasons behind their loss of reliability.

The second main focus of the thesis consists in the development of an alternative method that permits to obtaining a prevision of the maximum temperature reached in a bushing in service, in way as simple as possible.

An alternative method that evaluates the thermal behavior of a bushing with a good grade of accuracy already exists: it consists in the realization of a thermal simulation through a finite element analysis software. However, this method requires very specifics knowledge to can be realized, and for every simulation is necessary spending a lot of time before reaching a result.

The fourth chapter of the thesis is dedicated to the simulation analysis, due the importance of the method itself but even because several considerations made here are subsequently used in the development of the alternative method.

The chosen approach at the problem has been try to defining an equivalent thermal circuit of the bushing, thankfully the property of the heat flow to can be modeled with electrical components, and implementing a calculation program capable to resolve this circuit, giving also directly the final calculate temperature in various bushings zones.

These alternative method must have also a good ease of usage even by users without too much specific knowledge, and it can allow to reach the final result in a contained amount of time.

After the development of the circuital calculation, it has been realized a comparison with the results obtained through it with the ones given by test and simulations, in order to can evaluate their discrepancies. With these data, it is realized an analysis to estimate the accuracy of the method proposed, and also are made some considerations about the weak points of the circuital method itself and about the possible future improvements.

Unfortunately, the time necessary to can develop this method for all the bushings types would be too high respect the remaining duration of the internship, therefore it has been chose to focusing only about the family of PNO bushing.

1 BUSHINGS OVERVIEW

1.1 Introduction

The most general definition of what is a bushing is given by the IEC Standard 60137:

"*A bushing is a device that enables one or several conductors to pass through a partition such as a wall or tank, and insulates the conductors from it. The means of attachment (flange or any other fixing device) to the partition forms part of the bushing. The conductor may or may not be an integral part of the bushing.*"

A schematic example of a bushing is shown in Figure 1.1.

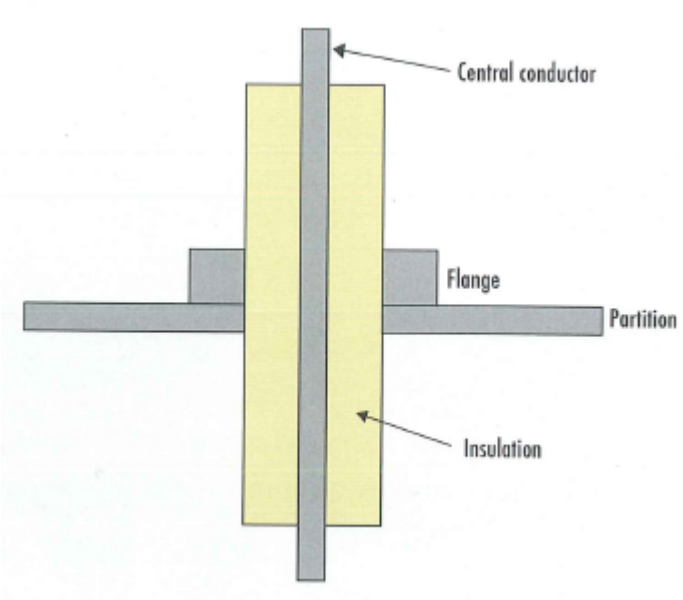

Figure 1.1 - Schematic Bushing Components Representation

Today a wide assortment of bushing types designed for different applications is available. The most common type features in outdoor transformers, and it is estimated to account for about the 60% of the total number of bushing in service; other important applications include gas-insulated switchgear (almost 20%), generators (almost 10%) and wall and test bushings (less than 10%).

1.2 Bushings Classification

Generally speaking, the physical characteristics and type of insulation of the bushings is driven by application requirements.

The first step of classification can be made between capacitance graded and ungraded bushings: this is related to the type of field control used internally in the bushings.

The second classification level is related to the type of insulating medium technology used inside the bushing, for example: oil, oil impregnated paper (OIP), resin, resin-bonded paper (RBP), resin impregnated paper (RIP), gas SF_6, SF_6 impregnated paper, SF_6 impregnated polypropylene, etc….

The third classification concerns the type of central conductor of the bushing. The current may be carried out or by a lead coming from the transformer and inserted in the central tube of the bushing or by a rod inserted also in the central tube of the bushing (draw rod and draw rod bushings have usually rated currents generally up to 1600 A) or else by the central tube itself (bottom connected bushings, with rated currents generally greater than 1600 A).

1.2.1 Ungraded Bushings

This is the first type of bushing that was developed, it is known as "*ungraded*" or "*noncondeser bushing".* During the early years, they were nothing more than a hollow porcelain shell filled with transformer oil through which passes a conductor or, alternatively, the insulator was made by a solid resin shell modelled onto the conductor (Figure 1.2). This technology was normally used up to 123 kV class of bushing, but then it has been overtaken by the second technology, that is graded insulation bushing.

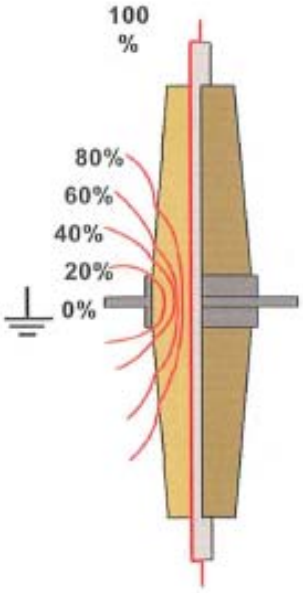

Figure 1.2 - Ungraded Bushing with Electrical Field Distribution

Today this type of bushing is for the most part used for medium voltage, normally up to 36 kV with porcelain shells for external applications and also with resin shells for the internal ones. The space between the external shell and the central conductor can be filled with oil (which is a specific type for bushing) or resin (even this is a specific type for bushing).

In few cases they are used for higher voltages (even no more than 123 kV), but the dimension of the insulating shells must increase and they become very large to withstand the internal electric fields, becoming a less convenient solution.

1.2.2 Capacitance-Graded Bushing

When the electrical networks became more sophisticated and the voltages increased, it was recognized that better distribution of the electric field across the bushing was required, especially for the higher voltages, where the traditional ungraded bushings could not withstand.

This resulted in the development of the capacitance-graded bushing, which is defined by the Standard IEC 60137 as "*bushings in which a desired voltage grading is obtained by an*

arrangement of conducting or semiconducting layers incorporated into the insulating materials".

The principle of grading is derived from the necessity of distributing and equalizing the stresses created by the natural electric field between the conductor and the earthed flange, as shown in Figure 1.3.

This is obtained by placing intermediate conductive layers, concentrically positioned, in order to distribute better the electric field radially (to stress the insulating material more uniformly) and axially (to control the field longitudinally).

This configuration results in a condenser built around the central bushing conductor, named as the condenser core. As the electric field is more uniformly distributed and controlled, this type is known as "*graded*" or "*condenser*" bushing.

Originally, the material used as dielectric was paper bonded on one side with a thin and uniform layer of epoxy resin, wound in concentric cylinders around the central conductor. The condenser foils were made of semi-conducting materials, such as graphite. Over the years other types of bushing were developed, however the insulated was obtained always by paper, at first treated with oil impregnation then, in later years, with resin impregnation.

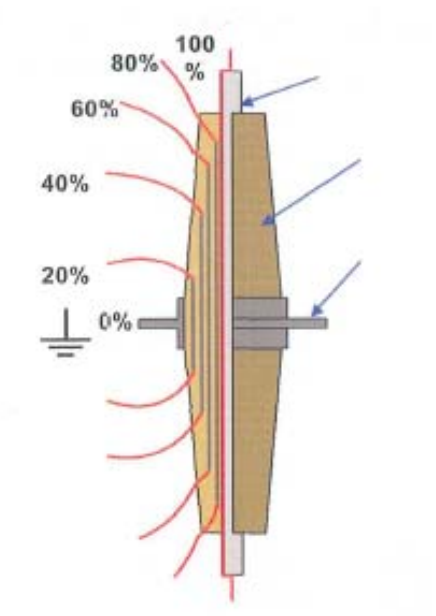

Figure 1.3 - Capacitance Graded Bushing with Electrical Field Distribution

The principals motivations that generated the development of field-graded bushings was the their capacity to give a good stress reduction, controlling it better and made it more uniform, improving resulting in margins of safety, decreasing the risk of electrical breakdown and giving the possibility to can use smaller diameters.

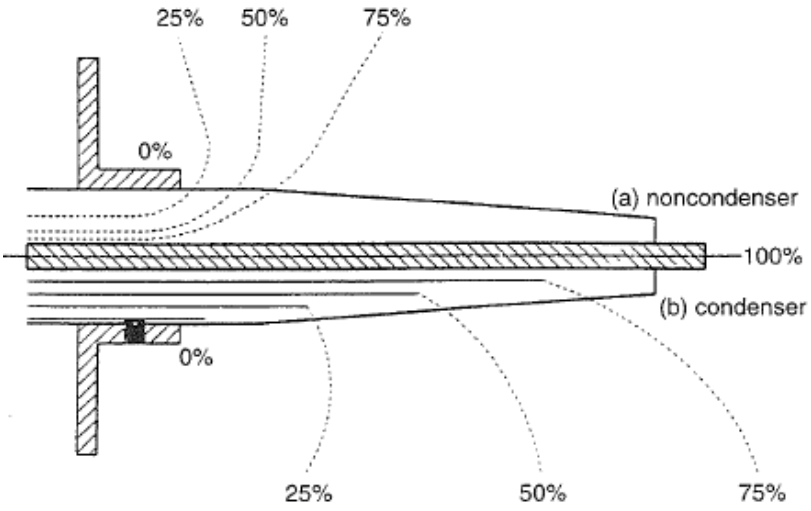

Figure 1.4 - Field Distribution in Non-Condenser and Condenser Bushing

The better field distribution respect the ungraded type is easily visible in the comparison reported in Figure 1.4.

From the designer point of view, the condenser core can be thought in two different modes.

In the first one, the conducting foils are placed in a way to maintain a substantially constant radial gradient, giving the best utilization of the dielectric material.

This choice brings about two consequences: every elementary capacitance must be constant (the condenser core is formed by several capacitances serially, each one formed by two conducting layers), and the distance between the layers must be constant, therefore the total voltage is uniformly divided and every dielectric cylinder is subjected to the same radial electric field. The geometric consequence is that the longitudinal distance between the layers changes, so the axial field does not remain constant (Figure 1.5).

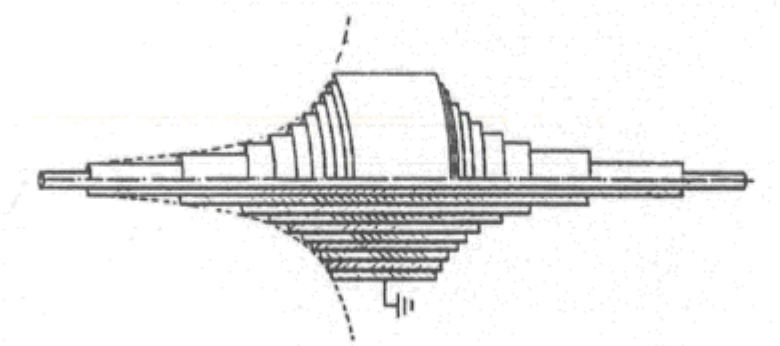

Figure 1.5 - Uniform Radial Field and Non-Uniform Axial Field Solution

The second way allows maintaining constant the axial field between the edges of conducting layers. This means that the elementary capacitances must be constant in this case, even if they have a uniformly divided axial voltage distribution, and now the longitudinal distance between the edges of the layers must be constant. The consequence is related to the radial distance between layers, which in this case is not constant, and the radial field is also no longer constant (Figure 1.6).

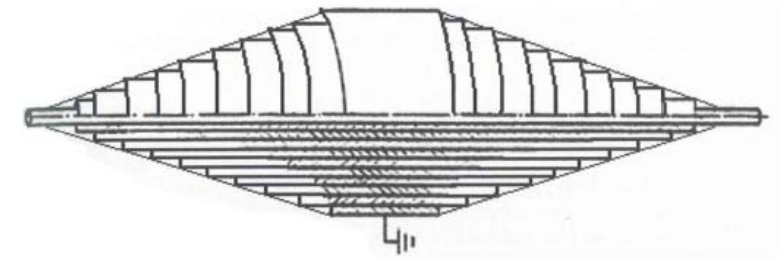

Figure 1.6 - Non-uniform Radial Field and Uniform Axial Field Solution

For transformer bushing is often preferable the second solution, because the transformer side is normally kept as short as possible, with the consequence of a high axial field, so the safest solution is maintaining the axial field as uniform as possible to control it.

The bushing designer must analyze all relevant parameters and must maintain the internal gradients sufficiently high to can be able to reduce the bushing dimensions, within the safe voltage stress limits. These ones must be managed in order to maintain them as uniform as

possible by careful optimization of the diameters and lengths of the foils, to avoid localized stresses in the bushing that could give rise to partial discharges.

1.3 Types of Bushing Insulations

1.3.1 Resin-Bonded Paper Bushing (RBP)

Resin-bonded paper bushing is defined by the standard IEC 60137 as "*bushings in which the major insulation consists of a core wound from resin-coated paper".*

This bushing is produced by winding a sheet of paper, coated with an uniform and thin layer of epoxy resin, around the central conductor. Strategically placed, a semi-conductive material such as graphite or other carbon-based material is placed between paper layers to create a field-graded bushing. At the end of the winding process, each layer is bonded to its neighbours by its own resin coating, which bonding is achieved by putting the condenser core in a furnace.

If it is necessary, this type of bushing can be improved with an insulating envelope, as porcelain or composite or another insulating material; the space between core and envelope is filled with another insulating material, which can be in liquid or solid form. When the envelope is not necessary at all (for example, in oil-to-oil type) or only in one side (for example, the air side of an air-to-oil bushing), then the part of the core is covered only by a suitable protective varnish, to prevent permeation of moisture into the resin bonded paper and is oven-cured.

Due to its construction, the dielectric material is not void free at all, especially between the paper layers. This could permits a partial discharge activity, starting from a voltage value about 1.3 - 1.5 per unit of the rated one. Depending upon their inception value, partial discharges can cause an erosion process through the bushing lifetime, they usually are initiated by an over voltage event or some mechanical damage.

The process can be very slow but with continuously increasing intensity. However, the by-products of the erosion process remain trapped in the solid dielectric, and the problem remains localized for a long time, while the bulk of the dielectric remains in satisfactory condition. As a consequence, this type has a long life expectancy despite the presence of partial discharges into its core.

This phenomenon is typical of solid dielectrics, but is absent in the liquid or gaseous ones, and is more critical at higher voltages. For this reason the resin bonded - paper bushings normally have an upper limit of 170 kV system rated voltage.

Their main vantages of RBP are a low cost and an excellent mechanical behaviour; while the disadvantage is the likely presence of partial discharges (refer also to the Standard IEC 60137).

1.3.2 Oil-Impregnated Paper Bushing (OIP)

These are bushings where the major insulation consists of core wound from untreated paper, which is subsequently dried, degassed and impregnated under vacuum with an insulating liquid, usually mineral or synthetic oil. The core is contained in an insulating envelope, with the space between them filled with the same insulating liquid used for the impregnation process. Here below, in Figure 1.7, is shown a typical OIP bushing and its components.

Since impregnation with fluid takes place under vacuum, the OIP have the vantage of being void free and consequently having the tendency to be free from measurable levels of partial discharges up to the test voltage. Therefore, they have the capacity to can reach the highest voltages levels (today up to rated values of 1100 kV, tested with an AC voltage that is even higher).

Another advantage of the OIP bushings is the capacity of their liquid dielectric to recover from small internal partial discharge transient events without starting an escalation process.

They require a hermetically sealed housing or shell, to hold the insulating liquid and to prevent that atmospheric humidity enters in the condenser core. This shell also adds the mechanical rigidity at the bushing.

If for some reason the external insulator has breaks, the bushing loses fluid and the discharge process begins. In some cases, there is also a risk to lose the bushing's function of hermetic closure of the transformer, which may also leak oil through the faulty bushing, with all the obvious consequences of discharge, arcing, fire, etc.

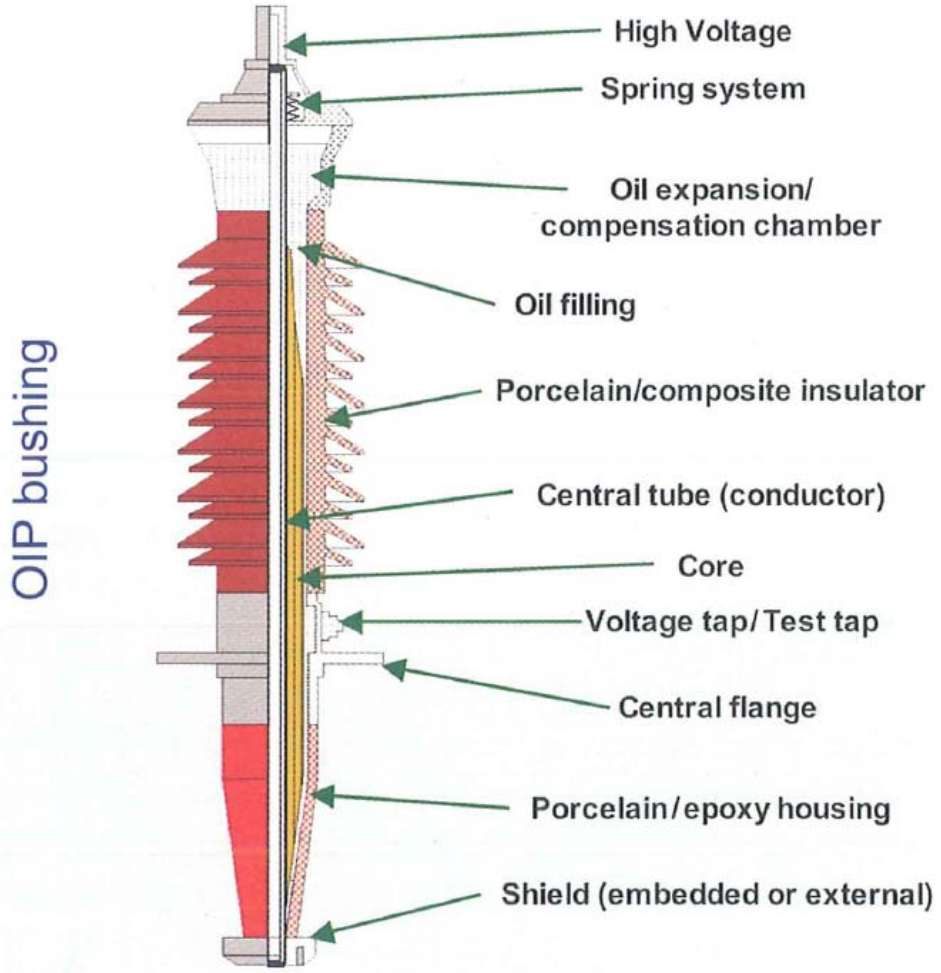

Figure 1.7 - Components of a Typical OIP Bushing

1.3.3 Resin-Impregnated Paper (RIP)

In this bushing, type the major insulation consists of a core wound from a roll of paper, in the same way as OIP bushings, but in this case it is later impregnated under vacuum with a curable resin. The core is often contained in an external insulating envelope of porcelain or hollow core composite, and the intermediate space between condenser core and envelope is filled with an insulating liquid or other medium, as shown in Figure 1.8.

A properly manufactured RIP bushing is completely void free and, thanks to this, tends to have no measurable partial discharges up to test voltage level. The main difference with OIP technology is that the RIP core is cured after impregnation and it results in a solid body, which is tight at both gas and oil and also mechanically tough.

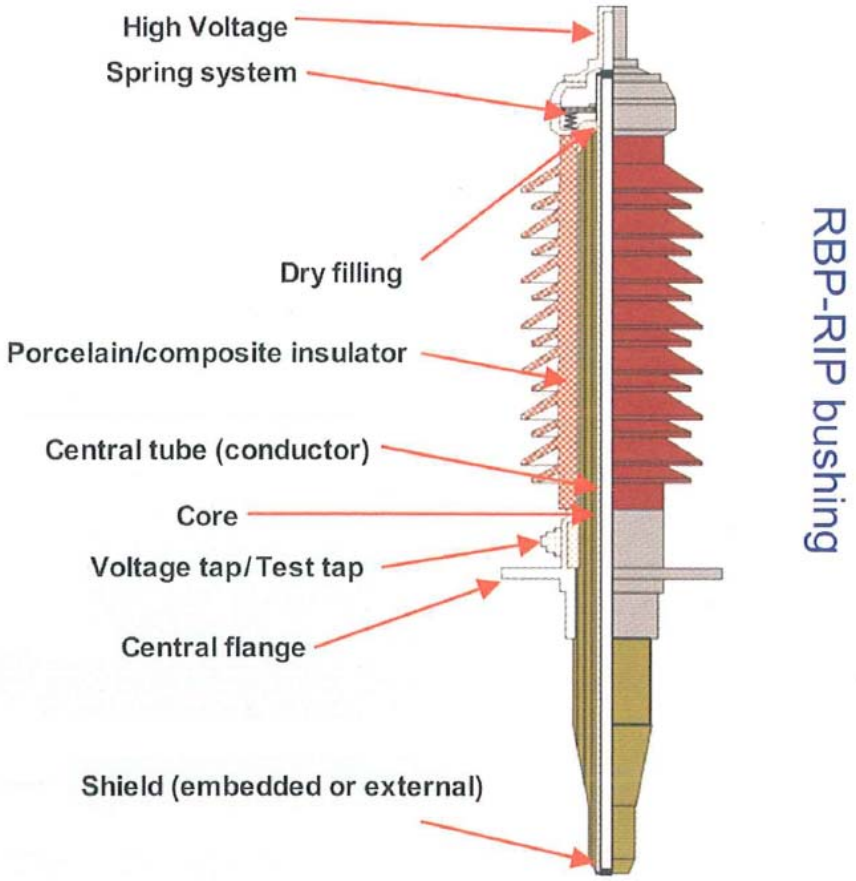

Figure 1.8 - Components of a RIP - RBP Bushing

This technology generally involves higher material and production costs, therefore normally carries a higher sales price than OIP. However, RIP cores offer certain advantages, including being relatively non-combustible and unaffected by humidity, as well as giving greater security in respect of potential oil leakages from the transformer tank through the bushing.

Furthermore, when equipped with composite housing, RIP bushings offer complete safety for personnel and adjacent equipment against the explosion risk.

Even if due to an over voltage event or mechanical damage, some partial discharge activity takes place in the dielectric and an erosion process starts, the by-products are encapsulated within the solid dielectric and the partial discharges remains localized for a long period, while the bushing's overall integrity remains intact. As a consequence, RIP bushings have a long life expectation.

Due to the difficulty of controlling the exothermic reaction that occurs during the curing process, RIP bushings currently are generally limited to 550 kV.

1.3.4 Gas Insulated Bushings

The main insulation of this bushing type is pressurized SF_6 (sulphur hexafluoride) gas, with the dielectric field controlled by metallic screens placed internally on the base and on the head of the bushing. As shown in Figure 1.9, there is an external insulating envelope of either porcelain or hollow core composite insulator. This type of bushing dues its conception to the necessity of a connection in GIS system, where the gas is already used. It can be designed as an open bushing, where the bottom part is in direct communication with the GIS system, in order to can have the gas in common; or as a closed bushing, where the bushing is completely tight and its insulation gas is totally separated from the one of the GIS system.

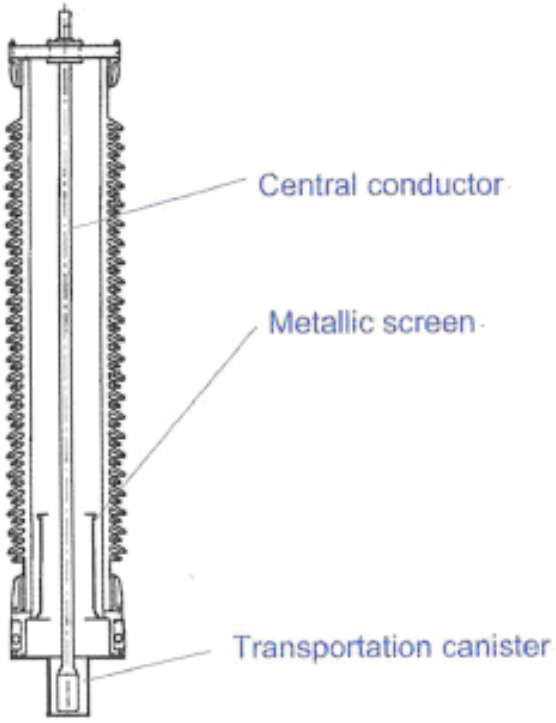

Figure 1.9 - An Open Type of Gas - Filled Bushing.

In the first case (open bushing) the final void treatment and gas filling will be made together with the GIS system. The bushing is transported and it is filled with SF_6 at a light overpressure of about 0.3 - 0.5 bar, in order to preclude humidity ingress, and close with a canister (as shown in Figure 1.9). At the site, the canister is removed and the bushing is assembled in the GIS system. This bushing's type is normally available until rated voltage up to 245kV, while for higher values the preferred solution is to adopt a semi graded bushing design; otherwise, the diameters of the external insulator become too large and expansive.

For the second bushing type (closed bushing) the void treatment and the gas filling are completed during the building process in the factory, in a way similar in many aspects at the one for OIP bushings. Afterwards, they are tested in the factory and, before shipment, the gas pressure is lowered to 0.3 - 0.5 bar to have a safe transport. Only after the final mounting at its own site the gas pressure can be restored at the rated value.

Gas insulated bushing is easy to assemble since it is formed only by a few components, and is therefore a good economic proposition, particularly for GIS or SF_6 filled transformer.

When the bushing is equipped with a hollow core composite insulator (and that are about the 80% of the closed types), it must be almost unbreakable against an explosion that could be result from internal discharge and arcing.

The major disadvantage of gas-filled bushing is the high planning pressure level, which must be at least equal to the one of the GIS or transformer upon it is finally mounted.

1.3.5 Gas Impregnated Bushings

This type has the main insulation formed by pressurized SF_6 gas and the dielectric field is controlled by metallic screens plus a condenser core.

The condenser is made from wound polypropylene sheet with concentrically disposed internal foils, similar to the other graded bushings described before. In this particular technology, the bushings are semi-graded, therefore the condenser core does not provide the unique field control device.

In addition, a floating electrode is positioned in the space between the flange and the central conductor, having a geometric shape designed to create two cylindrical capacitors, each one with similar capacitance (Figure 1.10).

As a consequence, the potential of the floating shield will be approximately half of the total voltage to earth imposed on the bushing.

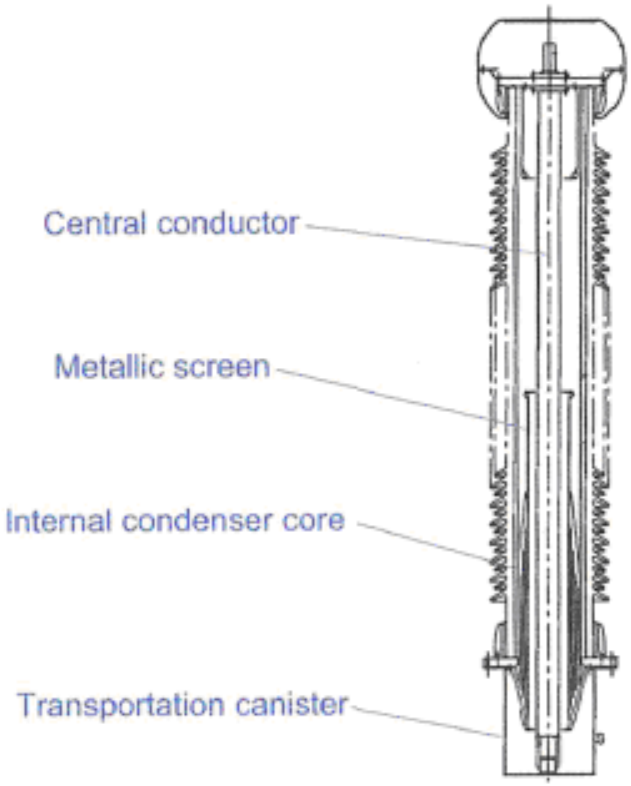

Figure 1.10 - Gas Impregnated Bushing

The condenser core is located between this floating metallic shield and the flange. For this reason this type of bushing is called "*semi-graded*". The foils are formed by aluminium sheets wound into the condenser in the same way as in the OIP bushing.

In this case, there is also the opportunity to select an open bushing in communication with the GIS or transformer filled ambient, or a closed one.

Main advantage of this technology is can make a reduction of the diameter of the bushing, and then the external insulator becomes smaller, lighter and less expensive.

The majority of these bushing types are equipped with a hollow core composite insulator, as a safety improvement. Normally this solution is adopted only for voltages that are greater than 245 kV.

1.4 Oil to Air Bushings

The Standard IEC defines them as:"*a bushing, one end of which is intended to be in ambient air and the other end to be immersed in an insulating medium other than ambient air*". Typically, the second insulating is oil, and that makes them the most common bushing for transformer applications.

Figure 1.11 - Oil to Air Bushing

The oil side insulator shell can be made of porcelain or epoxy resin. At the lower end of the higher voltage bushings of this type, there is usually a metallic deflector to shield the edges of the connection lead coming from the transformer. Between the flange and the oil side insulator there is a grounded part, where toroidal metering or protection current transformers may be mounted by the transformer manufacturer. This grounded length, or CT space, is agreed with customer requirements during the design phase of the bushing, and can normally vary since zero (no CT space expected) to 1000 mm.

The air side insulator shell can be made by porcelain or a hollow composite, in according to the customer specification. For many manufacturers, independent of the type of insulating shell, the bushing design is usually very similar to obtain the benefits of standardization.

1.4.1 Porcelain Insulator

Porcelain is the traditional insulator, used since the very beginning. It is a very solid, reliable, well tested and proven solution, with a long satisfactory history. At the present time, the use of porcelains OIP bushing covers is more than 90% of their production.

Furthermore, with the continuing developments and improvements of dielectric performance porcelain, diameters have been reduced and prices remain very competitive.

1.4.2 Composite Insulator

Composite hollow insulators comprise a glass resin internal tube and an external shell of silicone with integral sheds. There are three principal ways to apply the silicone covering of the central glass resin tube:

- The silicone may be injected molded directly during the extrusion process;
- The silicone may be extruded onto the tube with the sheds formed in the extrusion process;
- The individually molded sheds can be mounted and bonded together over the resin glass tube.

Today the use of composite insulators has increasing in the RIP bushing market, while for OIP technology this type of production amounts to less than 10% of the total.

The prime and most important advantage is the safety: there is no risk of disastrous in the way porcelains are not liable to fail mechanically, with an improved safety for personnel and apparatus in the vicinity.

Other important advantages such as hydrophobicity, which gives better performance under polluted conditions, limiting the need of insulator washing in heavily polluted areas, a proven high seismic withstand capability, and of course the lower weight.

The disadvantages are a reduced historical field experience in comparison with porcelain, damages given by rodents and birds and the problem of bio-growth.

1.5 Oil to SF_6 and Oil to Oil Bushings

Oil to SF_6 bushings are designed to have one side immersed in the transformer oil and the other one in the SF_6 environmental of the GIS.

Oil to oil bushings are very similar: even they have one side immersed in the transformer oil, but the other one is in an oil filled turret in order to be connected to a cable.

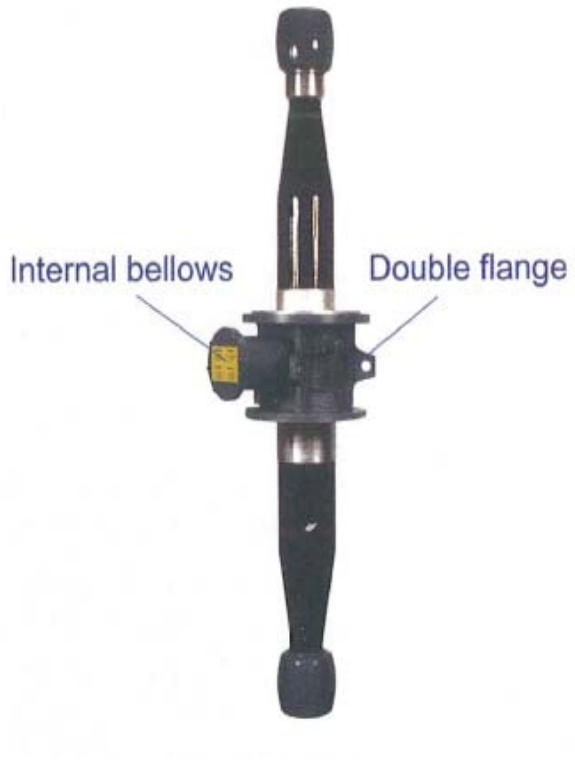

Their shape on either side is similar at the one of the oil side of a standard oil to air bushing, as shown in Figure 1.12. They can be made with either OIP or RIP technology.

Due to the fact that the mounting position can be in any of infinite number of planes (e.g. in horizontal, in vertical and any angle between them), the oil must completely fill the bushing to eliminate any potential gas spaces that could come into contact with critical high field zones of the condenser core, generating thus partial discharges. For this reason, OIP bushing are fitted with internal bellows to compensate the oil volumes variations due to changes of temperatures into the bushing during service conditions, as shown in Figure 1.12.

Figure 1.12 - Oil to Oil or Oil to SF_6 Bushing

Dual flanges are specially designed for the attachment of the bushing to the transformer tank and to the GIS ducting, with the space between them totally closed. Mounted externally are the compensation bellows, the power factor tapping and a pressure caliber with some alarm contacts, in order to monitoring the internal oil pressure. The external insulator of both sides is usually made in porcelain.

RIP bushings for the same applications do not have the problems of oil compensation, being dry types. Neither they require porcelain or epoxy resin insulator, however their shape is similar to that of OIP bushings as shown in Figure 1.12.

1.6 High Current Bushings

These types are normally used for medium voltage purposes (24-396 kV) when very high values of current are present, for example as the low voltage terminals of step-up transformers.

Usually the high current bushings are dry type, as RIP or more likely RBP (which are less expensive and with satisfactory dielectric performances for medium voltage applications). They are provided with a condenser core and the space between the external insulator and the porcelain is filled with a dry foam (as shown in Figure 1.13), therefore they can be mounted at any angle (in many cases, in fact, they are installed in horizontal position).

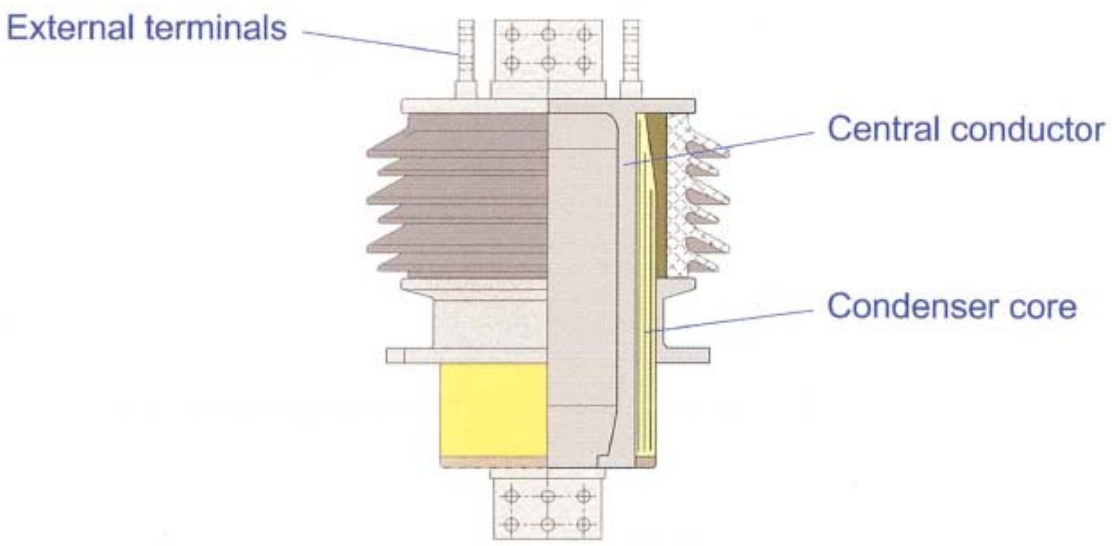

Figure 1.13 - Heavy Current Bushing

Due the internal conductor must carry a high current, it is very large. So these types of bushing have a typical shape that is larger and shorter than high voltages bushing. In some cases the dimensions allow the transformer oil circulation internally, through a hole in the bottom of the conductor, for a better cooling system. Normally the external conductor is formed by one or more plates, in according to the magnitude of the current, in order to reduce the current density to acceptable values, and reducing the circulating losses in the current-carrying joints.

The oil side does not require an additional insulator since it is of the dry construction type (the resin bonded condenser core is directly in contact with transformer oil), but on the air side a porcelain insulator is usually included.

The ungraded types, for example the ones without the condenser core, are not used for currents in excess of 9 kA, due to their requirement of very large flanges and large porcelain diameters necessary to withstand the corresponding voltages.

1.7 Oil Filled Cable Boxes

This assemblies are used on transformers when is required a cable connection. They are generally used where there is insufficient space for normal air clearances, or where the high voltage is transmitted through underground cables.

In Figure 1.14 it has been reported a typical application of an oil filled cable box at 145 kV. The cable entry is from the bottom but alternatively it may be either from above or horizontal connected, in according to customers requirements.

An oil fix cable box is the interface between the transformer and the cable, a simply oil filled chamber which encloses the cable termination ("item 2" in Figure 1.14) and the transformer termination ("item 4" in Figure 1.14), including the connection between them ("items 7" and "item 8" in Figure 1.14).

The cable termination is a component mounted to the end of the power cable, giving an accessible connection point. Cable connections can be either filled with insulation fluids, or be made of solid insulation elastomeric type, which would typically include capacitive controlled elements for dielectric field control. At low voltages, the cable can be directly connected to the connection link. The cable termination is usually inside the scope of the cable supplier.

1 Oil filled cable box
2 Cable termination
3 Oil filled termination box
4 Oil-oil bushing (mounted on transformer)
5 Shield electrode
6 Transformer turret
7 Connection link, copper tube
8 Connection link, copper cable
9 Connection access hand holes
10 Flange for connection to conservator, Buchholz relay
11 Cable box earthing connections
12 Flange for drain valve
13 Lifting eyelet
14 Flange for pressure relief device

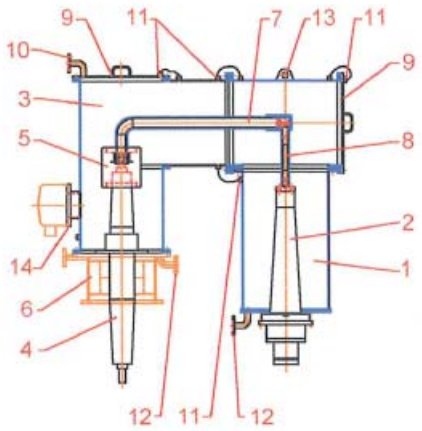

Figure 1.14 - Typical Application of Oil-Filled Cable Box for 145 kV with its Own Components.

The connection to the transformer is through an oil to oil bushing. When necessary, shield electrodes are used between the oil bushing and the connection link. The connection between the cable termination and transformer bushing is usually made of copper tube largely self-supporting. The termination points are made of either solid copper, silver or tin planted copper.

It is normally recommended having both the oil volumes in the main transformer and in the cable box are separately equipped with a Buchholz relay, but they would generally share the same conservator. Separate conservators are sometimes request and mounted. The cable box is usually designed to withstand full void and to be oil tight at the same test pressure as the main transformer tank. The oil filling of the cable box will normally be carried out with degassed oil under vacuum. Operating temperatures inside the box are similar to those of the transformer and are defined by the same international standards.

During the transformer test, the oil bushing and cable terminal are with no connection, temporary oil to air bushings are necessary to be linked to the oil to oil bushings. The cable box will probably have been designed with a specifically air to oil bushing and special shield electrode protection in mind, so the appropriate test equipment for that must be set up. The temporary test bushings would be mounted on the cable box so as to give suitable phase to phase and phase to earth clearances.

1.8 Air Filled Cable Boxes

Air filled cable box assemblies for transformers and reactors are generally used to terminate cables to bushings ("item 2" in Figure 1.15) while shielding all live parts from external contact and, additionally, they offer protections against environmental conditions.

They are designed to house transformer bushings with their terminations and connections, generally up to maximum voltage level of 36 kV. The power cables used to connect the bushings are fully supported through the gland plate ("item 13" in Figure 1.15) to ensure that no mechanical stress is applied to the bushing connection end. The oil to air bushings are used to bring the internal electrical connection of the transformer to the outside of its own tank.

Air filled cable boxes may be used in a way that the high and low voltage bushings are located in one common box or in separate boxes too.

Key :

1 Air filled cable box
2 Oil-air bushing
3 Transformer turret
4 Removable connection, Flexible copper link
5 Stand off insulator
6 Top cover plate
7 Connection hand hole
8 Cable glands
9 Cable earthing
10 Cable box earthing
11 Flange for breather connection
12 Lifting handles
13 Gland Plate

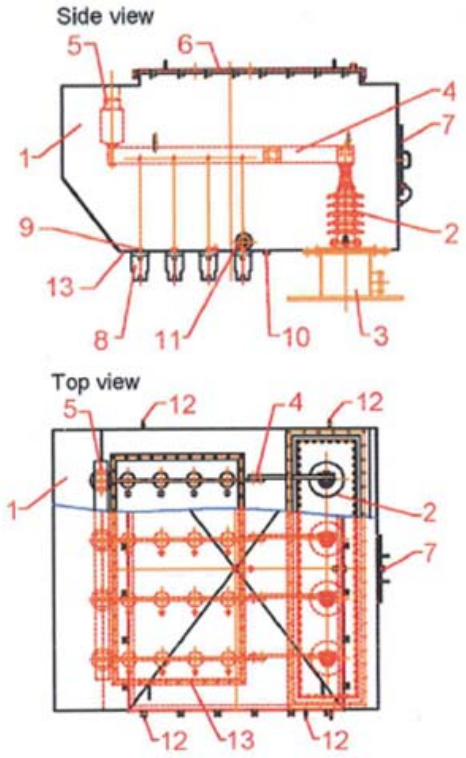

Figure 1.15 - Example of Air Filled Cable Box for 36 kV with its component

The box may be welded or bolted to the transformer cover plate (or it can be split in two sections, with one bolted and the other welded). In the example shown in Figure 1.15 all the cables of the three phases plus the neutral are inserted from the bottom side.

In certain transformer applications, a special type of cable box may be designed to suit its own specific high voltage, and will be in compliance with design criteria: electrical clearance requirements, accommodation of all cable fittings for terminations, accessibility for bushing terminal connections and conformance to relevant international specification.

1.9 HVDC Bushing

Valve bushings are critical components of the HVDC transformer and they must be designed to face with both a.c. and d.c. stresses, at normal operations and at higher levels.

This bushing type must possess all the relevant performance characteristics of an a.c. bushing, but the voltage distribution within it is also afflicted by the d.c. stresses. The voltage distribution for a.c. is controlled by metallic foils in the insulation and the voltage is uniformly

distributed by selection of their spaces and heights to achieve the required capacitance grading. The a.c. field distributions are not significantly affected by the oil end arrangements.

The d.c. distribution is controlled not by the capacitances between the foils and grounded components, but by the inclusion of higher resistance pressboard insulation in the oil. However the HVDC bushing may be designed in complete conjunction with the cleat bar agreements within the transformer as well as the insulated structure that will interface between the two.

There is a mismatch in the relative resistivities of the oil and porcelain, then alternative solutions have been considered to improve the control of the stress distribution. Special porcelain with a higher conductivity that is similar respect the one of the used oil, or the porcelain itself has been completely removed to reduce the changes in conductivity. Finite Element Analysis (FEA) is required to verify interface suitability.

The external part of the valve bushing must have enhanced creepage because of the collection of the pollution and dust attracted to DC field. The bushing may use a composite reinforced glass fiber insulator with silicon rubber sheds to allow high creepage and to take advantage for the reported improvements in DC performances.

1.10 Types of Bushing Conductor

There are various types of conductor that can carry the rated current through the bushing, and each type gives a different connection between bushing and transformer. It can be chosen: a draw lead connection, a draw or fix rod connection or a bottom connection. The choice may be a manufacture design decision or it may come directly from the costumer. The main discriminant is the value of the rated current of the bushing must carry out (which is generally higher than the operating current).

The type of bushing conductor is very important for the temperature rise measurement, enough to changes completely the approach at the problem.

1.10.1 Draw lead connection

In this type of connection the conductor that carrying the current is a lead, which coming directly from the transformer's winding, up to the multicontact placed in the bushing head.

The conductor that goes through the bushing is extractable and that is useful, for example, for the realization of several tests or during the transport operation.

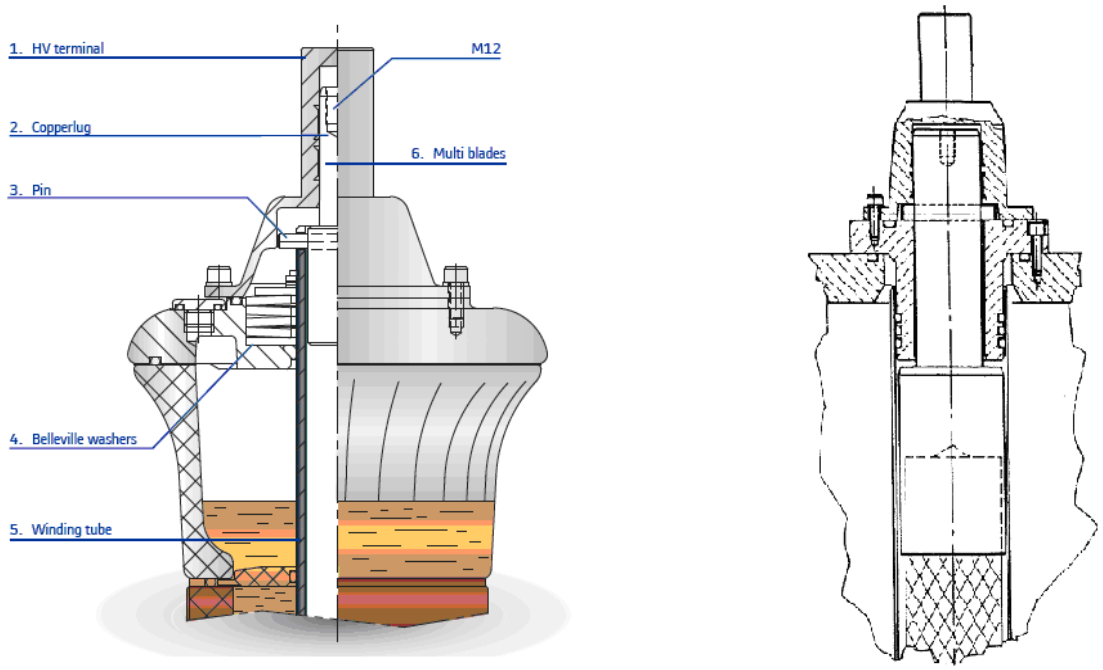

Figure 1.16 - Head of a Draw Lead Connection Bushing (of a PSO 52 ÷ 170 kV) and Joining Between Conductor and Multicontact.

In Figure 1.16 are shown, respectively on the right and on the left, the head of a draw lead bushing and the connection of the lead with the multicontact, which connects the conductor with the high voltage terminal.

It is possible the use of one or more copper leads, with the second solution that is the preferred one, because in this way the total equivalent section of the conductor is formed by many smaller leads and this allows a better use of the material (the limitations due to skin effect are in fact reduced). However the current density must not be higher than 2 ÷ 2.5 A/mm^2. This type of connection is typically chosen for rated current lower than 1600 A.

For a better bushing's tail insulation, it is advisable to protect the lead coming from the winding of the transformer with paper; it is suggested to insulate with a minimum diameter layer of minimum 1.5 mm and maximum of 2 mm smaller than the internal diameter of the tube (to permit the oil circulation).

1.10.2 Draw and fix rod connection

In this type of execution the conductor is usually removable to (draw rod connection), but sometimes the solution adopted does not permit the extraction (fix rod connection) .The conductor is rigid, as shown in Figure 1.17. There is the possibility to splitting the conductor in two (or even more) parts, in order to make easier the transport operations.

The mounting procedure is similar at the draw lead case, but there is no necessity of lug because the used conductor is placed inside the bushing for all its length, coming out from the bottom part to make the connection with the transformer lead.

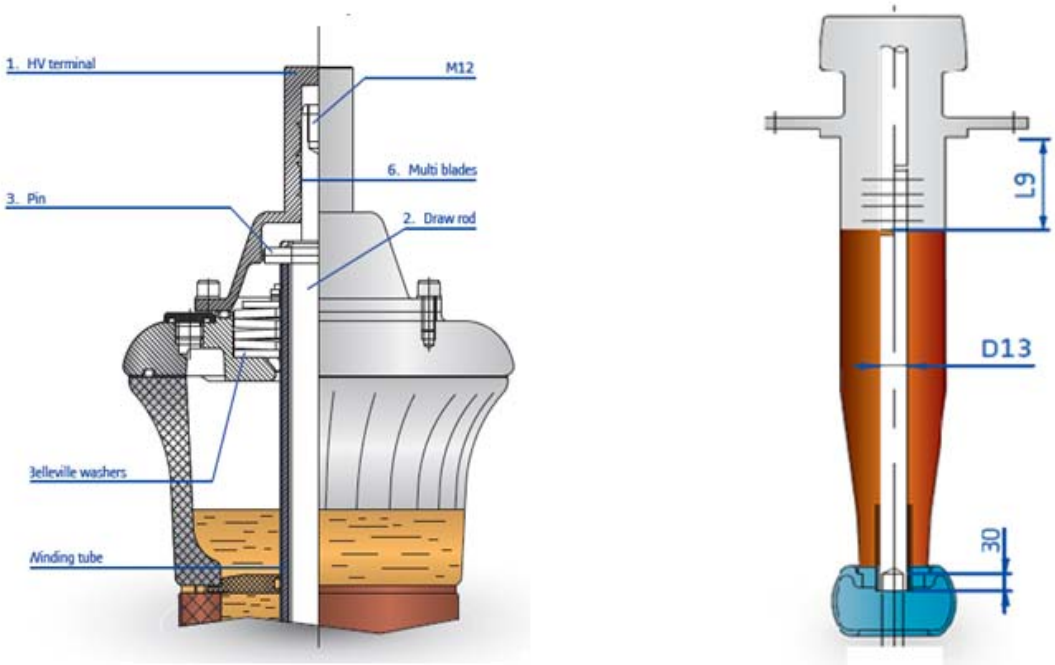

Figure 1.17 - Head and Tail of a Draw Rod Connection Bushing (of a PSO 52 ÷ 170 kV).

1.10.3 Bottom connection

In this type of execution the current is carried out directly by the central bushing conductor, from the bottom terminal (the one on the right in Figure 1.18) to the high voltage terminal (the one on the left in Figure 1.18). This type is selected usually for high values of rated current.

The conductor can be a tube or a rod, usually made in aluminum or copper, it depends mainly of the rated current value for which is designed the bushing. With this type of choice it is possible reaching highest rated current, usually it used for every value over 2000 A. When the

bushing is made, there are no possibilities to have access to the conductor, or even remove it. That's because the central tube (where the conductor passes through) must be sealed to the outside, and the connections with the transformer and the line are realized through two terminals.

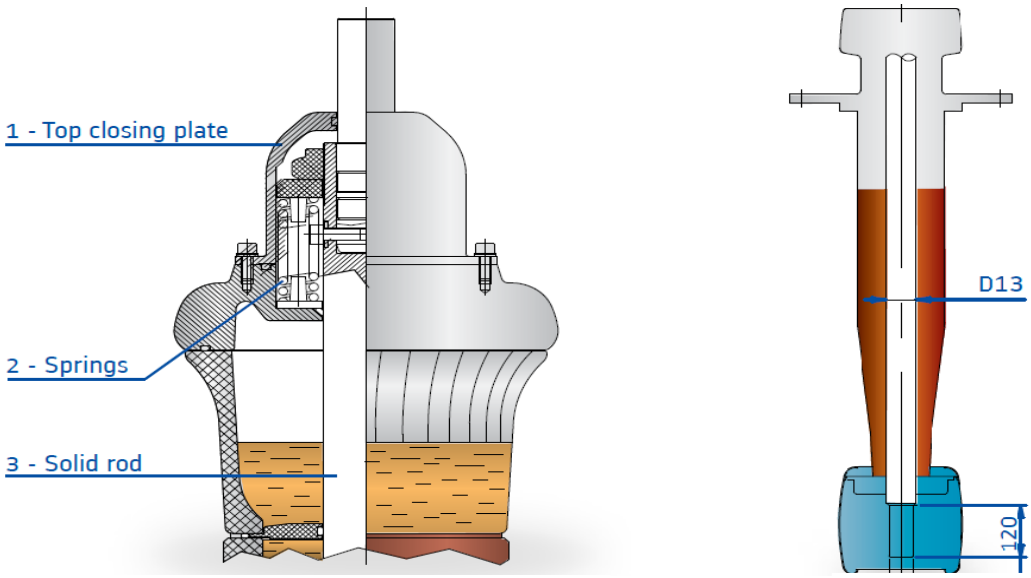

Figure 1.18 - Head and Tail of a Bottom Connection Bushing (of a PNO 245 kV).

2 TEST ARRANGEMENTS AND IEC STANDARD REQUIREMENTS

2.1 Introduction

The principal standard references about bushing's design are for sure the International Standards IEC 60137 ("*Insulated bushings for alternating voltages above 1000 V*", edition 06, published on 06/2008) and IEC 62199 ("*Bushings for d.c. application*", published on 05/2005). The first one is especially important, since the second one gives essentially the same indication, with the necessary calibrations and adjustments.

n fact, IEC 62199 is full of references at the IEC 60137, both for a lot of tests execution methods and for tests acceptance criteria.

Due the nature of the transformer bushings, the Standards IEC are also made in according with the test specifications of the power transformers, given by IEC 60076-3 "*Power transformers*" published on 2000.

2.2 Definitions

In the standards, there are many definitions, the really important ones to can well understand the various test descriptions and test requirements are reported in the following list (some of these definitions are better detailed in the Chapter 1):

- BUSHING= a device that enables one or several conductor to pass through a partition such as a wall or a tank, and insulates the conductors from it; the means of attachment (flange or fixing device) to the partition forms part of the bushing. The conductor may from an integral part of the bushing or be drawn into central tube of the bushing.
- LIQUID-FILLED BUSHING= bushing in which the space between the inside surface of the insulating envelope and the solid major insulation is filled with oil.
- COMPOUND-FILLED BUSHING= bushing in which the space between the inside surface of the insulating envelope and the solid major insulation is filled with an insulating compound.
- LIQUID-INSULATED BUSHING= bushing in which the major insulation consists of oil or another insulating liquid.
- GAS-FILLED BUSHING= bushing in which the space between the inside surface of the insulating envelope and the solid major insulation is filled with gas (other than ambient air) at atmospheric pressure or higher.
- GAS-INSULATED BUSHING= bushing in which the major insulation consists of gas at atmospheric pressure or higher.
- GAS-IMPREGNATED BUSHING= bushing in which the major insulation consists of a core wound from paper or plastic film (GIF) and subsequently treated and impregnated with gas the space between the core and the insulating envelope being filled with the same gas.
- OIL-IMPREGNATED PAPER BUSHING (OIP)= bushing in which the major insulation consists of a core wound from paper and subsequently treated and impregnated with an insulating liquid, generally transformer oil.
- RESIN-BONDED PAPER BUSHING (RBP) = bushing in which the major insulation consists of a core wound from resin-coated paper.

- RESIN-IMPREGNATED PAPER BUSHING (RIP) = bushing in which the major insulation consists of a core wound from untreated paper and subsequently impregnated with a curable resin.
- COMPOSITE BUSHING= bushing with an insulating envelope consisting of a resin impregnated fibre tube with or without a rubber compound covering.
- CAPACITANCE GRADED BUSHING= bushing, in which a desired voltage grading is obtained by an arrangement of conducting or semiconducting layers incorporated into the insulating material.
- INDOOR BUSHING= bushing, both ends of which are intended to be in ambient air at atmospheric pressure, but not exposed to outdoor atmospheric conditions.
- OUTDOOR BUSHING= bushing, both ends of which are intended to be in ambient air at atmospheric pressure and exposed to outdoor atmospheric conditions.
- OUTDOOR-INDOOR BUSHING= bushing, both ends of which are intended to be in ambient air at atmospheric pressure. One end is intended to be exposed to outdoor atmospheric conditions, and the other end not to be exposed to outdoor atmospheric conditions.
- INDOOR-IMMERSED BUSHING= bushing, one end of which is intended to be in ambient but not exposed to outdoor atmospheric conditions and the other end to be immersed in an insulating medium other than ambient air (e.g. oil or gas).
- OUTDOOR-IMMERSED BUSHING= bushing, one end of which is intended to be in ambient and exposed to outdoor atmospheric conditions and the other end to be immersed in an insulating medium other than ambient air (e.g. oil or gas).
- COMPLETELY IMMERSED BUSHING= bushing, both ends of which are intended to be immersed in an insulating medium other than ambient air (e.g. oil or gas).
- HIGHEST VOLTAGE FOR EQUIPMENT U_m= highest r.m.s. value of phase-to-phase voltage for which the equipment is designed in respect of its insulation as well as other characteristics which relate to this voltage in the relevant equipment standard.
- RATED PHASE-TO-EARTH VOLTAGE= maximum r.m.s. value of the voltage which the bushing withstands continuously between the conductor and the earthed flange or other fixing device, under the operating conditions.

- RATED CURRENT I_r= maximum r.m.s. value of current which the bushing can carry continuously under the operating conditions, without exceeding the temperature rise limits.
- RATED THERMAL SHORT-TIME CURRENT I_{th}= r.m.s. value of a symmetrical current which the bushing withstands thermally for the rated duration (t_{th}) immediately following continuous operation at rated current with maximum temperatures of ambient air and immersion media.
- RATED DYNAMIC CURRENT I_d= peak value of a current which the bushing withstands mechanically.
- HOLLOW INSULATOR= insulator which is open from end to end, with or without sheds.
- CREEPAGE DISTANCE= shortest distance along the surface of an insulator between two conductive parts.
- ARCING DISTANCE= shortest distance in air external to the insulator between metallic parts which normally have the operating voltage between them.
- TEST TAP, MEASURING TAP OR TAN δ TAP= connection, accessible from outside the bushing, insulated from the flange or other fixing device, made to one of the outer conducting layers of a capacitance graded bushing in order to allow measurements of dissipation factor, capacitance and partial discharge whilst the flange of the bushing is earthed.
- MAIN CAPACITANCE C1= capacitance between the high-voltage conductor and the test tap or the voltage tap of a capacitance-graded bushing.
- TAP CAPACITANCE C2= capacitance between the test tap or the voltage tap and the mounting flange of a capacitance-graded bushing.
- CAPACITANCE C= capacitance between the high-voltage conductor and the mounting flange of a bushing without a voltage tap or test tap.

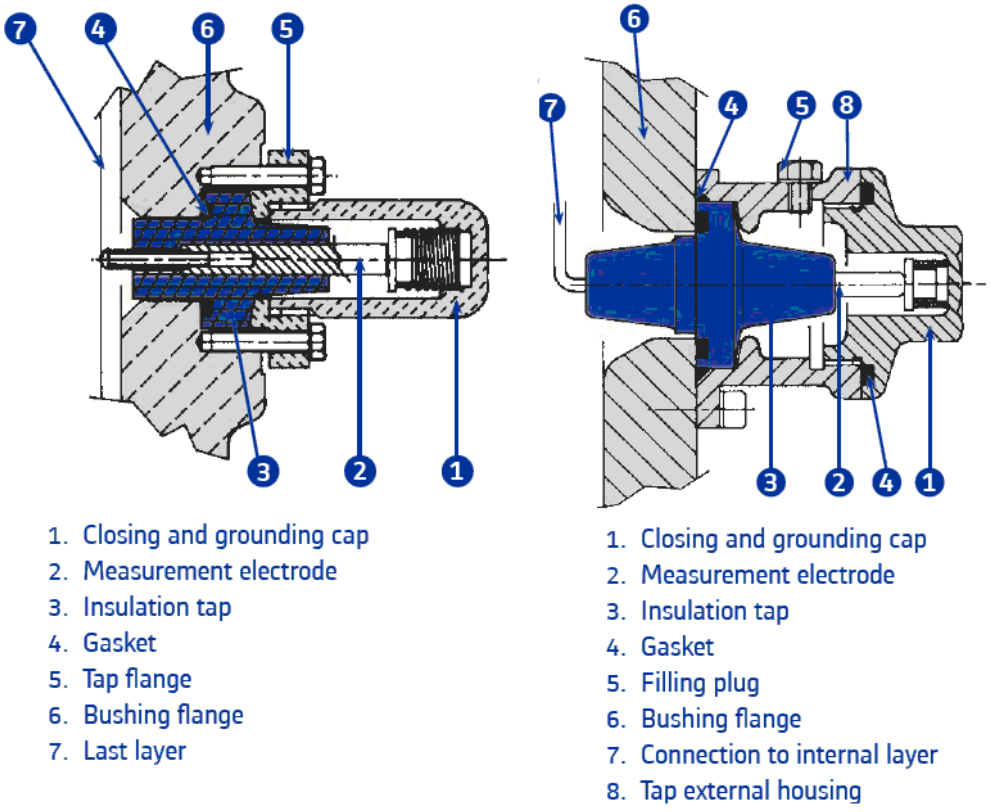

Figure 2.1 - Test Tap (on the Left) and Voltage Tap (on the Right).

2.3 Temperature Limits and Temperature Rise (IEC 60137 - 4.8)

The temperature limits of metal parts in contact with insulating material under normal operating conditions are as follows:

- 105 °C for oil-impregnated paper: Class A;
- 120 °C for resin-bonded and resin-impregnated paper: Class B;
- 130 °C for gas-insulated: Class C;

The temperature rise above maximum daily mean ambient air temperature in accordance with IEC 60137 - 5.3 (therefore 30 °C) of the hottest spot shall not exceed the values given in Table 2.1. In the case of other insulating materials, the temperature limits shall be stated by the supplier. References shall be made to IEC 60216-2 and IEC 60505.

For bushing terminals and connections, the temperature rises are also given in Table 2.1.

Description of component		Maximum temperature rise K	Maximum temperature °C	Comments[a]
Spring contacts	Copper and copper alloys, uncoated:			[d]
	- in air	45	75	
	- in SF_6	60	90	
	- in oil	50	80	[b]
	Tinned in air, SF_6 or oil	60	90	
	Silver/nickel-plated:			
	- in air or SF_6	75	105	
	- in oil	60	90	[b]
Screwed contacts	Copper, aluminium and their alloys, uncoated:			
	- in air	60	90	
	- in SF_6	75	105	
	- in oil	70	100	[b]
	Tinned:			
	- in air or SF_6	75	105	
	- in oil	70	100	[b]
	Silver/nickel-plated:			
	- in air or SF_6	85	115	
	- in oil	70	100	[b]
Terminals to be connected to exterior conductors by screws or bolts	Copper, aluminium and their alloys:			
	- uncoated	60	90	[c]
	– tinned	75	105	
	- silver or nickel-plated	75	105	
Metallic parts in contact with	Insulation class:			
	- A (OIP)	75	105	
	- E (RBP and RIP)	90	120	
	- (GIF)	[e]	[e]	
	- SF_6	100	130	
	- Oil		[e]	

[a] The temperature rise values are based on IEC 60943 with a maximum daily mean temperature of 30 °C. For further information reference should be made to IEC 60943, Table 6.

[b] For synthetic insulating liquids (silicone, esters), higher values may be agreed between purchaser and supplier.

[c] If heavy oxidation is to be expected, the temperature rise shall be limited to 50 K.

[d] A spring contact is a connection maintained by spring pressure for example a plug-in connection.

[e] The temperature limits shall be stated by the supplier.

Table 2.1 - Maximum Temperature Rise Over The Ambient and Maximum Temperature Allowed to Pass the Test

Bushings used as an integral part of apparatus, such as switchgear or transformers, shall meet the thermal requirements for the relevant apparatus. For transformer bushings, reference shall be made to paragraph 4.2 of the Standard IEC 60137.

For gasket in contact with metallic parts, special attention should be paid to the ability of the material withstand the temperature rise.

2.4 Temperature of Ambient Air and Immersion Media (IEC 60137 - 5.3)

Bushings shall be designed for operation temperatures not exceeding the limits given in Table 2.2. Considerations should be given to the operating conditions of completely immersed bushings and bushings operating in air-insulated ducting.

Moisture condensation on the surface of the indoor part of the bushing is to be prevented, if necessary by ventilation or heating.

2.5 Tests to Execute on a Bushing

The supplier shall provide a detailed type test certificate; the tests shall have been carried out on bushings of a design that does not differ from that offered to the purchaser.

The bushings shall not be damaged by the tolerated flashover in air when tested, but slight marks remaining on the surface of the porcelain insulating parts are acceptable.

For bushings of highest voltages for equipment greater than 52 kV the tests to check the dielectric, thermal and mechanical properties of bushings are reported in the following paragraphs.

2.5.1 Type test

Type tests have mandatory nature only for prototypes or for new series/models.

The order or possible combination of the tests is at the discretion of the supplier, except for the impulse voltage withstand test that shall be made before the dry power-frequency voltage withstand test. Before and after the series of type tests, measurements of dielectric dissipation factor and capacitance and of partial discharge quantity shall be carried out in order to check whether damage has occurred.

Subject		Temperature °C
Ambient air:		
– maximum		40
– maximum daily mean (open air)		30
– maximum daily mean (air-insulated ducting)		70
– maximum annual mean		20
– minimum		
• Indoors	Class 1 [a]	–5
	Class 2	–15
	Class 3	–25
• Outdoors	Class 1 [a]	–10
	Class 2	–25
	Class 3	–40
Oil in transformers:		
– maximum		
• for normal load		100
• for emergency duty [b]		115
– maximum daily mean		90
Other media:		
(gaseous and non-gaseous)		[c]

[a] The normal minimum ambient air temperature is Class 1.

[b] The values for oil in transformers are in accordance with IEC 60076-1 and IEC 60076-2. The value for emergency duty is in accordance with IEC 60076-7

[c] In the absence of other information, reference should be made in principle to the corresponding IEC apparatus standard for which the bushing is intended, whereby particular attention should be paid to bushings one end of which is to be immersed in gas.

NOTE 1 The daily mean temperature of the immersion medium should be calculated by averaging 24 consecutive hourly readings.

NOTE 2 By agreement between purchaser and supplier, other temperature ranges may be adopted.

Table 2.2 - Temperature of Ambient Air and Immersion Media.

The type tests are:

- Dry or wet power frequency voltage withstand test;
- Long duration power-frequency voltage withstand test;
- Dry lightning impulse voltage withstand test;
- Dry or wet switching impulse voltage withstand test;

- Thermal stability test;
- Electromagnetic compatibility test (EMC);
- Temperature rise test;
- Verification of thermal short-time current withstand;
- Cantilever load withstand test;
- Tightness test on liquid-filled, compound-filled and liquid-insulated bushings;
- Internal pressure test on gas-filled, gas-insulated and gas-impregnated bushings;
- External pressure test on partly or completely gas-immersed bushings;
- Verification of the dimensions.

2.5.2 Routine test

Routine tests must be done for all bushings, because they can reveal if there is any damage or some mistake that has occurred during the mountain operation.

The order or possible combination of the tests is at discretion of the supplier, except if the tests include impulse voltage withstand test. Before and after the dielectric routine tests, measurement of dielectric dissipation factor (tan δ) and capacitance shall be carried out in order to check whether damage has occurred. The measurement of partial discharge quantity shall be made before the last measurement of tan δ.

The routine tests are:

- Measurement of dielectric dissipation factor (tan δ) and capacitance at ambient temperature;
- Dry lightning impulse voltage withstand test;
- Dry power-frequency voltage withstand test;
- Measurement of partial discharge quantity;
- Tests of tap insulation;
- Internal pressure test on gas-filled, gas-insulated and gas-impregnated bushings;

- Tightness test on liquid-filled, compound-filled and liquid-insulated bushings;
- Tightness test on gas-filled, gas-impregnated and gas-impregnated bushings;
- Tightness test at the flange or other fixing device;
- Visual inspection and dimensional check.

2.6 Temperature Rise Test: Alternating Voltages (IEC 60137 - 8.7)

2.6.1 Applicability (IEC 60137 - 8.7.1)

The test is applicable to all type of bushings, excluding liquid-insulated bushings (the ones where the major insulation consist of oil or another insulating liquid), unless it can be demonstrated by a calculation based on comparative tests that specified temperature limits are not met.

2.6.2 Test method and requirements (IEC 60137 - 8.7.2)

Bushings, one or both ends of which are intended to be immersed in oil or another liquid-insulating medium, shall be appropriately immersed in oil at ambient temperature, except for transformer bushing, where the oil shall maintained at a temperature of 60 K ± 2 K above the ambient air.

In some applications (e.g. generator transformer) the transformer top-oil temperature is often restricted to value below the normal IEC limits. Subject to agreement between manufacturer and purchaser, the standard oil temperature rises of 60 K may be reduced to reflect the real transformer top oil temperature.

Bushings with a conductor drawn into the central tube shall be assembled with an appropriate conductor, the cross-section of which shall conform to Ir. when the transformer oil is in communication with the bushing central tube, the oil level shall not exceed one-third of the height of the external part.

The end of bushings, which are intended for immersion un a gaseous insulating medium other than air at atmospheric pressure, shall normally be appropriately immersed in an enclosure insulated with gas at minimum pressure (the pressure which the bushing is filled before being put in service),the gas being at the ambient temperature at the beginning of the test.

Gas-insulated bushings shall beat ambient temperature at the beginning of the test.

For transformer bushings operating in air-insulating ducting, the airside shall be enclosed, in an appropriate chamber. During the test, the air in the chamber shall be heated to 40K±2K above the ambient air, either by self-heating indirectly.

An appropriate numbers of thermocouples or other measuring devices shall, as far as possible, be placed along the bushing conductor, central tube or other current-carrying parts, as well as possible on the flange or other fixing device, so as to determine the hottest spot of the bushing metal parts in contact with insulating material with reasonable accuracy.

The ambient air temperature shall be measured with lagged thermometers placed around the bushing at the mid-height and a distance of 1 m to 2 m from it.

A satisfactory degree of lagging is obtained by placing the thermometers in oil-filled containers with a volume of approximately 0.5 l.

The temperature of the oil or gas shall be measured by means of thermometers placed at a distance of 30cm from the bushing and, in case of oil, 3 cm below the surface of the oil.

Temporary external connections used for this test shall be of such dimensions that they do not contribute unduly the cooling of the bushings under test. These conditions are assumed to be fulfilled if the temperature decrease from the bushing termination to a point at 1m distance along the connection does not exceed 5 K, or the thermal gradient along the external conductor is 5 K per metre for short connections.

The test shall be continued until the temperature rise is sensibly constant. This is considered to be the case if the temperature does not vary more than ±1 K during 1 hour.

In order to provide data for thermal modelling of bushings, operating under different current loading and ambient temperature conditions, it is recommended by agreement to carry out overload tests and to record time functions of all temperature readings.

To avoid the destruction of the insulation in the case of bushings with the conductor embedded in the insulating material, the temperature of the hottest spot may be, by agreement between purchaser and supplier, be determined as follow:

The maximum conductor temperature θ_M is deduced by the Equation 2.1 and Equation 2.2:

$$\theta_M := \frac{\left[3\left(\theta_A + \frac{R_C}{R_A \cdot \alpha}\right) - \left(\frac{3}{\alpha}\right) - \theta_1 - \theta_2\right]^2 - (\theta_1 \cdot \theta_2)}{3 \cdot \left[2\left(\theta_A + \frac{R_C}{R_A \cdot \alpha}\right) - \left(\frac{2}{\alpha}\right) - \theta_1 - \theta_2\right]} \quad [°C]$$

Equation 2.1 - Temperature Hot Spot

$$M = \left[3\left(\frac{R_C}{R_A} \times \frac{1}{\alpha} + \theta_A\right) - \frac{3}{\alpha} - \theta_1 - \theta_2\right] - \theta_M$$

Equation 2.2 - Coefficient M

If the result of the second equation is M positive, the higher temperature of the conductor is θ_M, and it is situated in any point of the conductor between the two extremities. If the result M is negative or zero, the higher temperature or the conductor is θ_2.

The point of maximum conductor temperature lies at distance L_M from the cooler end.

$$L_M := \frac{L}{1 + \sqrt{\frac{(\theta_M - \theta_2)}{(\theta_M - \theta_1)}}} \quad [mm]$$

Equation 2.3 - Distance L_M From the Hot Spot to the Bushing Cooler End

Where:

- α= is the temperature coefficient of resistance at which conductor resistance R_A is measured;
- θ_1= is the measured temperature at the cooler end of the conductor, in degrees Celsius;
- θ_2= is the measured temperature at the hottest end of the conductor, in degrees Celsius;

- θ_A= is the uniform reference temperature of the conductor, in degrees Celsius;
- θ_M= is the maximum temperature of the conductor, in degrees Celsius;
- L= is the length of the conductor;
- L_M= is the distance from the cooler and of the conductor to the point of highest temperature;
- R_A= is the resistance between the ends of the conductor at uniform temperature θ_A;
- R_C= is the resistance of the conductor carrying I_r after stabilisation of temperature.

2.6.3 Acceptance (IEC 60137 - 8.7.2)

The bushing shall be considered to have passed the test if the permissible temperature limits in accordance with IEC 60137-4.8 are met, and there is no visible evidence of damage.

2.7 Temperature Rise Test: D.C application (IEC 62199 - 8.4)

2.7.1 Applicability (IEC 62199 - 8.4.1)

The test is applicable to all type of bushings.

2.7.2 Test method and requirements (IEC 62199 - 8.4.2)

Test shall be carried out in accordance with IEC 60137.

The applied current it is different depending upon the application of the bushing: for the ones that carry substantially d.c. current, the applied current shall be no less than the rated continuous d.c. current. If a d.c. source is not available, an alternating 50 Hz or 60 Hz supply may be used. In such a case, the test current shall be used with correction for the skin effect of the a.c. supply as calculated in Equation 2.4.

$$I_{testac} := \sqrt{I_{dc}^{2} \cdot \frac{R_{dc}}{R_{ac}}} \quad [A]$$

Equation 2.4 - Equivalent a.c Test Current for Bushings That Carry Usually d.c. Current

For bushings that carry substantially a.c. currents, the test current I_{testac} is a 50 Hz or 60 Hz calculated by:

$$I_{eqac} := \sqrt{\sum_{h} \left(I_{h}^{2} \cdot K_{h} \right)} \quad [A]$$

Equation 2.5 - Equivalent a.c Current

$$I_{testac} := \sqrt{I_{eqac}^{2} \cdot \frac{R_{dc}}{R_{ac}}} \quad [A]$$

Equation 2.6 - Equivalent a.c Test Current for Bushings That Carry Usually a.c. Current

2.7.1 Acceptance (IEC 62199 - 8.4.2)

The bushing shall be deemed to have passed the test if the limits of IEC 60137 (reported in Table 2.1) are met.

2.8 Temperature Rise Test: Draw Lead and Draw Rod Bushings

With the bushings having an extractable conductor, the evaluation of the temperature hottest spot can be realized with a direct measure. This is possible thankfully to these conductor types, where the measurement devices can be placed inside the bushing and even directly on the current carrying conductor. The used devices to take over the values of temperature are some thermocouples.

2.8.1 Thermocouples

A thermocouple consists of two conductors of different materials (usually metal alloys) that produce a voltage in vicinity of the point where the two conductors are in contact. The voltage produced is dependent on, but not necessarily proportional to, the difference of temperature of the junction to other parts of those conductors. This is called thermoelectric effect or *Seeback effect*.

Any junction of dissimilar metals will produce an electric potential related to temperature. Thermocouples for practical measurement of temperature are junctions of specific alloys that have a predictable and repeatable relationship between temperature and voltage, with different alloys used for different temperature ranges.

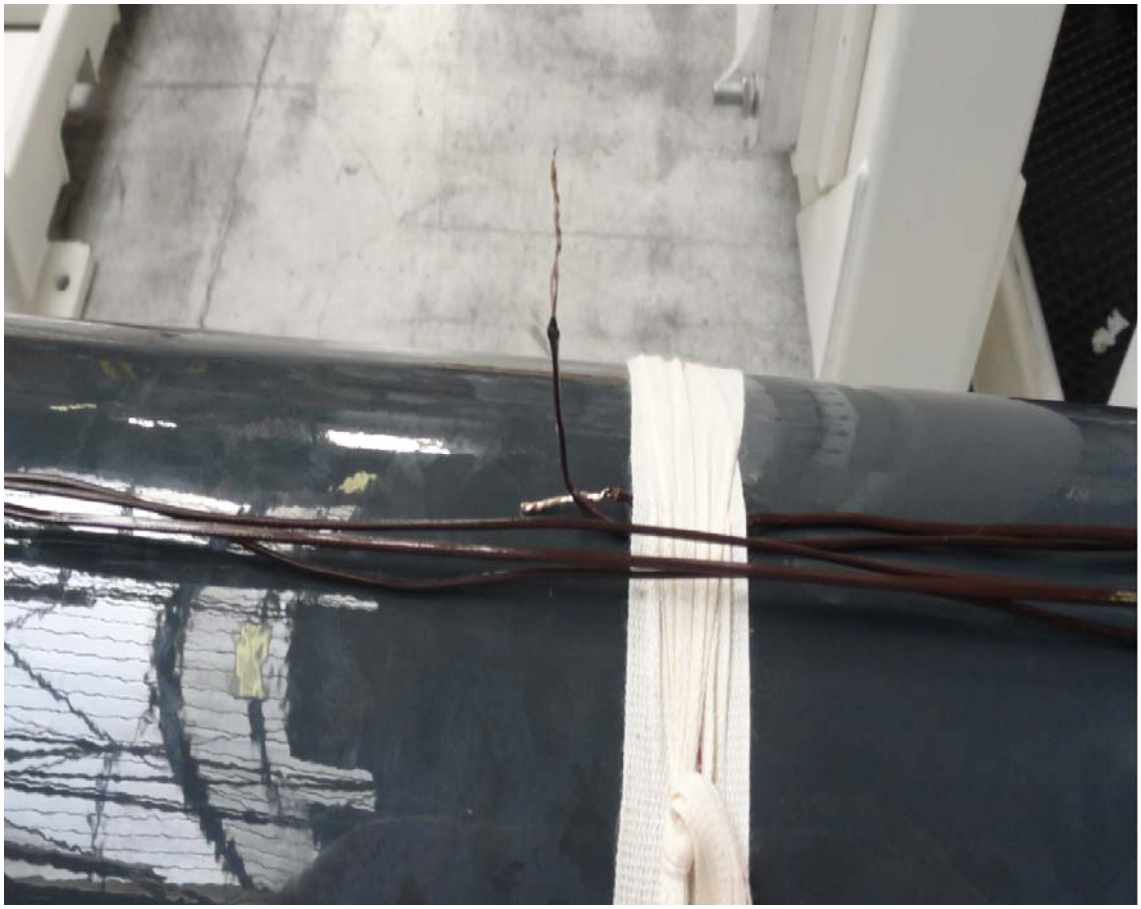

Figure 2.2 - Two Thermocouples Positioned on the Conductor of the PHI Bushing, in the Gas Side: One is Placed Along the Conductor to Measure its Temperature in That Zone, One is Up in Air to Measure the Internal Gas Temperature.

Commercial thermocouples are usually inexpensive, interchangeable, supplied with standard connectors, and they can make a measure of a wide range of temperatures. In contrast to most other methods of temperature measurement, thermocouples are self-powered and do not require external form of excitation. They have an accuracy limitation: system errors of less than one degree Celsius can be difficult to achieve. However, for the measures of temperature rise test of a high voltage bushing this is a negligible error, due the high values reached.

In the test realized in the Alstom Grid-Passoni&Villa factory the thermocouples used are of the J Type, which work in a temperature range of 0 ÷ 750 °C for continuous service and (-180) ÷ 800 °C for short periods.

2.8.2 Realization of the Test

The test is carry out in the following mode: some thermocouples, usually about ten, are placed inside (especially directly on the conductor) and outside of the bushing. At least one of them must be dedicate to notice the ambient temperature and another one must be dedicate to notice the oil tank temperature.

A typical example of thermocouples disposition during a temperature rise test can be seen in Figure 2.3.

In order to respect the Standard IEC indications, the temperature of the oil presents in the tank must be maintained at a fixed value of 60 K ± 2 K over the ambient air.

The measures of temperature are realized and reported every half an hour or every hour, since the thermal stability is reached; this mean when the variation of temperature noticed by the same thermocouple is less than 1 K during 1 hour.

After having satisfied this condition, the test has reached the steady state condition and the taken values considered the final temperature, which can be used to make a confrontation with the limits given by the Standard IEC 600137.

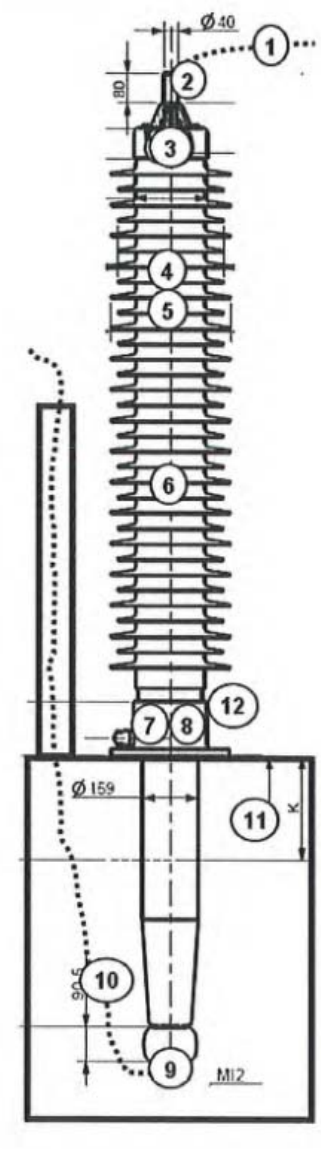

Thermocouples positioning	
T1	Air side - Cu lead 1m
T2	Air side - Al top terminal
T3	Air side - Cu lead joint
T4	Air side - internal Cu lead 2/3 h in air
T5	Air side - external Cu lead 2/3 h in air
T6	Air side - external Cu lead 1/3 h in oil
T7	Air side - internal Cu lead flange
T8	Air side - external Cu lead flange
T9	Oil side - bottom Cu terminal
T10	Oil side - Cu lead 1m
T11	Oil
T12	Ambient temperature

Figure 2.3 - Thermocouples Placing During the Temperature Rise Test of a PNO 170.750.800

If the measured maximum temperature value, after having report it at the reference ambient temperature of 30 °C used in the Standard IEC, and the highest temperature rise result minor of their relatives limits, than the test is considerable positive and the bushing has passed it.

This method of measurement has a good accuracy, the final uncertainty given by this process is about the 1%.

Figure 2.4 - A Draw Lead Bushing Mounted on an Oil Tank During The Temperature Rise Test

2.8.3 Critical Points of the Test Realization

At a first glance, the direct measure appears an easy procedure to realize. However, there are two critical points where is mandatory giving the maximum attention, especially during the selection of the measurement circuit components.

The first problem is making a right selection of the leads that connect the up and bottom bushing terminals with the power supply. In fact, if the chosen lead section is too big there is a

too high heat flow directs from the bushing to the feeding circuit, creating a cooling effect that gives an underestimate temperature hot spot.

On the contrary, if the chosen lead section is too small the consequences are duals: there is a too high heat flow directs from the feeding circuit to the bushing, creating a warming effect that gives an overestimate temperature hot spot.

Both these two cases could heavily modifies the final test result

In the ideal world the connections should made an adiabatic system, but since this is very hard to obtain in the real world the IEC Standard gives a limit to can consider the test correctly executed (gradients of temperature are acceptable when they do not exceed the 5 K from the bushing end to a point positioned at 1 m of it along the connection).

The parameter to take into account during the choice is the current density given by the leads; it is usually included in a range that goes from 1.5 A/mm^2 to 2.5 A/mm^2.

The second problem is given by the fact that in these bushing types (draw lead and draw rod), the central current carrying conductor is not fixed inside the bushing. Therefore, there is the risk to take a conductor section for the test that is different of the effective one used by the customer.

The reasons of these uncertainties are various: because there are insufficient data (e.g. in draw lead case, where conductor comes directly from the transformer winding and its dimensions are usually not known to the manufacture), to having not in the test chamber the exactly reproduction of the supplier conductor or due to the fact that the leads assembled to create the conductor have an irregular final shape difficult to replace.

This second critical point is present and important during both the bushing designing and the creation of a model for a thermo-magnetic simulation with a FEA program. On the test repost must be inserted the section of the leads used during the temperature rise evaluation.

2.9 Temperature Rise Test: Bottom Connected and Fix Rod Bushings

In these types of bushings the ends of the air side and the oil side are closed and they cannot be opened, therefore is impossible inserting some thermocouples inside and along the current carrying conductor. For this reason, realize a direct measure of temperature inside the bushing

is impossible, the points only of the conductor accessible are the connections with top and bottom terminals.

2.9.1 Test Preparation

The preparation of the temperature rise test of the test is the same illustrated in the previous paragraph (2.8.2), but now the thermocouples can be placed only outside the bushing.

A typical (and acceptable according to the standard) disposition of these measuring devices can be seen in Figure 2.5. The picture comes from a temperature rise test carried out in the Alstom Grid-Passoni&VIlla factory.

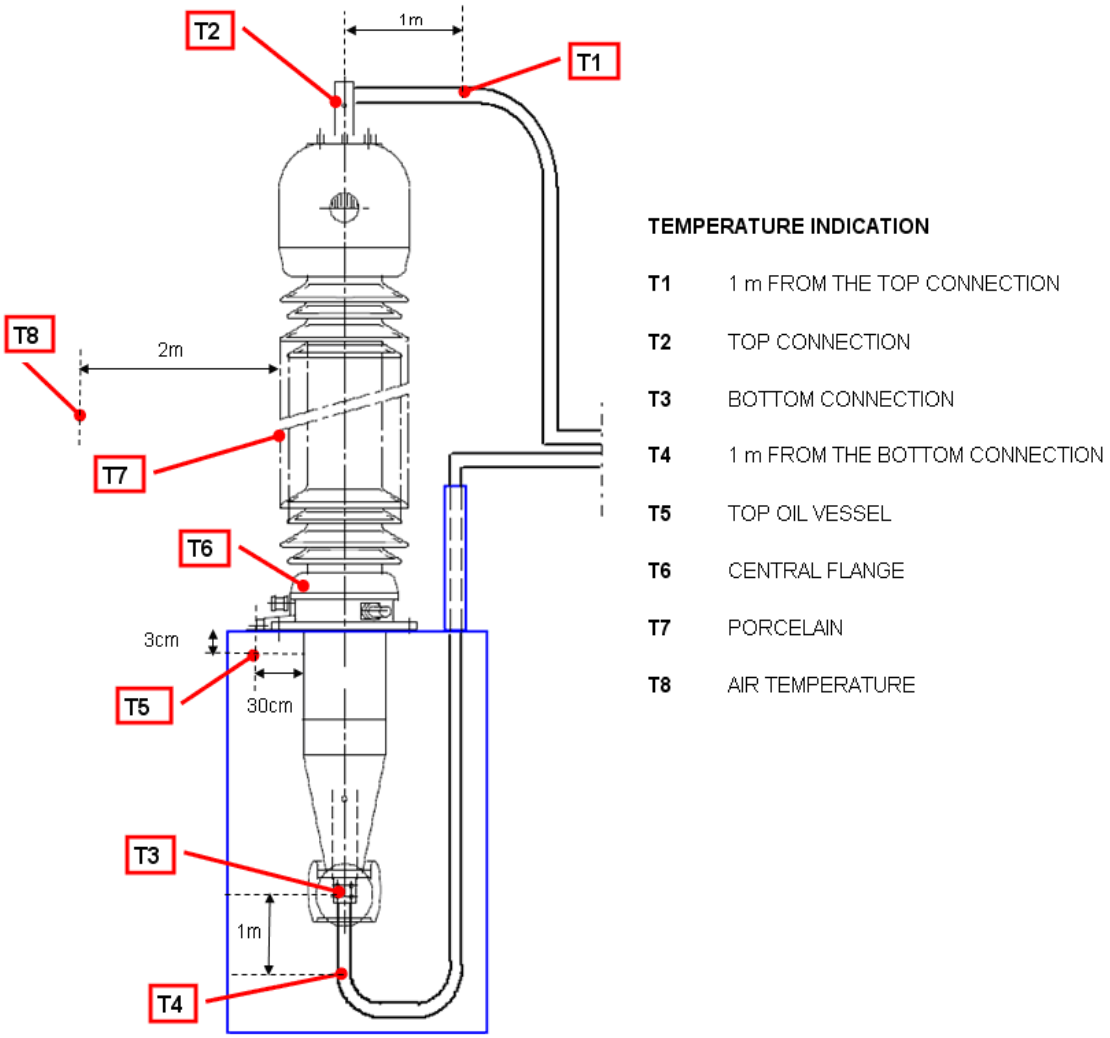

Figure 2.5 - Thermocouples Disposition for the Temperature Rise Test of PNO 800.2550.2500

2.9.2 Cold Resistance Measurement

After the thermocouples disposition, the first step is find the value of resistance between the bushing ends, which will be used in the IEC Formula (Equation 2.1) as the conductor resistance value at the uniform temperature (there called resistance "R_A"). This parameter is called "cold resistance" and to obtain it is realized a d.c. voltmetric measure, based on the circuit reported in Figure 2.6.

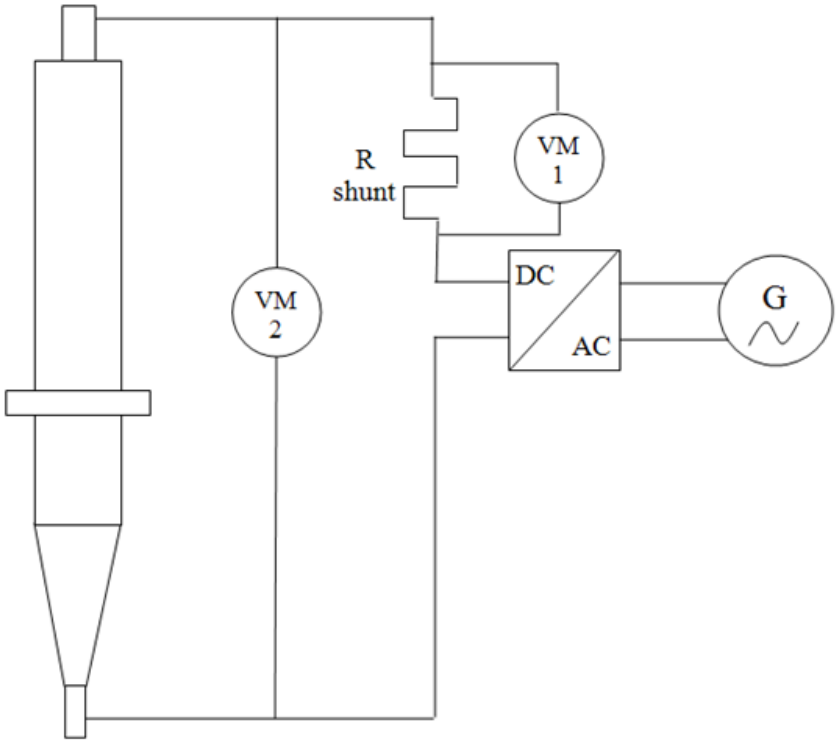

Figure 2.6 - Cold Resistance Measuring Circuit

The components present in the circuit are:

- A generator that gives the bushing feeding current;
- An AC/DC converter;
- A reference shunt, with a well know value of resistance;

- Two voltmeters.

In the Table 2.3 are reported some characteristics of the instrument usually used in the Alstom Grid-Passoni&Villa factory during the temperature rise test realization.

VOLTMETER	**VM1**	-	range :	-	accuracy 0,01
		-	manufact. :	*AGILENT 34401A MY4701·LE 5211*	
VOLTMETER	**VM2**	-	range :	-	accuracy 0,01
		-	manufact. :	*AGILENT 34401A MY4701·LE 5210*	
		-	**Rz :**	**117,47 $\mu\Omega$**	accuracy 0,01
SHUNT		-	range :	500A / 60mV	
		-	manufact. :	*TINNOVA* *LE 5209*	

Table 2.3 - Measuring Devices Characteristics

The generator at the measuring circuit gives a d.c. current. The current passes through the shunt, where is connected the first voltmeter. The voltage value given by this device is used to calculate the exact value of the d.c. feeding current in the circuit, with the application of the Ohm's law (Equation 2.7).

$$I_{DC} := \frac{V_{VM1}}{R_{shunt}} \quad [A]$$

Equation 2.7 - The Feeding d.c. Current During Cold Resistance Measuring

Since the current that pass through the bushing conductor is the same one through the shunt (they are connected in series), its value is well know.

The voltage at the bushings terminals is also notice thankfully the second voltmeter connected here, then it is possible calculate the so-called cold resistance of the conductor, using the Equation 2.8 .

$$R_{cold} := \frac{V_{VM2}}{I_{DC}} \quad [\Omega]$$

Equation 2.8 - Bushing Cold Resistance

This measure is replaced for N times, usually about ten. Afterwards, starting to all the values of cold resistance obtained, an average one is extrapolated through an arithmetic mean process, as reported in the Equation 2.9.

$$R_A := \frac{1}{N} \cdot \sum_{i=1}^{N} \left(R_{cold_i} \right) \quad [\Omega]$$

Equation 2.9 - Bushing Cold Resistance Average Values

2.9.3 Bushing Shutdown Resistance Measurement

The second phase of the measurement process permits to define the shutdown resistance, which is the value called "R_c" in the Standard IEC Formula (Equation 2.1).

The bushing is feeds with an a.c. test current, which could be:

- The rated current;
- An equivalent of the rated value, e.g. happens when the bushing is designed for some foreign market and is necessary report the rated current value given at the destination market frequency to the equal one at 50 Hz;
- An arbitrary current, but this case happens when the final goal is making a study about the bushing thermal behaviour at several values of current different to the rated one. To pass the temperature rise test is, however, mandatory feed the bushing with the rated current (or an equal one).

Even in the case of fix rod and bottom connected bushing the choice of the leads that connect the terminals to power supply is a critical point, in the same way was already explained in paragraph 2.8.3.

The a.c. current must feed the measuring circuit since the bushing has reached the thermal steady state.

Afterwards, the a.c. feeding current must be interrupted and replaced with a d.c. current, which has a significant lower rated value, so it is possible realize the measure with the same circuit used for the cold resistance. This procedure allows the usage of measuring devices designed for low currents, giving an important costs saving. This changing operation must be done as fast as possible, it is typically completed in about 1 minute ÷ 1 minute and half.

It is important to notice that the temperature values of the ambient, of the tank oil, of the top and bottom connection recorded before the current shutdown are those used as parameters in the IEC Formula (in Equation 2.1 and Equation 2.2).

The shutdown resistance method now follows the same pattern of the cold resistance case: is applied the Ohm's voltage low at the ends of the two voltmeters, in order to find, as first, the current that circulates in the circuit and then the bushing resistance (practically, are applied again Equation 2.7 and Equation 2.8).

However, now the sampling instants of time are plenty more respect the previous point, at the end of this measure there must be about twenty-five or thirty resistance values. It must be taken one sample about every 30 seconds.

With all these values is realized a graph, in the y-coordinate are inserted the resistances calculated, while in the x-coordinate are placed the time instants where the relative samples have been taken. Their measurement units are not seconds but minutes reported in hundredths (e.g. the sample taken at 1 minute and 30 seconds must be inserted at the y-coordinate equal to 1.5).

The final goal of this process is finding the conductor resistance value at the instant t= 0, that is the one of when was passing the a.c. test current and that represent the R_c in the Standard IEC Formula.

To identify this value, starting from the samples taken is make a regression curve with the OLS (Ordinary Least Square) method, which minimizes the sum of squared vertical distances between the observed responses in the data collection and the responses predicted by the

linear approximation. The results obtained with this process can be considered a good approximation of the real value.

An example of this curve, taken from a test report of the PNO.800.2550.2500, is reported in Figure 2.7.

This measurement process is obtained by the power transformers Standard IEC 60076-3:2000, while there are no indications of how the resistance R_c must be measured in the bushings Standard IEC 60137. Therefore, it is possible that others manufacturers adopt different methods to obtain it.

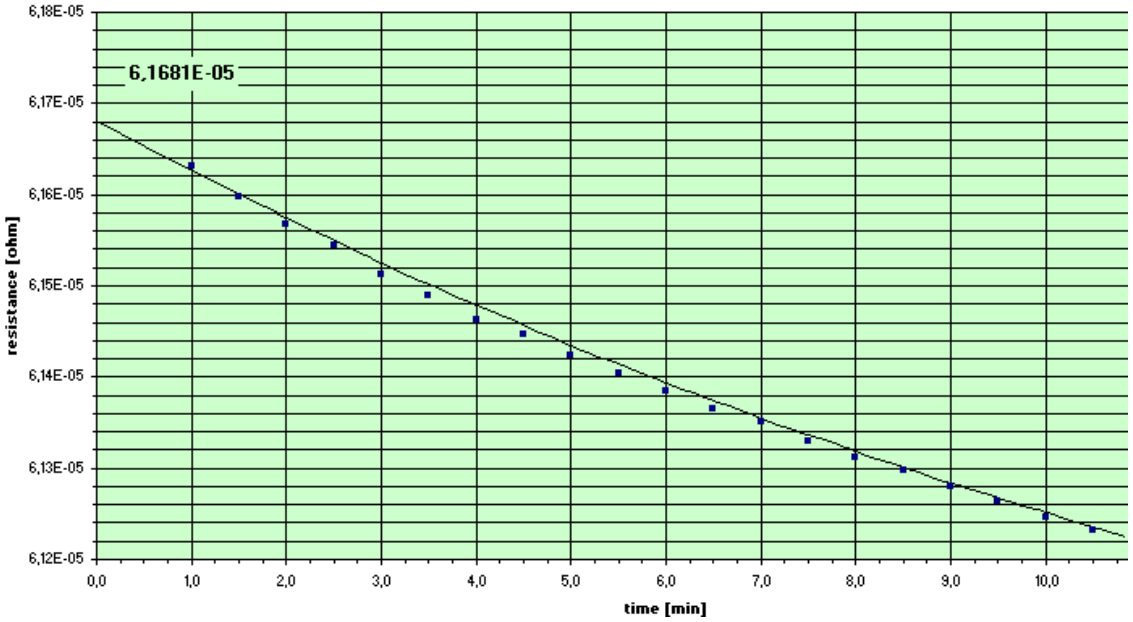

Figure 2.7 - Regression curve from temperature rise test on a PNO 800.2550.2500, the founded resistance value a t=0 is Rc= 61,681 μΩ

Having found the value of the conductor resistance when the rated current pass through the bushing, all the data that are necessary to applying the IEC Formula are well knows. Therefore is possible calculate the bushing maximum temperature using the Equation 2.1, Equation 2.2 and Equation 2.3.

3 ANALYSIS OF THE TEST HISTORICAL RESULTS

3.1 Introduction

In this chapter, after a quickly presentation of the methodology used in Alstom Grid-Passoni&Villa to recognize the bushing type from its proper name, it have been reported some collections of data taken from the realized tests, in order to can understand which are the typical values of maximum temperature expected and to make some considerations above the realization of the temperature rise test itself and even about the validity of the Standard IEC 60137.

3.2 Bushing type code

In the following paragraphs are inserted the temperature rise data taken from the test reports realized by the company Alstom Grid-Passoni&Villa in the last years. The tests were made both in its own factory and in external test chambers.

Each series of bushing has its proper name that depends: to the designed technology, to some dimensional characteristics, if it has been thought as a transformer bushing or a through wall bushing, etc. The type name comes from an abbreviation of these main properties.

The complete explanation of the principal bushing families analyzed in the next paragraphs are reported in the Table 3.1.

Family Name	Italian	English	Insulating Technology	Bushing type
PNO	Passante Normale Olio	Normal tail oil bushing	OIP Oil Impregnated Paper	Transformer bushing
PNR	Passante Normale RIP	Normal tail RIP bushing	RIP Resin Impregnated Paper	Transformer bushing
PSO	Passante Short Olio	Short tail oil bushing	OIP Oil Impregnated Paper	Transformer bushing
PAO	Passante ANSI Olio	IEEE Standards oil bushing	OIP Oil Impregnated Paper	Transformer bushing
POBO	Passante Olio Blindato SF6 Olio	Oil to SF_6 transformer bushing	OIP Oil Impregnated Paper	Transformer bushing
PCTO	Passante Cavo Trasformatore Olio	Cable to transformer oil bushing	OIP Oil Impregnated Paper	Transformer bushing
PWS	Passante Wall SF_6	Wall bushing SF_6 type	SF_6	Through wall bushings
PHI	Passante HVDC Ibrido	Normal tail HVDC bushing hybrid type	Hybrid (OIP and SF_6)	HVDC Through wall bushings

Table 3.1 - Bushing Family Name Explication

3.3 Data from Test Reports

A test report is a document where are reported the bushings responses at the tests, with even indications of how they have been made (e.g. environmental conditions, characteristics of devices and instruments used, presence of particular conditions, etc).

In the following paragraphs are showed all the results of the temperature rise test performed in the last four/five years by Alstom Grid - Passoni&Villa.

Some of them are coming from test reports of final products, they are mandatory because a bushing needs to work inside the limits given by the International Standard in order to be sold, usually the test's activity is realized in presence of the customer or a CESI inspector or another external part to ensure the correct application of the standard and the respect of the limits.

Some other are coming from internal test reports, usually made to achieve different objectives, which may be: knowing the thermal behaviour of a bushing prototype, seeing what values of current/voltage can be reached before damaging the product, having a major amount of data for specific bushing types, etc.

The number of total test results available, however, is very small if it is compared with the average production of the factory, which amount about at several hundreds of bushings for year.

The reason is dues at the fact that the temperature rise test is a so defined "type test" and then is not obligatory carried out it for all the bushings produced: when a specific type has passed it, the test is assumed satisfied also for every other bushing of the same family or with very similar electrical, mechanical and geometrical characteristics.

Even test realized with only research and development finality are few, because making them involves not negligible both economic costs and an amount of time (time where, furthermore, the test chamber cannot be use to testing the bushings intended for sale, blocking the production process).

3.3.1 Data Organization

Since the interesting data for the subject of this thesis are not easily and immediately identifiable in a complete test report, it is necessary rewrite them in a clearer form for a better organization.

The first thing is recognizing that the bushings with removable conductor (draw lead and draw rod types) have a pretty different measurement method for the temperature rise test if compared to bushings with non-removable conductor (fix rod and bottom connection types). Therefore, they should be treated as two different cases and it is a good thing split them in two different series of tables.

Beyond the basic bushing characteristics, the most significant data are: the values of the highest temperature, the maximum temperature rise over the ambient and the place where they are located. Therefore, these informations are highlighted in the follows tables to can easily recognize them.

To can better understand the sense of the measurement process (and if the measure itself gives a reasonable response) are also reported the most significant thermocouples lectures and, for the non-removable conductor types, the parameters necessary to the application of the Standard IEC Formula (shown in Chapter 2).

3.4 Test Report Results: Bushing with Removable Conductor

Bushings with removable conductors are the ones where it is possible make a direct temperature measure just placing the thermocouples on all the bushing.

To report these test data, the method chosen is the following one: in the Table 3.2 are inserted the values of the measurements realized with the thermocouples placed in the most significant bushing zones and their relative temperature hot spots, while in the Table 3.3 are inserted the values of the temperature rise over the ambient and the position along the bushing where them and the hot spot are individuated.

BUSHING				MEASURES WITH THERMOCOUPLES					
Name	Type of buhing	L [mm]	I test [A]	Ta[°C]	Toil[°C]	Ttop [°C]	Tbottom [°C]	Tmax [°C]	Tmax at 30°C [°C]
PNO.145.650.1250	Draw Rod	2220	1250	17,1	77,5	76,7	80,1	92	104,9
PNR.170.750.800	Draw Rod	2695	850	20,2	80,1	40,9	88,3	95,8	105,6
PNO.170.750.1250	Draw Rod	2420	1250	16,8	74,9	72,6	81,2	90,4	103,6
PNO.245.1050.800	Draw Lead	4390	800	20,3	83,4	44,1	83,1	83,1	92,8
PNO.245.1050.1250	Draw Lead	3750	1250	22,1	82	46,8	84,1	84,1	92
PNO.420.1425.1250	Draw Lead	5670	1250	29,4	91,6	51,5	92,6	92,6	93,2
PNO.420.1425.1600	Draw Lead	5670	1600 - after 15h	32,1	89,3	52	96,1	110,9	108,8
PNO.420.1425.1600	Draw Lead	5670	1600 - after 24h	29,4	91,5	49,1	109,7	112,2	112,8
PNO.525.1800.1250	Draw Lead	6760	1250	23,1	81,4	62,1	89,1	94,9	101,8
PWS.800DC.2100.4305	Gas/combined insulation	21320	3500	18,75		34,7	61,8	61,8	73,05
PWS.800DC.2100.4305	Gas/combined insulation	21320	4000	17,57		39,5	74,7	74,7	87,13
PWS.800DC.2100.4305	Gas/combined insulation	21320	4700	19,15		50	90	90	100,85

Table 3.2 - Bushing with Removable Conductor, Hot Spot

BUSHING				TEMPERATURE RISE				
Name	Type of buhing	L [mm]	I test [A]	ΔToil [K]	ΔTtop [K]	ΔTbottom [K]	ΔTmax [K]	HOT SPOT POSITION
PNO.145.650.1250	Draw Rod	2220	1250	60,4	59,6	63	74,9	Inside conductor, at 2/3 of total height
PNR.170.750.800	Draw Rod	2695	850	59,9	20,7	68,1	75,6	Internal conductor at flange height
PNO.170.750.1250	Draw Rod	2420	1250	58,1	55,8	64,4	73,6	Inside conductor, at 1/3 of total height
PNO.245.1050.800	Draw Lead	4390	800	63,1	23,8	62,8	62,8	Bottom Terminal
PNO.245.1050.1250	Draw Lead	3750	1250	59,9	24,7	62	62	Bottom Terminal
PNO.420.1425.1250	Draw Lead	5670	1250	62,2	22,1	63,2	63,2	Bottom terminal
PNO.420.1425.1600	Draw Lead	5670	1600 - after 15h	57,2	19,9	64	78,8	Internal conductor at flange height
PNO.420.1425.1600	Draw Lead	5670	1600 - after 24h	62,1	19,7	80,3	82,8	Internal conductor at flange height
PNO.525.1800.1250	Draw Lead	6760	1250	58,3	39	66	71,8	Internal conductor at flange height
PWS.800DC.2100.4305	Gas/combined insulation	21320	3500		15,95	43,05	43,05	H.V.screwed contact - outdoor side
PWS.800DC.2100.4305	Gas/combined insulation	21320	4000		21,93	57,13	57,13	H.V.screwed contact - outdoor side
PWS.800DC.2100.4305	Gas/combined insulation	21320	4700		30,85	70,85	70,85	H.V.screwed contact - outdoor side

Table 3.3- Bushing with Removable Conductor, Temperature Rise

The voices in the two previous tables mean:

- Name= name of the bushing;
- Type of bushing= intended as which type of conductor of the bushing;
- L= total bushing length, in [mm];
- Itest= current which has been executed the test, in [A];
- Ta= temperature of the ambient, in [°C];
- Toil= temperature of the tank's oil where is immersed the bushing oil side, in [°C];
- Ttop= temperature of the bushing top terminal, in [°C];
- Tbottom= temperature of the bushing bottom terminal, in [°C];
- Tmax= higher temperature measured by the thermocouples, in [°C];
- Tmax reported at 30°C= Tmax - Ta + 30°C , here the value of Tmax is reported at the reference temperature of 30 °C to can make a easily confrontation with the given limits, in [°C];
- ΔToil= Toil - Ta, temperature rise of the tank's oil over the ambient, in [K];
- ΔTtop= Ttop - Ta, temperature rise of the top connection over the ambient, in [K];
- ΔTbottom= Tbottom - Ta, temperature rise of the bottom connection over the ambient, in [K];

- ΔTmax= Tmax - Ta, temperature rise in the hottest spot over the ambient, in [K];
- Hot spot position= where are located the highest both temperature and temperature rise.

3.5 Analysis of the Results: Bushing with Removable Conductor

Observing all the results of the tests, one of the first thing that strikes the attention is the fact that the values the highest temperatures and temperature rises obtained have both a trend that is unpredictable, even if the bushing characteristics (e.g. the bushing length, the rated voltage, the rated current, etc.) are well know. There is not an unequivocal link between them and the resulting hottest spot value.

The final maximum temperature and temperature rise are knowable only after the test is carried out, there is not another simple way to obtain them.

Actually, the possibility to can estimate them with a certain accuracy exists: realizing a bushing model and making a thermo-magnetic simulation over it to calculate the temperature distribution. However, this method requires a lot of hour of work, usually days, and quite complicated problem settings (but this approach is still important and is well analyzed in the subsequent chapter).

Another interesting point is observing in which zones the highest temperatures are located: in the majority of the cases, the hot spot results placed either on the bushing bottom terminal or on the inner conductor at the flange height. This is an understandable and expected result.

In fact, the bottom part of the bushing is immersed in a tank filled of oil with a temperature of about 90 °C, so it is reasonable thinking that the heat generated by the current flow along the conductor is dissipated with many difficulties in such ambient.

Even the flange zone is expected, since the heat flow along the conductor tends to transport it towards to the bushing top terminal (it is usually the colder one). Therefore, in the zone where is mounted the flange, there is both a heat flow from the bottom part and an additional layer, the flange itself, that obstructs the radials heat dissipation, favouring the warming process.

Observing the results, there is a particular test that requires some explanations. It is the PNO.420.1425.1600, from which is notable a possible critical point of the Standard IEC 60137 itself. The test was realized in the following way: after 15 hours of feeding, the variations of

temperature becomes smaller than 1 K in 1 hour, and therefore, according to the Standard indications, the thermal stability has been reached, the lectures realized at those moments represent the final temperature values and the test can be considered over.

However, the feeding was maintained and the test and the measures have been continued. As result, even with variations smaller than 1 K, the temperature has increased significantly until have been reaching 24 hours from the beginning of the test. This means that the effective thermal stability has been reached about 9 hours after the time defined by following the Standard IEC indications.

The final hottest spot found with the extended duration, as consequence, results higher of about 4 °C respect the highest temperature measured after just 15 hours of bushing's feeding, an incrementing value that is not negligible at all.

3.6 Test Report Results: Bushing with Non-Removable Conductor

Since the measurement method for these bushings types must follows a more complicated process, there are more sensible data to collect respect the cases seen in the previous paragraphs.

In fact, to contain them the tables created have several voices extra respect the previous case.

Beyond the basics characteristic, in the Table 3.4 there are inserted all the parameters that are necessary to can apply the Standard IEC Formula, while the Table 3.5 has the same function of, respectively, the Table 3.2 and the Table 3.3 already seen in the paragraph 3.4.

However, this time the lectures given by the thermocouples represent only a partial evaluation of the thermal behaviour, due the impossibility to place them in the inner bushing, but they can be used to make a helpful comparison with the results obtained through the calculation.

The major part of the tables voices are explained yet, in the Chapter 2 for what concerns the IEC formula parameters and in previous paragraph for the ones in Table 3.5.

The voices that need a rapid explanation are the follows:

- θm= values of temperature hot spot given by the application of first equation in the IEC Formula;

- θmax= effective values of temperature hot spot given following the Standard IEC indications. It is equal to θm if the coefficient M is a positive number, otherwise it is equal to the temperature measured on the hottest bushing terminal;
- θmax reported at 30°C= θmax - Ta + 30 °C , here the value of θmax is reported at the reference temperature of 30 °C, to can make a easily confrontation with the Standard limits, in [°C];
- Hot spot position= where are located the highest both temperature and temperature rise, in according with the IEC Formula results indications.

BUSHING		I TEST	IEC FORMULA METHOD													
Name	Type of buhing	I test[A]	Ra [μΩ]	Rc[μΩ]	θa [°C]	θ1 [°C]	θ2 [°C]	α [1/°C]	L [mm]	θm [°C]	M	Lm [mm]	θmax [°C]	θmax at 30 °C [°C]	Δθmax [K]	HOT SPOT POSITION
PNO 170.1425.2500	Fix rod	2000	31,344	33,894	23,5	60,9	83,3	3,91E-03	2650	29,5	-41,4	1145	83,3	94,1	64,1	Bottom terminal
PCTO.170.750.1250	Fix rod	1250	59,6	64,8	19,8	43,7	89,3	4,00E-03	1617	25,7	-33,9	562	89,3	92,1	62,1	Bottom terminal
PNO.420.1425.2000HL	Bottom connection	2000	69,778	88,96	17	63	71,2	4,02E-03	7170	94,7	27,4	3852	94,7	104,3	74,3	Internal conductor at flange height
PNO.550.3000	Bottom connection	3000	26,48	31,86	24,4	51,5	84,8	3,83E-03	7093	88,7	12	5364	88,7	94,3	64,3	Internal conductor at flange height
PNO.550.1675.5000	Bottom connection	5000	24,114	30,226	25,2	72,4	88,3	3,93E-03	7133	95,5	12,89	4578	95,5	97,2	67,2	Internal conductor, above at flange height
PNO 800.2550.2500	Bottom connection	2500	51,503	61,681	19,9	47,6	81,3	3,97E-03	9020	81,3	-1,29	8557	81,3	88,3	58,3	Bottom terminal
PNO - 1100kV - 3150A	Bottom connection	2500	71,708	79,078	23,95	55,9	86,8	3,91E-03	13200	37,8	-29,75	4989	86,8	92,2	62,2	Bottom terminal
PNO - 1100kV - 3150A	Bottom connection	2900	71,708	79,963	23,95	61,8	87,2	3,91E-03	13200	41,6	-30,35	5275	87,2	93,3	63,3	Bottom terminal
PNO - 1100kV - 3150A	Bottom connection	3150	71,708	80,691	23,95	65,4	88,2	3,91E-03	13200	44,6	-30,14	5349	88,2	94,3	64,3	Bottom terminal
PNO - 1100kV - 3150A	Bottom connection	4000	71,708	81,97	23,95	78,6	87,8	3,91E-03	13200	49,1	-33,78	6135	87,8	92,8	62,8	Bottom terminal
PNO.1100.2400.2500	Bottom connection	1500	74,293	80,122	27,7	41,7	85,7	3,85E-03	13200	35,3	-17,83	3485	85,7	86,9	56,9	Bottom terminal
PNO.1100.2400.2500	Bottom connection	2000	74,293	82,365	27,7	53,2	89,8	3,85E-03	13200	44,5	-19,89	4016	89,8	88,2	58,2	Bottom terminal
PNO.1100.2400.2500	Bottom connection	2500	74,293	86,376	27,7	53,4	88,2	3,85E-03	13200	11	57,21	5619	11	12,2	-17,8	In the conductor, at 2/3 of total height

Table 3.4 - Bushing with Non-Removable Conductor, Hot Spot by IEC Formula

BUSHING		I TEST	MEASURES WITH THERMOCOUPLES						TEMPERATURE RISE			
Name	Type of buhing	I test[A]	Ta [°C]	Toil [°C]	Ttop [°C]	Tbottom [°C]	Tmax [°C]	Tmax at 30 °C [°C]	ΔToil [K]	ΔTtop [K]	ΔTbottom [K]	ΔTmax [K]
PNO 170.1425.2500	Fix rod	2000	19,2	81,4	60,9	83,3	83,3	94,1	62,2	41,7	64,1	74,9
PCTO.170.750.1250	Fix rod	1250	27,2	86,5	43,7	89,3	89,3	92,1	59,3	16,5	62,1	62,1
PNO.420.1425.2000HL	Bottom connection	2000	20,4	79,9	63	71,2	71,2	80,8	59,5	42,6	50,8	50,8
PNO.550.3000	Bottom connection	3000	24,4	84	51,5	84,8	84,8	90,4	59,6	27,1	60,4	60,4
PNO.550.1675.5000	Bottom connection	5000	28,3	89	72,4	88,3	88,3	90	60,7	44,1	60	60
PNO 800.2550.2500	Bottom connection	2500	23	81,1	47,6	81,3	81,3	88,3	58,1	24,6	58,3	58,3
PNO - 1100kV - 3150A	Bottom connection	2500	24,6	85	55,9	86,8	86,8	92,2	60,4	31,3	62,2	67,6
PNO - 1100kV - 3150A	Bottom connection	2900	23,9	85,4	61,8	87,2	87,2	93,3	61,5	37,9	63,3	69,4
PNO - 1100kV - 3150A	Bottom connection	3150	23,9	85,8	65,4	88,2	88,2	94,3	61,9	41,5	64,3	70,4
PNO - 1100kV - 3150A	Bottom connection	4000	25	86,3	76,6	87,8	87,8	92,8	61,3	51,6	62,8	67,8
PNO.1100.2400.2500	Bottom connection	1500	28,8	86	41,7	85,1	85,1	86,3	57,2	12,9	56,3	57,5
PNO.1100.2400.2500	Bottom connection	2000	31,6	90,2	53,2	89,8	89,8	88,2	58,6	21,6	58,2	56,6
PNO.1100.2400.2500	Bottom connection	2500	28,8	88,4	53,4	88,2	88,2	89,4	59,6	24,6	59,4	60,6

Table 3.5 - Bushing with Non-Removable Conductor, Hot Spot by Thermocouples and Temperature Rise

3.7 Analysis of the Results: Bushing with Non-Removable Conductor

The meaning parameters to notice, for what concerns the principal objective of this analysis, are those that highlights that the Standard IEC Formula has began to show some limits of applicability, and that some results obtained with the usage of this method can be very odd and inaccurate.

The first strange thing that can be notice observing the tables, is how frequently the response of the Standard IEC method gives a negative value of the parameter "M", individuating in this way for many times the maximum temperature as the one placed at the bottom connection of the bushing.

The high recurrence of this result is strange, because even if it is true that we could expected the final highest temperature placed in the lower zone on the bushing (for the reasons already explained in the paragraph 3.5), the hot spot should be localized more frequently in the zone around the flange (due the presence of the heat flow coming from the current carrying conductor plus the one oil tank bottom) than to the bottom terminal connection.

Furthermore, this should be true especially for the bushings with the higher rated voltages, whose have bigger dimensions (they are tallest respect the ones with the lower voltages, with even various meter of difference) but also grater heat flows from the bottom to the top of the bushing.

The second and most important sign of that the Standard IEC method does not give always correct results, even if it is properly applied, are some final maximum temperatures that simply have not physical sense. For example, it is the case of PNO.1100.2400.2500, where the formula gives a final maximum temperature value equal to 12.2 °C. It is evident that such a value has no sense to exist in the reality.

This is the only clearly case that I have found among the recent years of temperature rise test reports, but this because when a strange result as the previous happens, the engineers of Alstom Grid - Passoni&Villa have decided to take as final hottest spot, previously agreement with the customer, the highest value measured by thermocouples (usually the temperature of the bottom connection), enclosing when is possible the thermal simulation of the bushing.

3.7.1 Execution of the PHI.820.2100.4500 Temperature Rise Test

Thankfully to the particular characteristics of this type of bushing, a special temperature rise test was realized in the Alstom Grid - Passoni&Villa factory. In fact, this bushing belongs at the PHI family (Passante HVDC Ibrido): it is a hybrid type where the insulation inside the bushing is formed by two distinct parts, each one made with a different insulating material.

In the bushing upper part the insulating medium is the SF_6 gas, while in the bottom part the insulating medium is oil-impregnated paper wound around the conductor. Therefore, the first zone is called the "GAS side" and the second one is called the "OIP side". The two parts made by different insulating materials could be threaten like two stand-alone bushing.

Into the GAS side was realized a direct measure of temperature, since is possible placing the thermocouples inside the bushing and along the conductor, while for the OIP side this is not possible and must be applied the indirect method given by the Standard IEC. In this way is evaluated the thermal behaviour in the two parts of the bushing, and confronting the two maximum temperatures obtained is defined the maximum one for the total body.

It is important to specify that the PHI is a very particular type: it is not possible obtain good results by applying the Standard IEC indirect method on the GAS side, due its strong fluid-dynamic phenomena. Therefore, the two different measure are necessaries to define the temperature evaluation on all the bushing.

The test has been repeated with four different feeding currents, in order to better understand the thermal behaviour.

In the Figure 3.1 is shown the disposition of the thermocouples on the bushing during the temperature rise test execution. In this schematic drawing:

- The blue tube represents the conductor body;
- The azure part represents the GAS side;
- The green part represents the OIP side

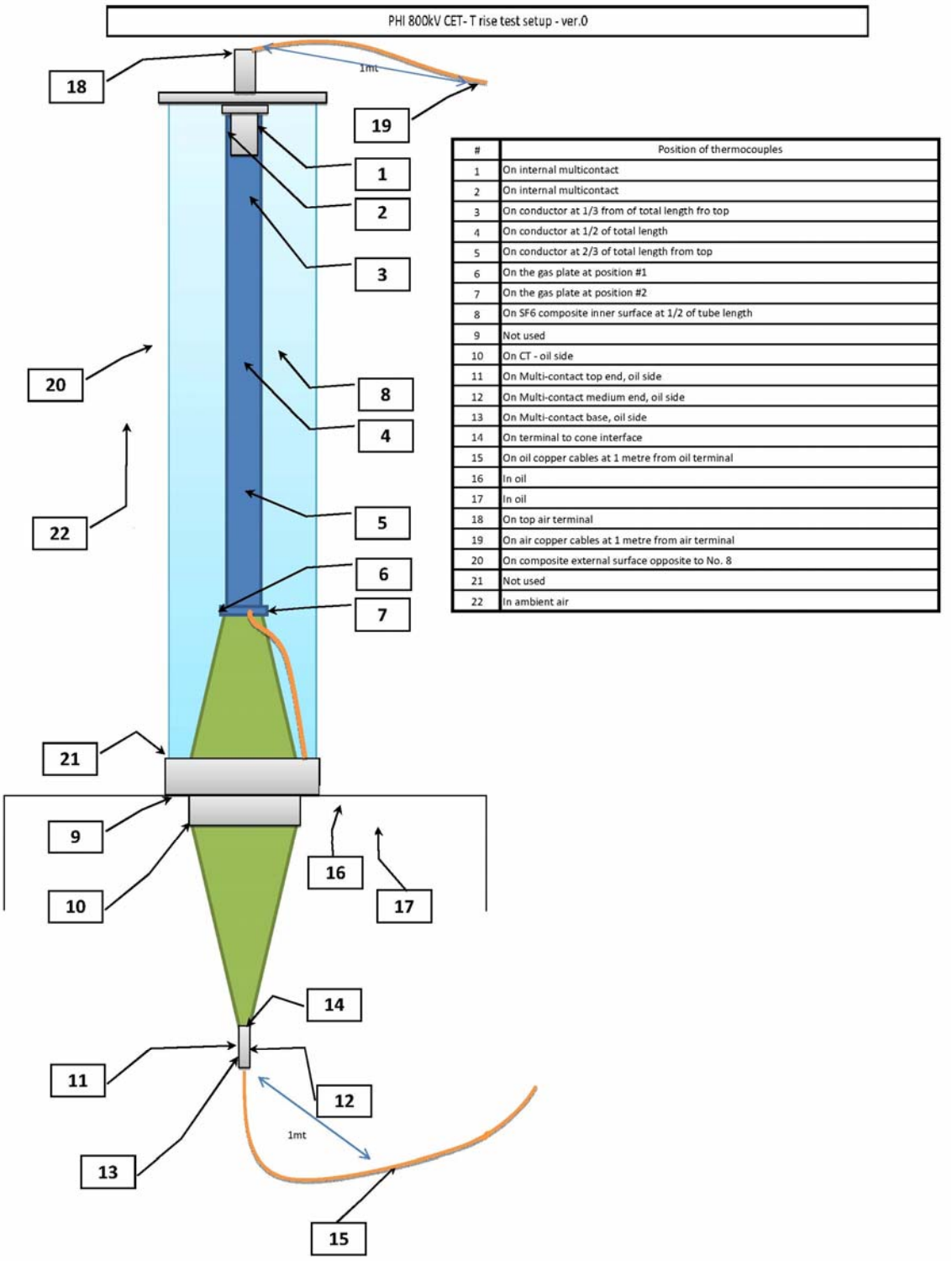

#	Position of thermocouples
1	On internal multicontact
2	On internal multicontact
3	On conductor at 1/3 from of total length fro top
4	On conductor at 1/2 of total length
5	On conductor at 2/3 of total length from top
6	On the gas plate at position #1
7	On the gas plate at position #2
8	On SF6 composite inner surface at 1/2 of tube length
9	Not used
10	On CT - oil side
11	On Multi-contact top end, oil side
12	On Multi-contact medium end, oil side
13	On Multi-contact base, oil side
14	On terminal to cone interface
15	On oil copper cables at 1 metre from oil terminal
16	In oil
17	In oil
18	On top air terminal
19	On air copper cables at 1 metre from air terminal
20	On composite external surface opposite to No. 8
21	Not used
22	In ambient air

Figure 3.1 - Thermocouples Positioning on the PHI 820.2100.4500

MEASURES WITH THERMOCOUPLES																						
I test[A]	T1 [°C]	T2 [°C]	T3 [°C]	T4 [°C]	T5 [°C]	T6 [°C]	T7 [°C]	T8 [°C]	T9 [°C]	T10 [°C]	T11 [°C]	T12 [°C]	T13 [°C]	T14 [°C]	T15 [°C]	T16 [°C]	T17 [°C]	T18 [°C]	T19 [°C]	T20 [°C]	T21 [°C]	T22 [°C]
2500	49,7	53,1	55,2	55,1	56,4	65,4	68,9	53,8	83,3	87,3	90	90,1	90,1	90,4	90,1	89,8	89,6	46,8	45,2	40,1	79,7	34,1
3500	57,7	62,9	63,3	62,3	63,3	71,4	75,1	57,3	85,1	88,9	92,1	92,1	92,3	92,1	91,4	90,4	90,6	53,9	57,7	40,1	80,9	33,2
4500	65,3	72,8	70,4	68,2	69,4	76,4	81,9	62,2	86,8	90,8	95	95,2	95,2	95,4	93,5	92,1	92,3	60,9	63,4	40,5	83	30,5
5000	73,4	83,4	80,4	77,1	78,1	84,5	88,4	68,2	87,8	91,3	95,8	96	96	96,2	93,2	91,8	91,8	69,3	82,5	44,2	84	35

Table 3.6 - Thermocouples Measurements during the Temperature Rise Test on PHI.820.2100.4500

BUSHING DETAILS		I TEST	IEC FORMULA METHOD												
Name	Bushing side	I test[A]	Ra [μΩ]	Rc[μΩ]	θa [°C]	θ1 [°C]	θ2 [°C]	α [1/°C]	L [mm]	θm [°C]	M	Lm [mm]	θm [°C] by IEC	Δθ= θm - θa [K]	HOT SPOT POSITION
PHI.820DC.2100.4500	GAS side	2500	38,38	41,297	32	46,8	68,9	3,79E-03	5295	45,7	-5,16	962	68,9	36,9	Bottom terminal of the GAS side
PHI.820DC.2100.4500	OIP side	2500	33,418	39,081	32	68,9	90,1	3,79E-03	6500	68,6	2,65	712	68,6	36,6	Under the OIP side top terminal
PHI.820DC.2100.4500	Total bushing	2500	71,797	80,399	32	46,8	90,1	3,79E-03	11795	45	8,978	1958	45	13	About 2 m under the top terminal
PHI.820DC.2100.4500	GAS side	3500	38,38	39,554	32	53,9	75,1	3,79E-03	5295	53,2	-3,81	786	75,1	43,1	Bottom terminal of the GAS side
PHI.820DC.2100.4500	OIP side	3500	33,418	42,374	32	75,1	92,2	3,79E-03	6500	75,1	-0,92	330	92,2	60,2	Bottom terminal of the OIPside
PHI.820DC.2100.4500	Total bushing	3500	71,797	81,943	32	53,9	92,2	3,79E-03	11795	51,1	10,7	2438	51,1	19,1	About 2,5 m under the top terminal
PHI.820DC.2100.4500	GAS side	4500	38,38	40,056	32	60,9	81,3	3,79E-03	5295	59,8	4,97	992	59,8	27,8	Bottom terminal of the GAS side
PHI.820DC.2100.4500	OIP side	4500	33,418	43,755	32	81,3	95,4	3,79E-03	6500	80,4	-3,75	1297	95,4	63,4	Bottom terminal of the OIPside
PHI.820DC.2100.4500	Total bushing	4500	71,797	83,814	32	60,9	95,4	3,79E-03	11795	50	22,3	3883	50	18	About 4 m under the top terminal
PHI.820DC.2100.4500	GAS side	5000	38,38	45,546	32	69,3	88,4	3,79E-03	5295	88,7	-2,52	4684	88,4	56,4	Bottom terminal of the GAS side
PHI.820DC.2100.4500	OIP side	5000	33,418	40,396	32	88,4	96,2	3,79E-03	6500	84,1	-7,26	2433	96,2	64,2	Bottom terminal of the OIPside
PHI.820DC.2100.4500	Total bushing	5000	71,797	85,309	32	69,3	96,2	3,79E-03	11795	52,9	26,66	45494	52,9	20,9	About4,5 m under the top terminal

Table 3.7 - Temperature Rise Test on PHI.820.2100.4500 Results by IEC Method

3.7.2 Analysis of the PHI.820.2100.4500 Temperature Rise Test Results

In Table 3.6 are reported all the thermocouples measurements realized after the steady state condition has been reached, for each value of the test current; in the Table 3.7 are reported the hottest spot given by the application of the IEC Method and its parameters (just as seen in the previous Table 3.4). At every test current are collected the data for: the GAS side only, the OIP side only and the bushing in its whole form.

As yet mentioned, for both the GAS side and the total bushing body the indirect method is not applicable. However, it has been used even on these zones to can having an evaluation not for the temperatures (it can be seen in the table how their values are very odd) but for the accuracy of the indirect method to calculate the cold resistance Ra (paragraph 2.9.2) and the shutdown resistance Rc (paragraph 2.9.3) of the conductor.

In fact, if the measurement processes are right the summation of the partial resistances of the GAS side and OIP side must be equal to the one of the total bushing. Observing the Table 3.7, it can be seen how this proportion is always respect.

in Figure 3.2 is make a graphic representation of the thermal behaviour in the GAS side using the lectures of the temperatures, starting from the one placed at the top terminal (thermocouple "T18") down to the last one on the GAS side bottom terminal (thermocouple "T7").

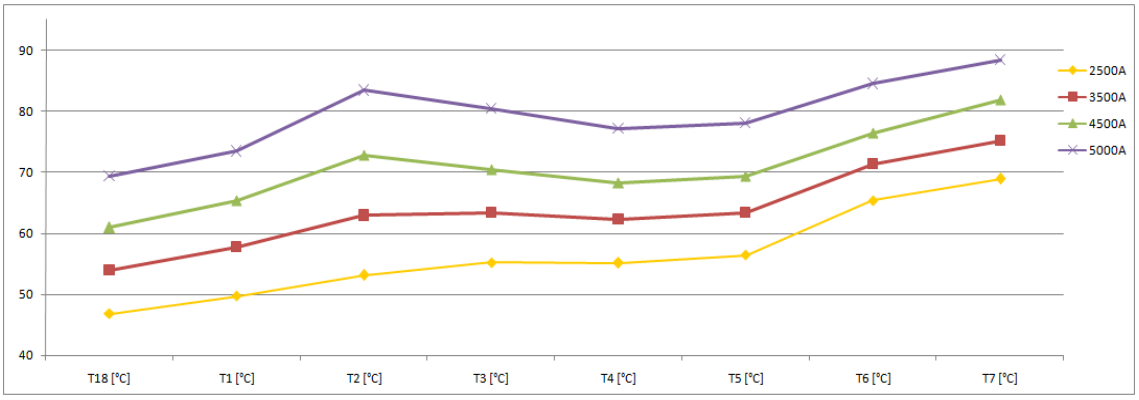

Figure 3.2 - Thermocouples Values on the Bushing GAS Side

This map of temperatures shows a reasonable behaviour: the ones in the same zones increases proportionally with the value of the feeding current and the colder parts are those near at the top connection of the bushing. It can be seen how the hottest spot measured for each case of the four different current values is always placed on the GAS side bottom terminal.

In Figure 3.3 are reported the hottest spot founded in the OIP side and in the GAS side.

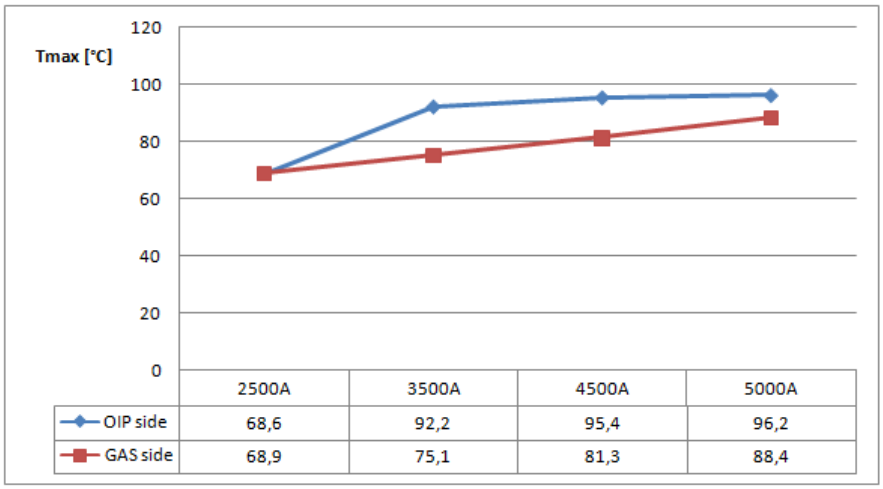

	2500A	3500A	4500A	5000A
OIP side	68,6	92,2	95,4	96,2
GAS side	68,9	75,1	81,3	88,4

Figure 3.3 - Maximum Temperatures Calculated for OIP side and GAS side

The final maximum temperature is given by a comparison of the two sides and it correspond for every case with the one given by tithe OIP side. But the first value is too low to be effectively real: the maximum temperature recorded by thermocouples in this case is equal to 90.1 °C (at the bottom connection), about 22 degrees higher than the maximum given by IEC method. It is even strange for the others cases that the hot spot is always found on the bushing bottom connection.

In conclusion, with this test it has been verified the correctness of the chosen method used in Alstom Grid-Passoni&Villa factory to measure the resistance value of the conductor, and is shown how the indirect measurement method given by the IEC is not reliable at all, especially when the parameter M results positive and then must be taken as hottest spot the one given by the Equation 2.1.

3.8 Critical points of the International Standards IEC 60137 and IEC 62199

After having seen all these inconsistencies between the expected results and the obtained ones, the next step is wondering about the reason that are behind of the discrepancies given by the application of the Standard IEC indications.

To better understand the IEC Formula itself is necessary to know where it comes from, which hypothesis there are at the base of the method, which calculation process was follow to reach the final form inserted in the Standard IEC. With this information, should be easier identifier the critical points that afflict IEC formula and under which limits it is valid.

All the complete informations can be found in the technical paper "36(s)21" of the International Electrotechnical Commission. For what concerns ours interests, here below are reported the fundamentals things taken from the document.

The principal hypothesis at the base of the model, which was proposed by Japanese National Committee to the IEC in January 1991, are two:

- Heat generation per unit length along the bushing conductor is almost constant at every part of it, due the temperature coefficient of electrical resistivity of the conductor is small (it is usually made of copper or aluminium);
- Heat conducts only axially along the conductor, due the radial heat diffusion through the surrounding insulation is neglected because heat conductivity of any insulating material is much smaller than that of the metal-made conductor.

The starting formulas at the base of the demonstration consider that the amount of heat flow Q on the abscissa x along the conductor is proportional to the distance from the hottest point (as shown in Figure 3.4 and described in Equation 3.1) and that the temperature distribution ϑ respect to x is obtainable by the differential equation shown in Equation 3.2.

$$Q := r \cdot I^2 \cdot (Lm - x)$$

Equation 3.1 - Heat Flow Q in Function of the Distance From the Hottest Point

Where:

- Lm= distance between cooler and of conductor t point of highest temperature;
- r= resistance per unit length;
- I= current.

Moreover:

$$Q := C \cdot S \cdot \frac{d\theta}{dx}$$

Equation 3.2 - Heat Flow Q in Function of the Temperature Distribution

Where:

- C= heat conductivity of conductor;
- S= sectional area of conductor.

These previous informations enable us to make some considerations.

While considering as constant the heat generation per unit length along the conductor is an acceptable hypothesis, it is instead too unrealistic assuming that the heat flow passes through the bushing only in the axial direction and for nothing through the radial's one.

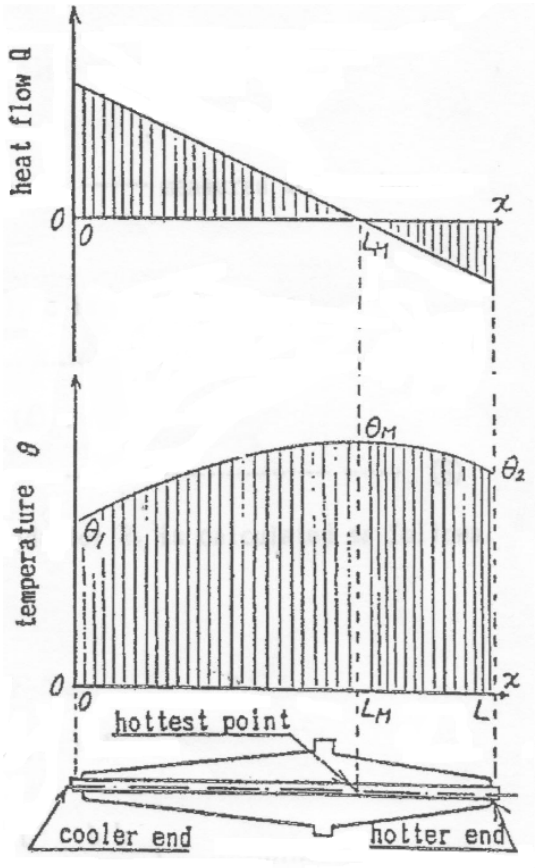

Figure 3.4 - Heat Flow and Temperature Distribution

This can be considered an acceptable hypothesis only for bushings with small dimensions, where the radial dissipation is very low and can be neglected. This is understandable, since the method was proposed at the IEC about twenty years ago, when the majority of the bushings have small constructive dimension respect nowadays. In the last years the bushings rated voltages have increased in a considerable way, and, as a consequence, even the dimensions have followed this trend too.

Another critical point comes to the fact that this formula was designed in a time where the majority of the insulation material was the impregnated paper, so it has been developed taken as model the behaviour of a solid material. But nowadays the bushings can be easily filled with gas (for example, SF_6 or hydrogen) or liquid (for example, the mineral oil), with these types

must be introduced some new parameters to take into account, for example, the convective motion of these fluid and their corresponding heat transfer coefficients.

This last weak point does not regards only the formula used to calculate the hottest spot, but can be extended to all the Standards IEC 60137 and IEC 62199 in a more general speech. In fact, the Standards impose the same test requirements and arrangements, besides the same limits too, to all the bushings with a rated voltage above 1000 V. However, this is a category highly heterogeneous.

There are a lot of possible bushing types: insulated with solid or gaseous material, filled with liquid or under vacuum, designed with an oil circulation systems or without them, with dimensions that range from a height in the order of several tens of centimeters to twenty meters even. It is hard to believe that all which is content in the Standards IEC can be applied without differences at all the range of the bushing types that have rated voltage above 1000 V.

An evident example of this fact is the situation shown before, in the paragraph 3.5, where is reported the case of the discrepancy in the reaching of the thermal stability between the Standard indication and the real measure, with a result of several hours and some degrees of difference.

This is logical, a body with higher dimensions respect another one similar have for sure a greater thermal inertia respect this last one, and therefore the deserved time of the first body to reaching the steady state is for sure higher if compared to the time necessary at the second body.

All these reasons, with some more of the others, contribute to make the method given by International Standards IEC 60137 and IEC 62199 pretty unreliable for the estimation of the temperature rise for certain types of bushing as, for example, the ones with great dimensions or the ones with inner fluids that have not negligible convective motions.

4 ALTERNATIVE WAYS TO ESTIMATE THE BUSHING THERMAL BEHAVIOR

4.1 Introduction

After having understood the several difficulties to make a good temperature rise test and to reach through it an accurate value of the temperature rise profile the bushing, the following paragraphs will be focused on some alternative methods to can obtain the bushing thermal behaviour. The principal and most important one is for sure the use of the FEA (Finite Element Analysis) with a calculating system, in order to create a thermal simulation of the bushing. Thankfully to the performances achieved by the modern computers is possible obtain a temperature map on the body of the bushing with a good accuracy, respect the real behaviour.

4.2 How Design the Mechanical Model

The first step to make a correct thermal simulation is for sure can be able to create a very good mechanical model of the bushing body.

This is not a simple passage: to making a good model is necessary understand whose details are important for the thermal simulation and instead whose are negligible.

This first problem setting is fundamental to can eliminate a lot of unnecessary objects to reach the final temperature evaluation, because if the model is designed with too many details then the simulation process may be too heavy for the computer. In the worst scenario, the overload could make impossible obtaining the simulation final result.

To realize the bushing mechanical model is necessary using a software that permits the operations of both creation and modification in the simplest way. In Alstom Grid-Passoni&Villa the chosen program is a 3D-CAD (*Computer Aided Design*) called "*Pro-Engineer*", which has the very useful option, among the others, to can be directly interfaced with the FEA software used for the thermo-magnetic simulation.

An example of how looks a mechanical model of a bushing (in this case the analyzed one is a PNO.550.1675.3000) specifically created for a thermal analysis is reported in Figure 4.1.

The last thing to create around the model is the component called Air Box, which represents the bushing surrounded environmental, on which are applied some of the imposed boundary conditions. It must be make with the right dimensions, if it results too small the final result may be heavily altered by the boundaries influence. Typically, the Air Box is a cylinder with a diameter about ten or even twenty times of the one of the conductor, with air as assigned material.

Such as immediately evident observing the Figure 4.1, the components that presents more changes after the simplify process are the porcelain envelopes representations, both for the oil side one and the air side one. They are designed as pure cylinders, without the sheds present in the real object. The fact that their presence or absence do not influence in significant way the final temperature rise has been confirmed by some simulation performed by the Alstom Grid - Passoni&Villa engineers, moreover their presence would include several complications (e.g. the simulation could not be threaten as static but as dynamic one, which requires more difficult settings and heavy power calculation) .

Another evident simplification can be found on the flange, where was suppressed all the holes there placed (their duty is containing the screws that allow the installation of the bushing on the transformer tank).

Figure 4.1 - Mechanical Bushing Model in Order to Realize a Thermal Simulation

The flange is another of the most modified components, all its own particular construction shapes are replaced with more simply shapes, to obtain a piece that has the (fundamental) axisymmetric geometry.

4.2.1 Simplifying the Model

Speaking in general, it is a good and recommended simplification the suppression of all the follows parts of the mechanical model:

- The holes;
- The O-ring spaces;

- The grooves;
- The bolts;
- The screws;
- The porcelain's sheds;
- The springs.

All these part are unnecessary for the thermal point of view, and they must be deleted. They are all very small objects, with dimensions in the order of a few millimetres, and when the finite element analysis program will go to analyzing the model, the necessary calculation power to make polygon mesh in these small parts could be too high for the system.

For the same reason, fittings and arches must be replaced with right angles, since the curved portions are the ones that require a highly refined mesh.

This step represents one of the major difficulties during the realization of the thermal simulation: a bushing has not many different components to represent, they are about twenty at the maximum, but those have usually have an high difference of dimensions. Some parts are smaller than others even of one or two order of magnitude, and this could regards even different zones of the same components (e.g. the endings of the wounded OIP are very thinly respect the OIP in the centre of the bushing). It is not easy create a mesh that permits an accurate analysis on these small parts and at the same time does not make too heavy the calculation.

The problem is not negligible, it is simply impossible to make a simulation with a too heavy model, even modern computers have well-defined limitations that can not be exceeded.

The components that have the higher influence on the result of the thermal simulation must be created with the smallest possible number of simplifications. This means a representation for all the current carrying components (therefore, the conductor materials) as closer as possible to the reality, while the insulating materials can be heavily simplified with only few consequences.

However, even well adopting all the previous simplifications, it is pretty hard for the thermo-magnetic software been able to work using a satisfying refined polygonal mesh on such a 3D

model. The solution adopted is the following one: instead of the complete model, for the analysis is taken only a piece of the total body. For example, a typical case is having a section with amplitude of 3.6 degrees, which is an hundredth of the total model.

This last simplification works great, lightens a lot the mole of calculations request at the computer and does not modify at all the accuracy of the final thermal behaviour evaluation. The conditions to satisfy to can apply it are two: the respect of the proportions even for the input values (in an section of an hundredth of the total, the feeding current inserted must be an hundredth of the rated one too, then the 3000 A of the example in Figure 4.1 become 30 A), and the bushing must have axisymmetric geometry.

Fortunately, this last is a propriety that naturally belongs at almost all components that formed the bushings, since their models are given principally by cylindrical components. The only pieces that are often with a rectangular shape (and then are not axisymmetric) are the two terminals, but in these cases to resolve the problem is enough creating instead of them two cylinders equivalents by the electrical point of view (which means that they maintain the same specific losses of the rectangular terminals).

4.3 Thermomagnetic Simulation on a Bushing

To realize a finite elements analysis in Alstom Grid-Passoni&Villa are used the coupled software *MagNet* and *ThermNet* for what concerns the thermo-magnetic simulations under steady state conditions, and the software *Fluent* for what concerns the thermal simulations under fluid-dynamic conditions.

In this thesis, the types of bushing on which is the focus can be analyzed in a good way even with just the first two programs, therefore the fluid-dynamic state analysis and the software *Fluent* are only mentioned.

This last one is a program that was commercialized just quite recently, due the high performances request to working, and is for sure not user-friendly: requires a lot of time to learn the right way to use it. The engineers of the R&D section have spent months of work to individuate the better parameters settings to obtain a configuration finalized for the bushings analysis.

4.3.1 Magnetic Simulation Settings

The simulation is divided in two phases: as first is realize a magnetic simulation with *MagNet* and only in a second time is make the thermal one with *ThermNet*. The objective of the first analysis is evaluating the bushing losses due to the current flow, before use them as sources of heat in the second simulation.

Once the mechanical model is created, is necessary import it in *MagNet*. Thankfully to the facility of communication between *MagNet* and *Pre-Engineer* this action is both very easy and fast to carry out.

Afterwards, it is the assignation at each component of the bushing model the right corresponding material. This is one of the most hard point of the simulation, because beyond the standard materials given by the software is necessary build a user-defined database where are inserted both the physical and mechanical characteristics of all the particular types of material used in the bushing realization.

The research of these data is made on various references (as contacting the supplier of the material, or search in the books), it can take a long time and sometimes can be even inconclusive (in these case are used parameters of similar materials).

An example of bushing in *MagNet* with a complete material assignation is reported here below in Figure 4.2.

It is necessary refine the solving polygonal mesh on every singular bushing component. To do not load too much the calculation, is a good thing realize a highly refine mesh only where is more interesting evaluating the magnetic field (e.g. on the conductor and on the terminals) while leaving a low refine one on the parts less interesting (e.g. on the air box). A typical solving mesh distributed on the model is reported in Figure 4.3.

The input parameter for this type of analysis is given by the rated current that feeds the bushing, proportionally at the mechanical model section taken (as explained in the paragraph 4.2.1).

The last thing to do before launching the simulation is the definition of the boundary conditions.

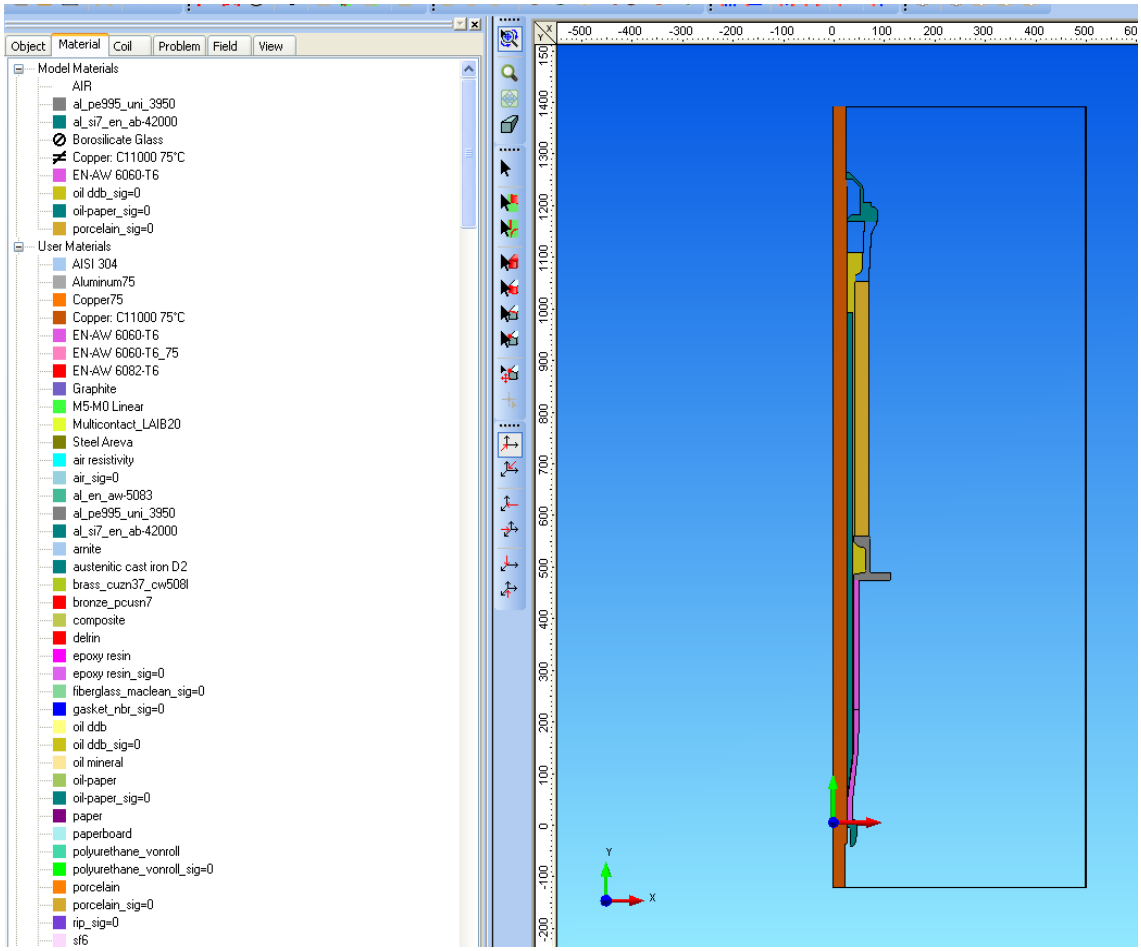

Figure 4.2 - Section of the Bushing Model Imported in MagNet, with all Material Assigned

For our case is necessary enforce the magnetic field as direct normal respect the two faces of the Air Box that cut the model's section vertically.

This is an imposition in order to can respect the Gauss's law of magnetism, also known as one of the Maxwell's equations, which states that the magnetic field has divergence equal to zero.

After having launched the solving process, the software can calculates a lot of bushing parameters like, for examples, the current density or the magnetic field distribution, and the one that interest us: the values of the losses due to the passage of the current flow through the bushing.

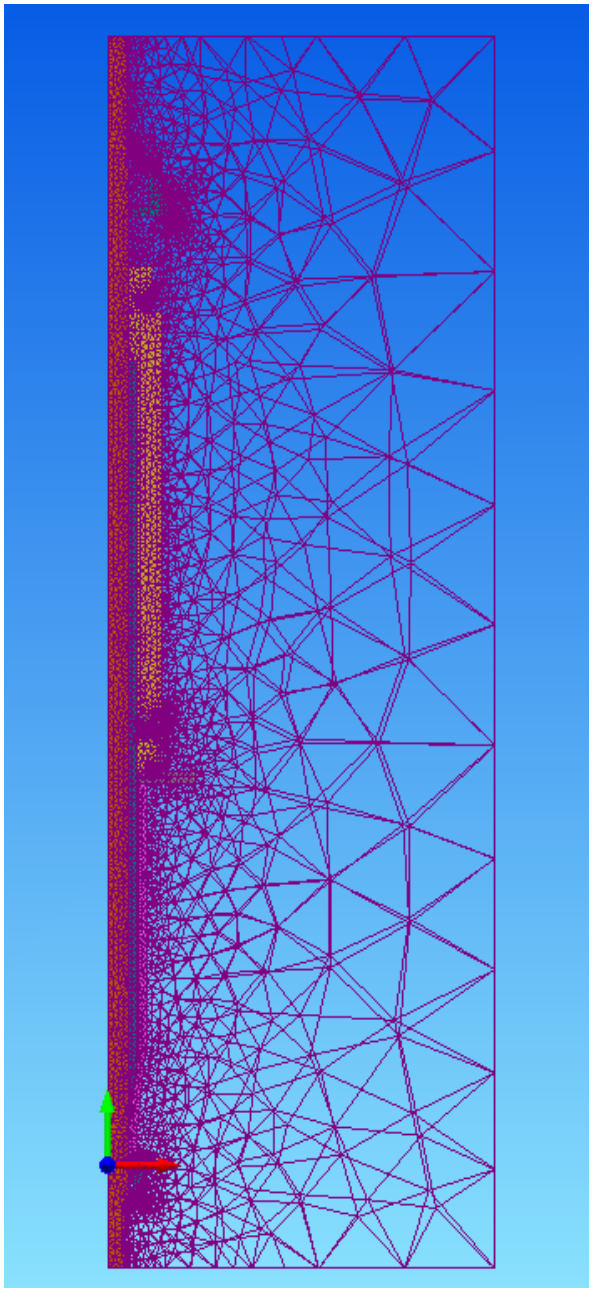

Figure 4.3 - Solving Mesh Distribution

4.3.2 Thermal Simulation Settings

The model must be now imported from *MagNet* to *ThermNet*, in order to define the thermal behaviour. The two software have been designed by their producer (they are both properties of Infolytica Corporation) to can work easily together, then the importing process is realized as an immediate operation. All the previous material assignation and mesh definition made

during the magnetic simulation settings, and even its obtained results, are maintained during the importing process, all these operations must not be done again.

The only settings to set up before launching the solving calculation are two: the suppression of the component Air Box (which is not a necessary component now) and, most important, the assignation of the specific boundary conditions for the thermal simulation.

The boundaries imposed must define, for the first, the environmental temperatures around the bushing zones. These values inserted that are chosen taking into account the indications of the Standard IEC 60137. Afterwards, the boundaries must define the heat transfer coefficient "*h*" of the mediums that surround the bushing, which depends both to the external surface dimension and (in a stronger way) to the physical properties of the surrounding material.

This coefficient is a fundamental parameter to can calculate the heat transfer between a fluid and a solid; it represents the proportionality between the heat flux and the thermodynamic driving force that causes it (for example, the difference of temperature). The coefficient is given by the follow formula:

$$h := \frac{Q}{A \cdot \Delta T} \quad \left[\frac{W}{m^2 \cdot {}^\circ C} \right]$$

Equation 4.1 - Heat Transfer Coefficient Definition

Where:

- Q= is the heat flow, in [W];
- h= is the heat transfer coefficient, in [W/(m^2·K)] or [W/(m^2·°C)];
- A= is the heat transfer surface area, in [m^2];
- ΔT= is the temperature gap between the solid surface and the surrounding fluid, in [K] or [°C].

It is very difficult estimate with high precision the heat transfer coefficient, for the simulations in Alstom Grid-Passoni&Villa it has been chosen to take the typical values reported in Table 4.1.

They have been derived by specific heat transfer literature and even confirmed through a comparison with the measures realized by thermocouples and thermoscan. All of them have been selected with the objective to maintain the thermal simulation under the most conservative conditions as possible.

Surface Position and Surrounding Medium	Environmental Temperature [°C]	Heat Transfer Coefficient [W/m^2C]
Vertical surface in air	30	8
Horizontal surface in air	30	4
Vertical surface in oil	90	80
Horizontal surface in oil	90	40
Vertical surface in H_2	60	100
Horizontal surface in H_2	60	50

Table 4.1 - Boundary Conditions for Thermal Simulation

It is now possible lunching the thermal simulation solving process. The best solution is using the "Coupled Solution" in the program options, whit that the software does not take just the previous calculate losses, but permits at *ThermNet* and *MagNet* to can work together in an iterative cycle to find the better temperature distribution:

1) The power losses are calculated with the magnetic simulation, where the physical characteristics that depending to the temperature (for example, the electrical resistivity of the materials) are calculated taking some references values;

2) The resulting losses are used in the thermal simulation to calculate the behaviour of the temperatures in every bushing component;
3) These temperature values are taken and inserted in the magnetic settings instead of the reference ones;
4) The first passage is done again, losses are recalculate, obtaining more accurate values;
5) The second passage is done again, etc.

Both the possibility to can use the coupled solution and define a good number of iterative cycles is strictly linked to the lightness of the model. If it requires a too heavy calculation, the computer performances could not be sufficient and becoming impossible the usage of this option to obtain a refine final solution.

In Figure 4.4 is shown the temperature distribution above all the bushing model obtained through a thermal simulation.

4.3.1 Critical Points of the Simulation Approach

How it has been already mentioned in previous paragraphs, there are several points that make not easy and not rapid the realization of a good thermo-magnetic simulation. It is necessary overcame several difficulties (which can easily became serious enough to do not permit the running of the simulation), having a certain level of knowledge, dealing with high costs and employing a not negligible amount of time.

The first important problem to overcome is achieve the level of knowledge necessaries to realize the simulation. This is not referred only at the physics behind the problem, but even the capacity to use the three different software.

Therefore, to can reach a good level of confidences with the used programs are mandatory two things. The first one is a training course to can learn some stuff as the meaning of the various commands, the available settings and the logical behind the software implementation. The second one is a high experience level, acquired only spending some time working with them.

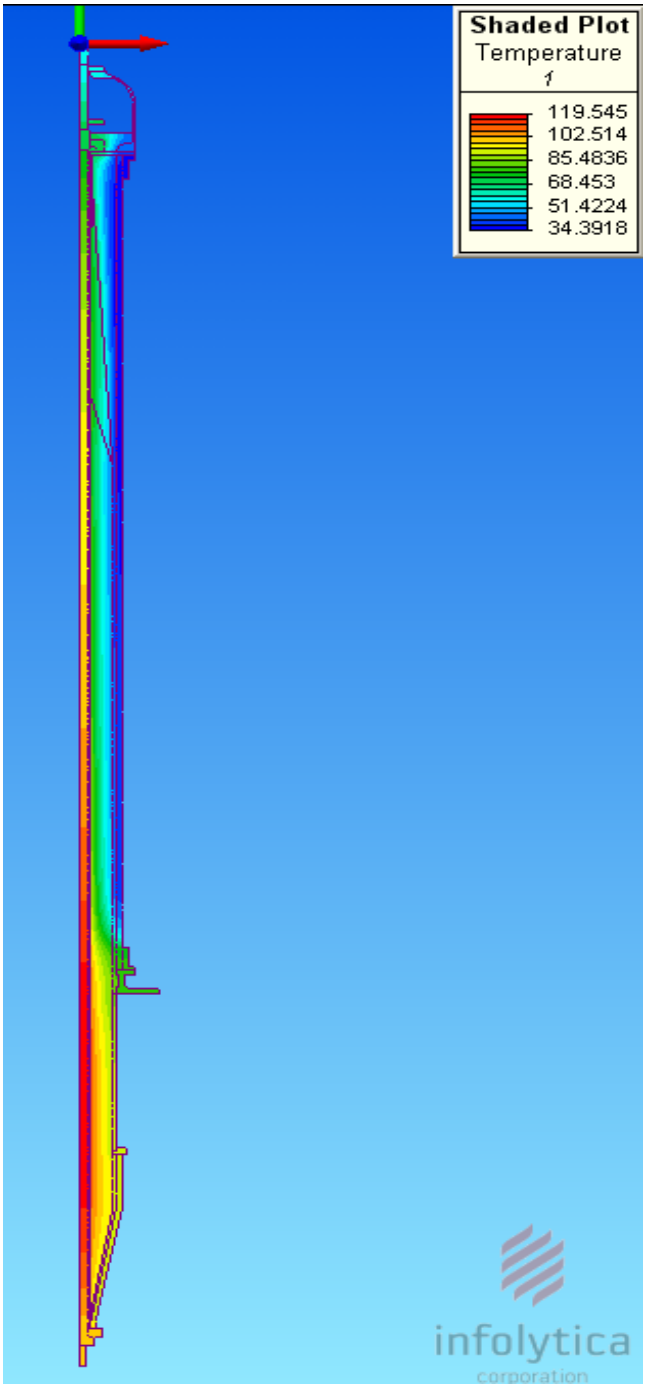

Figure 4.4 - Temperature Map on the Bushing

This mean that must be used a great quantity of both time and money only to can begin the simulation set up. To can give some references amount, the costs of software licenses, of the high performances computers and of the training courses are in the order of tens of thousands of euro.

Beyond the time spent to learn how can using the software, it must to be added the amount of ours that is required for making every simulation itself, because from the starting mechanical model creation until the achievement of final temperatures distribution are usually necessary several hours of work, or even days.

The second critical point of this approach is the complexity of the bushing model construction: it must be closer to the reality but at the same time it must be simplified as much as possible. This problem concerns both the mechanical model and the thermo-magnetic simulation settings (e.g. the refining of the mesh or finding the exactly physical parameters values of each material employed or the better boundary conditions definitions).

If the simplification process is too strong, the results find at the end of the simulation will not have any physical sense; but in the other hand if the simplification process is too light the simulation can not be accomplished because even the modern computers performances can not stand to such a quantity of calculation. Moreover, when these two situations happen is usually hard recognize the mistake before the simulation process enters in its last part (or even at the end of it), with the result to wasted all the time spent working on the simulation.

4.4 Conclusion About Simulation Method

The utilization of the thermo-magnetic simulation approach to evaluate the thermal behaviour of a bushing is a solution that, if correctly carried out, gives a final result that represents a very good approximation of the reality, and permits to have a good idea of the heat flow in every component of the bushing. It is a resource very helpful, especially during the bushing designation process.

However, to be applied requires a large employment of resources in terms of time, work and knowledge.

4.5 Alternative Method to Estimate the Temperature Rise

In the months passed in Alstom Grid-Passoni&Villa working on this thesis, one of the my first approach to can find a method for evaluating the bushing thermal behaviour, was make some research about the alternatives solutions proposed by other engineers and researchers who have already tried to find an answer at this problem.

The technical reports found have been very few, unfortunately. Each one of them illustrates a different method and gives a final formula that permits to calculate the bushing maximum temperature rise profiles. Here below the principal concepts of these methods are reported in a rapid way.

4.5.1 IEEE Method

In the standard IEEE C57.19.100-1995, "*Guide for Application of Power Apparatus Bushings*", is given the follow formula to estimate the maximum temperature rise for bushings in steady state condition, with no appreciable dielectric losses and without cooling ducts:

$$\Delta\theta_{HS} := K_1 \cdot I^n + K_2 \cdot \Delta\theta_0$$

Equation 4.2 - IEEE Temperature Rise Profile Evaluation Formula

Where:

- $\Delta\theta_{HS}$= is the steady-state bushing hot spot rise over the ambient (°C);
- $\Delta\theta_o$= is the steady-state immersion oil rise over the ambient (transformer top oil rise) (°C);
- I= is per unit load current based on bushing rating;
- K_1= constants with a value that range from 15 to 32, obtained by test;
- K_2= constants with a value that range from 0.6 to 0.8 , obtained by test;
- n= constants with a value that range from 1.6 to 2.0 (with 1.8 as most common value) obtained by test;

4.5.2 Lapp Insulator Company Method

The method is contained in the technical paper "*An improved method for estimating temperature rise of a bushing loaded above nameplate rating*" written by Daxiong Zeng, an engineer that works in the bushing division of the Lapp Insulator Company, and the final formula that allows to calculate the temperature rise profile of the bushing is reported in Equation 4.3.

$$\Delta\Theta(I,z) := F_1(z)\cdot I^2 + F_2(z)\cdot\Delta\theta$$

Equation 4.3 - Lapp Insulator Temperature Rise Profile Evaluation Formula

Where:

- $\Delta\Theta(I,z)$= temperature rise profile at current I and at oil temperature rise $\Delta\theta$;
- z= axial coordinate along the bushing centreline;
- I= load current in per unit;
- $F1(z)= \Delta\Theta(1,z) - \Delta\Theta(0,z)$, incremental temperature rise profile generated by heat losses at one unit current;
- $\Delta\Theta(1,z)$= temperature rise profile at zero current, obtained by test;
- $\Delta\Theta(0,z)$= temperature rise profile at rated current of 1 p.u., obtained by test;
- $F2(z)= \Delta\Theta(0,z)/ \Delta\theta_0$ temperature rise profile generated by temperatures difference between the boundaries.
- $\Delta\theta_0$= rated oil temperature rise;
- $\Delta\theta$= actual oil temperature rise, obtained by test.

4.5.3 NGK Method

This method is illustrated in the "NGK Review - Overseas Edition" number 32, in the article "*Temperature rise characteristics on OIP bushings with circular fluid convection*", where are reported two possible formulas. The first is the one at the base of the development and is reported in Equation 4.4.

$$R := \delta \cdot \left(k \cdot j^2\right)^a \cdot D^b \cdot L^c + A_0$$

Equation 4.4 - Starting Formula of the NGK Method

Where:

- R= highest temperature rise of the bushing;
- k= skin effect factor of conductor;
- J=current density of conductor;
- D= outer diameter of conductor;
- L= total length of bushing;
- δ, a, b, c, A_0= unknown constants, obtainable by test on the bushing;

Starting from Equation 4.4 in this technical paper are made some passages to obtain a more simply applicable formula. The result is:

$$R := C\left(\frac{Q}{A_{ext}}\right)^a + Z_0$$

Equation 4.5 - NGK Temperature Rise Profile Evaluation Formula

Where:

- $Q= I^2 \cdot r \cdot k$, heat generated in the bushing by the current flow;
- I= load current;
- r= electrical resistance of conductor;
- Aext= Top surface area (top porcelain + metal torso);
- C, Z_0= unknown constants, obtainable by test on the bushing;
- a= unknown constant that takes into account the non linearity of the heat transfer system, less than 1 and obtainable by test the bushing.

4.6 Critical Points of the Alternative Methods

All those formulas and methods viewed in previous paragraphs are for sure correct under the theoretical point of view, but, at the end, they are also pretty useless for the practical scope of this thesis and even generally speaking, principally for two reasons.

As first one, in every formula more than one parameter (two or even three) are maintained unknown by the choice of the author (some research was commissioned by companies, it is logical that they do not want give the complete method obtained by their R&D department to the free disposition of their competitors), and deduce them in a system that present only one formula is impossible.

The second reason is that in all these methods there are some parameters that can be determined only forming some temperature test realized on the bushing. This means that the objective of these formulas is for sure estimating correctly the maximum temperature rise value for a bushing, but they need an already built bushing on which make test to obtain fundamental parameters. They are not thought to be employed during the design process of a bushing.

5 DEFINITION OF A BUSHING EQUIVALENT THERMAL CIRCUIT

5.1 Introduction

After having observed in the previous chapter the effective uselessness of the alternative analytic methods and the several difficulties to can make a good thermal simulation, it has been decided to try a different approach at the problem.

It has been chosen to create an equivalent thermal circuit of the bushing itself associated with a calculating program capable to resolve it, in a way as simply and rapid as possible.

In the following paragraphs is explained how has been developed the equivalent thermal circuit, which hypothesis and simplifications were taken to realize the starting bushing model and the theoretical notions at the base of the creation of both the equivalent model and the resolving program.

5.2 Bushing Model: Hypothesis and Simplifications

The final objective of the thesis is find a method which can give an estimation value of the maximum temperature rise on a bushing, but giving also an elevate importance at both easily and rapidity of usage.

It is important to specify that this method has been developed only for the family of the PNO bushings, where the insulation material is the oil-impregnated paper.

At the beginning of the study, the idea was create a method capable to adapts itself at the various bushing types, but the amount of time necessary to can reach good results with this solution would have been excessively high respect the duration of the stage. Therefore, it has been chosen to concentrate only about one family of bushings.

5.2.1 Bushing Model

The logical used to create the model of the bushing from which extrapolate the thermal circuit is very similar at the one used during the model realization of a thermo-magnetic simulation (as seen in Chapter 4). However, with this method is unnecessary the creation of a mechanical model with a drawing software.

The purpose is could considering as necessary to know only some easily defining parameters of the bushing geometry (radius and lengths) and which are the specify materials that compose it.

For sure the total amount of simplification realized to make this model are both heavier and more numerous respect the ones made during the simulation process, but the final target of this alternative method is find a good approximate value of the bushing hottest spot and do not calculate a very highly accurate one.

During the initial phases of the method definition, the important thing was understand if the development was proceeded in a right direction, so it has been chosen to give the priority at the simplicity of the model, letting the possibility to make later a refining process.

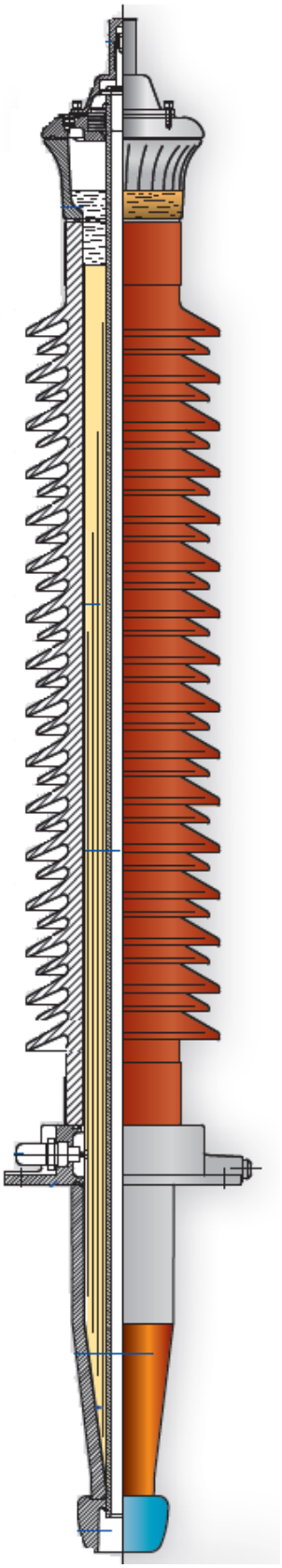

Figure 5.1 - Typical PNO Bushing

In Figure 5.1 is reported a drawing of a typical PNO bushing in a closer representation respect the real ones. Creating an equivalent thermal circuit starting from a bushing like this would be pretty hard, therefore to can reach our final model are realized the following simplifications:

- All the ones already described in the Chapter 4 are adopted also here: the porcelains sheds, the screws, the holes, the bolts, etc.;
- Sometimes under the flange is present an extension tube (usually made in aluminium) to allow the installation of a current transformer to make measurements. This tube does not be considerate and it must be replaced by the oil-side external porcelain. This decision make easier the calculation of the equivalent thermal resistances and the modify changes the model but in a conservative way (a thermal conductor is replace with an insulator);
- There is usually a very thin tube, metallic materials made like aluminium, on which is wound the oil-impregnated paper. Due its smaller dimension, its contribution to the thermal circuit is negligible and it can not be considerate;
- The head of the bushing: this component has very particular both shapes and materials (e.g. it could be made mostly in glass, because one of its utility is permits to checking the level of the oil). It would be very difficult create a good model of this component, then the decision is delete it and replacing with an extension of the porcelain (and the others inner materials). This is for sure a heavy simplification, but it is in a more conservative way and, mostly, is about a zone where do not worth having a

great accuracy, since the temperature hottest spot is placed with high probability at the central or lower part of the bushing, and not at the top one;

- The natural convective movements in the inner oil can be neglected, since has been demonstrated in past simulations that their effects on these bushings thermal behaviour are negligible;
- The flange shape must be simplified: it is replaced by a round piece with rectangular section. The height remains the same of the flange, but as length of this component is taken the maximum radius of the flange (is a conservative choice). This allow us to treat all the flange section as an unique piece, this will be useful in the subsequent passages (Figure 5.2);
- In order to can treat the oil-side components as uniform ones is necessary that they have the same radius in the entire zone between flange and bottom connection, so for all of them are calculated the equivalent cylindrical sections (Figure 5.2);
- Some components, like the head, are not filled only with oil but they have even a part with air or vacuum (to permit, for example, the expansions of the inner oil due to the thermal changes). For reasons of simplicity, in the model this space is considered filled with only oil;
- The total height of the bushing model is measured starting from the top conductor face to the bottom conductor face, excluding in this way the terminals. This is because they are very complex to modelling and their real shapes are often unknown (in fact, during the designation process their characteristics are usually hypothesized).

After all this simplification, the model looks like pretty different respect the starting one reported in the drawing in Figure 5.1.

A section of the final bushing model, which is at the base of the equivalent thermal circuit, is reported in the schematic drawing in Figure 5.2. The differences between the two pictures are immediately clear even with a rapid confrontation.

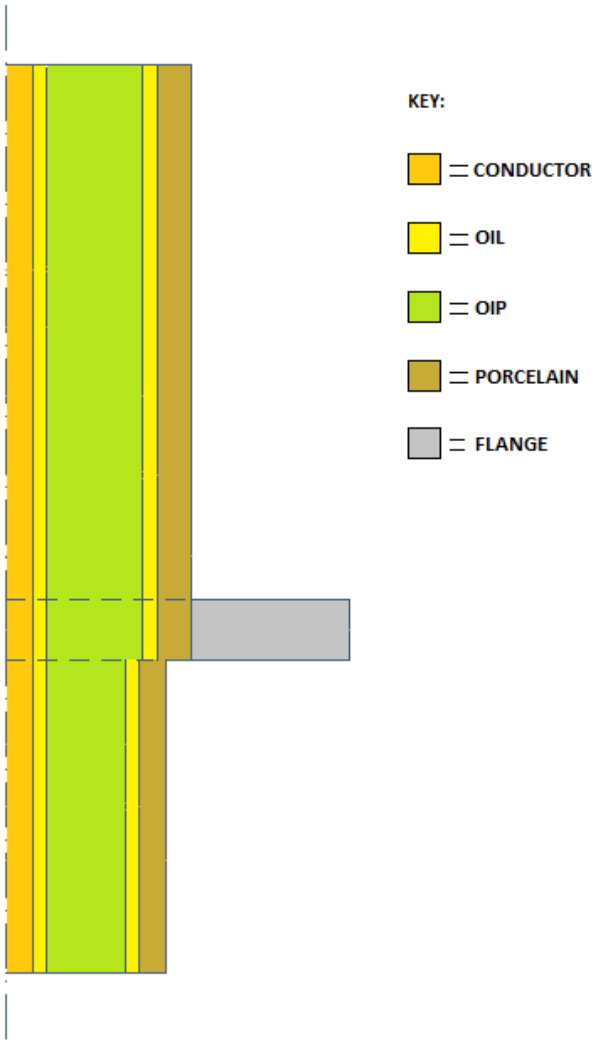

Figure 5.2 - Schematic Sectioned Bushing Model for the Equivalent Thermal Circuit

5.3 Equivalent Thermal Circuit

Starting from the bushing model in Figure 5.2, it can be developed its equivalent thermal circuit. This is possible thankfully to the property of the heat flow, which can be modelled by analogy as an electrical circuit.

Since the objective is calculating the maximum temperature of the bushing when the thermal stability is reached, the system analyzed is in steady state. Therefore, the thermal impedances are formed only by thermal resistances, without considering the thermal capacitances (they are useful in transient regime, where they take care of the inertia of the system).

5.3.1 Electric - Thermal Equivalents Models

Each thermal physical quantity, as temperature or heat flow, can be modelled with an equivalent electrical component.

The heat flow is represented by the current, and the heat sources are modelled by constant current source. The value of the current source is obtained by the calculation of the losses due to the current flow in the conductor, in [W].

The temperatures are represented by voltages, and where the temperatures are known or imposed then they are modelled by constant voltage sources, in [°C] or even in [K].

The thermal resistances are the representation of the property that indicates the heat difficulty to pass through a material, in [K/W] or [°C/W]. They depend to both geometry and types of materials; for this analysis the geometrical reference model is the hollow cylinders multilayer, as the schematic one reported in Figure 5.3.

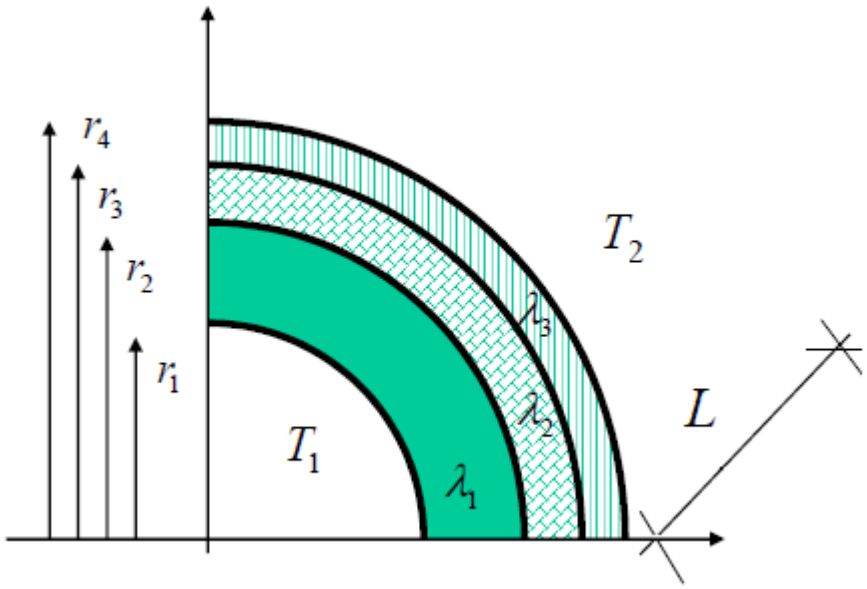

Figure 5.3 - Schematic Model of an Hollow Cylinders Multilayer

The first point to highlight is the necessity to make a distinction between the thermal resistances calculate in the radial direction and the ones calculate along the axial direction, since they are obtained with a different formulation.

The second difference among the resistances types is if they are due to the heat conduction or to the heat conductivity. The heat conduction represents the heat transfer through any medium (either solid or liquid or gaseous) due to a temperature gradient, with a heat flow spontaneous from a body at a higher temperature to a body at a lower temperature. The heat conductivity is a heat transfer present only in fluids medium (then liquid, without excessively higher viscosity, and gaseous ones) that are in contact with another medium (even a solid body) that has a different temperature.

There is a third type of heat transfer: the thermal radiation, but for the family of PNO bushings its contribute is negligible, while becoming important, for example, for the bushings insulated in gas, like the PHI types.

The axial thermal resistances in the model are due only by conduction effect and they are calculating by applying the formula reported in Equation 5.1.

$$R_{ax_i} := \frac{L}{\pi \cdot \lambda_{.i} \left[\left(r_i\right)^2 - \left(r_{i-1}\right)^2 \right]}$$

Equation 5.1 - Axial Thermal Resistances

Where:

- L= length of the cylinder, in [m];
- λ_i= thermal conductivity coefficient of the cylinder's material, in [W/Km];
- r_i= external radius of the cylinder, in [m];
- r_{i-1}= inner radius of the cylinder, in [m].

The radial thermal resistances, instead, are given by both conduction and convection, since they regards various material types. Their formulations are reported, respectively, in Equation

5.2 for the ones due to the heat conduction and in Equation 5.3 for the ones due to heat convection.

$$R_{\lambda i} := \frac{\ln\left(\frac{r_i}{r_{i+1}}\right)}{2\pi L \cdot \lambda_i}$$

Equation 5.2 - Radial Thermal Resistance Due to Heat Conduction

Where:

- L= length of the cylinder, in [m];
- λ_i= thermal conductivity coefficient of the cylinder material, in [W/Km];
- r_i= inner radius of the cylinder, in [m];
- r_{i+1}= external radius of the cylinder, in [m].

Moreover:

$$R_{.conv_i} := \frac{1}{h_{.i} \cdot 2\pi L \cdot r_{.i}}$$

Equation 5.3 - Radial Thermal Resistance Due to Heat Convection

Where:

- L= length of the cylinder, in [m];
- λ_i= thermal convection coefficient of the cylinder material, in [W/m^{2}K];
- r_i= radius of the cylinder, in [m];

Once defined the value of each resistance, is possible obtain the total radial resistance of the multilayer model in Figure 5.3. As first step, it is realized the equivalent thermal circuit, which can be seen in Figure 5.4, where every layer is modelled as a series resistance.

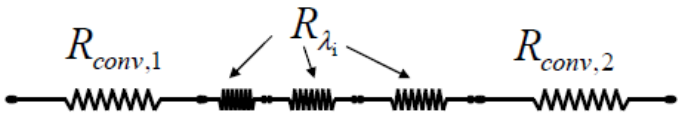

Figure 5.4 - Equivalent Circuit of the Radial Resistance

Therefore, the equivalent thermal resistance is given by:

$$R_{eq} := R_{conv_1} + \sum_i R_{\lambda i} + R_{conv_2}$$

Equation 5.4 - Total Radial Resistance

All these relationships are largely used in the development of the bushing equivalent thermal circuit.

5.3.2 Defining of Equivalent Thermal Circuit

In order to obtain the equivalent thermal circuit, the bushing model presented in Figure 5.2 must be divided in some sections. For each section considered, a radial line must be added to the circuit. Higher is the number of the taken sections and greater is the level of refinement of the model, which results closest to the reality.

However, it is also true that with a great number of lines the equivalents circuit and components and the resolving program are much more complicate to define, then it has been chosen to split the bushing in a few sections as possible during the development process, letting even here the possibility to improve this subdivision in future method expansions.

The bushing model has been divided in the following three sections:

- One that goes from the flange's top surface to the flange's lower surface, giving the radial line called L_1;
- One that goes from the flange's top surface to the top conductor's face, giving the radial line called L_2;
- One that goes from the flange's lower surface to the lower conductor's face, giving the radial line called L_3.

The model is therefore split in three very asymmetrical sections, with each one that has a very different height. For example, the height of the line L_2 could be even greater than an order of magnitude respect the one of the line L_1.

This solution has been adopted because the highest hot spot and the maximum temperature rise with high probabilities will be individuate in a zone placed around on the flange or between the flange and the bottom connection (for the reasons already explained in the Chapter 3).

Therefore, is preferable focusing the analysis on these zones respect of all the bushing air side, on which the temperature evaluation gives results having only partial interest.

In Figure 5.5 is reported the equivalent thermal circuit of a typical PNO bushing, where the thermal resistances represent the materials conduction/convection, the current sources represent the heat generated by the current flow and the voltage sources represent the imposed boundary conditions of both ambient air and tank oil temperatures.

The precise and complete definition of every circuital component can be find the Chapter 6.

DEFINITION OF A BUSHING EQUIVALENT THERMAL CIRCUIT

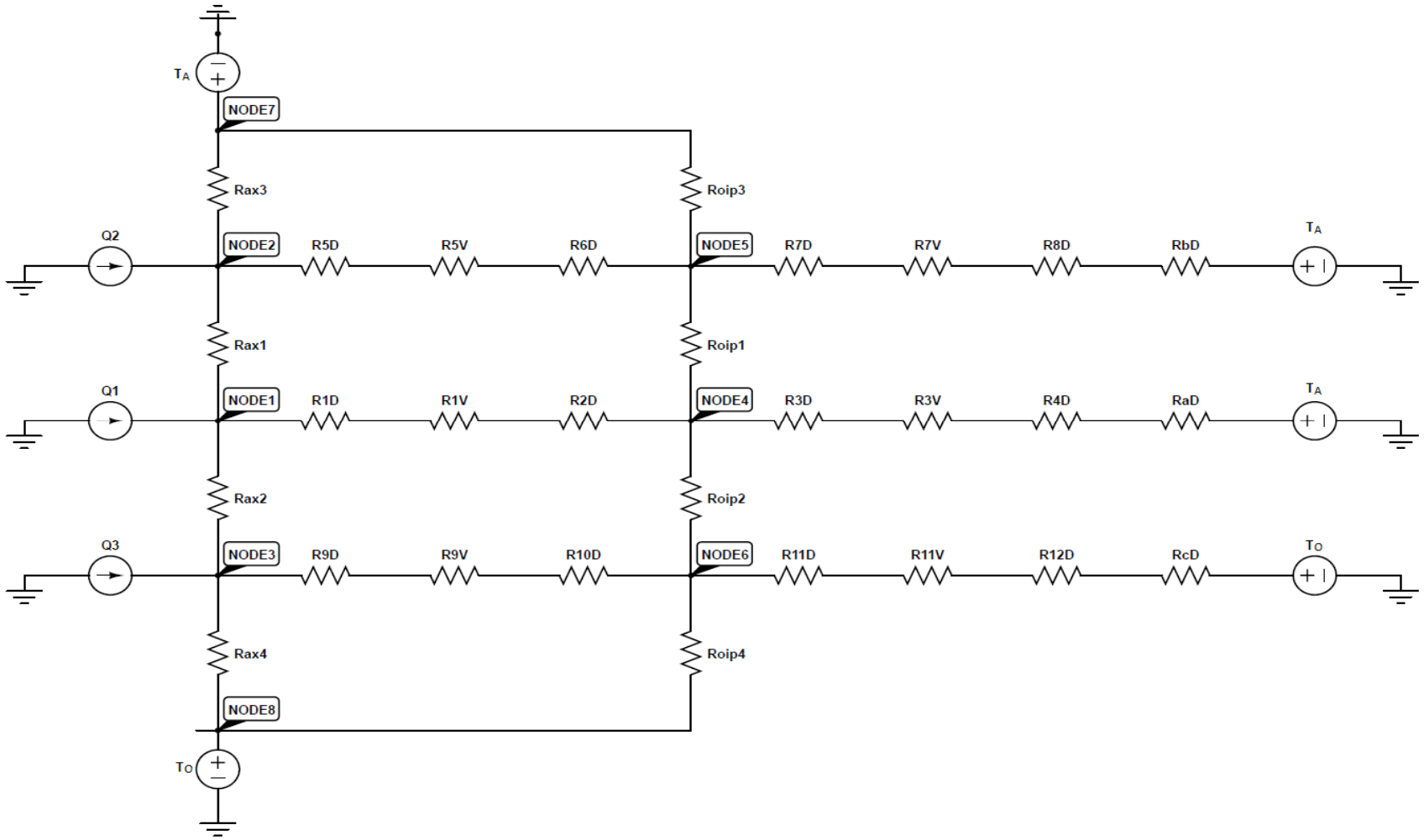

Figure 5.5 - Equivalent Thermal Circuit of a PNO Bushing

Where:

- Q_x= heat flows given by the current flow in the bushing's conductor, modelled as ideal current sources;
- RxD= thermal radial resistances due to the heat conduction of the materials;
- RxD= thermal radial resistances due to the heat convection of the materials;
- Rax_x= thermal axial resistances of the conductor;
- $Roip_x$= thermal axial resistances of the oil impregnated paper;
- T_A= temperature of the ambient that surrounds the bushing air side, modelled as ideal voltage sources;
- T_O= temperature of the oil in the tank that surrounds the bushing oil side, modelled as ideal voltage sources;

The final objective is obtain the values of the temperatures on the components of the bushing, this means create a calculation program able to solve the circuit in Figure 5.5, finding the nodal voltages values that represent the unknown temperatures. Especially meaning are the ones of the "NODE 1", "NODE 2" and "NODE 3", which represent the temperatures on the conductor body.

5.4 Resolving Method of the Circuit

After having defined the equivalent circuit, it is necessary create a resolving program in order to can calculate the values of the temperatures analytically.

The better resolving system to apply at this circuit is the Nodal Analysis method, because with it is possible calculate the nodal voltages (which are the final targets) directly and with few passages. In addition, the equivalent thermal circuit is easily modifiable to can satisfy the necessary conditions to can apply the Nodal Analysis.

5.4.1 Nodal Analysis Method

The nodal analysis is a method that permits to determining the voltages between the nodes in an electrical circuit. The circuit must be formed only by current sources and component with an admittance representation. If there are voltage generators, they must be replace with their equivalent current sources (modify nodal analysis method).

A front of a circuit with "*n*" nodes and "*l*" sides, the solution equations necessary are (n-1), and its general solution is obtained resolving the following system:

$$\begin{bmatrix} a_{1,1} & a_{1,2} & \cdots & a_{1,(n-1)} \\ a_{2,1} & a_{2,2} & \cdots & a_{2,(n-1)} \\ \vdots & \vdots & \ddots & \vdots \\ a_{(n-1),1} & a_{(n-1),2} & \cdots & a_{(n-1),(n-1)} \end{bmatrix} \begin{bmatrix} V_1 \\ V_2 \\ \vdots \\ V_{n-1} \end{bmatrix} = \begin{bmatrix} b_1 \\ b_2 \\ \vdots \\ b_m \end{bmatrix}$$

Figure 5.6 - Resolving System of the Nodal Analysis

Where:

- $a_{i,i}$= are the diagonal terms, given by the summation of all the conductances that converge at the node "i" and taking the result as negative;
- $a_{i,j}$= are the terms out of the diagonal, given by summation of the conductances between the nodes "i" and "j";
- V_i= are the nodal voltages at the nodes "i" and are the unknowns factors of the system;
- b_i= summation of the currents given by the generators that converge in the node "i", it must be taken negative if entrants.

To calculate the nodal voltages values is enough multiplying the inverted matrix of the conductances result with the current sources matrix, since all their others data are definable.

5.4.2 Necessaries Circuital Modifications

Some circuital modifications are necessary to can apply the nodal analysis at the circuit in Figure 5.5. In fact, as already explained in the previous paragraph (5.4.1), it is necessary a circuit having only current sources but in the our circuit there are several voltage sources. Therefore, it is necessary substitute them with their equivalent current generators.

For the ones that have in series a resistance, the equivalent current sources it is immediately obtainable through the simply application of the Norton's theorem.

Generally speaking, in Figure 5.7 is illustrated how, taking a voltage source Vn with in series a resistance R, the application Norton's theorem permit to define the equivalent current source.

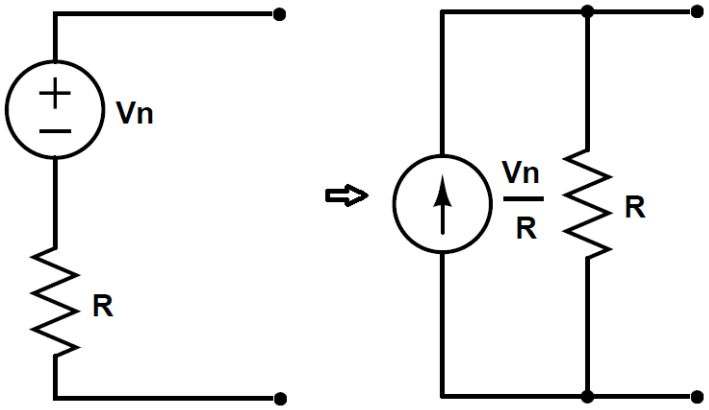

Figure 5.7 - General Application of the Norton's Theorem

In the starting circuit in Figure 5.5 are present some voltage sources apparently without a resistance in series. However, it is always possible for these components implement the transformation seen above, with only a further passage.

In Figure 5.8 is reported graphically this passage for a piece of the thermal circuit (is the part that models the bottom zone of the bushing). The same work it must be done for the remaining two voltages sources.

After making these modifies, the equivalent thermal circuit has the right form to can be resolved.

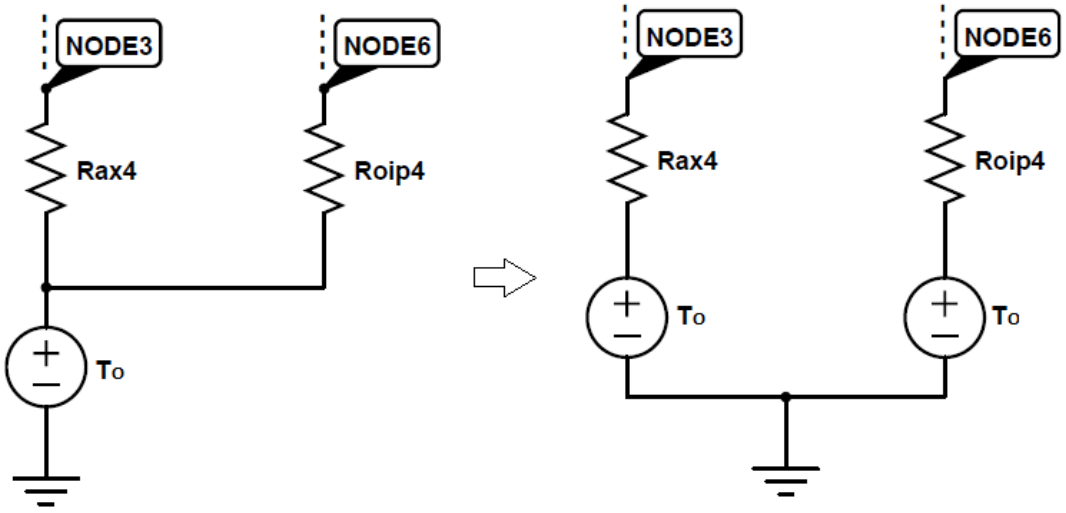

Figure 5.8 - Passage to Can Have Each Voltage Source in Series With a Resistance

5.4.3 Resolution of the circuit

In order to can make easier the study of the problem, all the resistances in series presents on every line must be summed where is possible, in this way the circuit results more compact and the number of components to treating during the construction of the matrix decreases.

Since the method used is the nodal analysis, all the resistances must be transformed in their equivalent conductances, with the immediate passage reported in Equation 5.5.

$$Gi := \frac{1}{Ri}$$

Equation 5.5 - Equivalent Conductance of the Resistance

The resulting equivalent thermal circuit is reported in Figure 5.9

Starting from this circuit, is possible realizing the matrix ofthe current generators (Figure 5.10) and the matrix of the conductances (Figure 5.11), having in this way defined all the parameters necessary to can calculate the nodal voltages, and then to have an evaluation of the temperature values reached in the bushing (Equation 5.6).

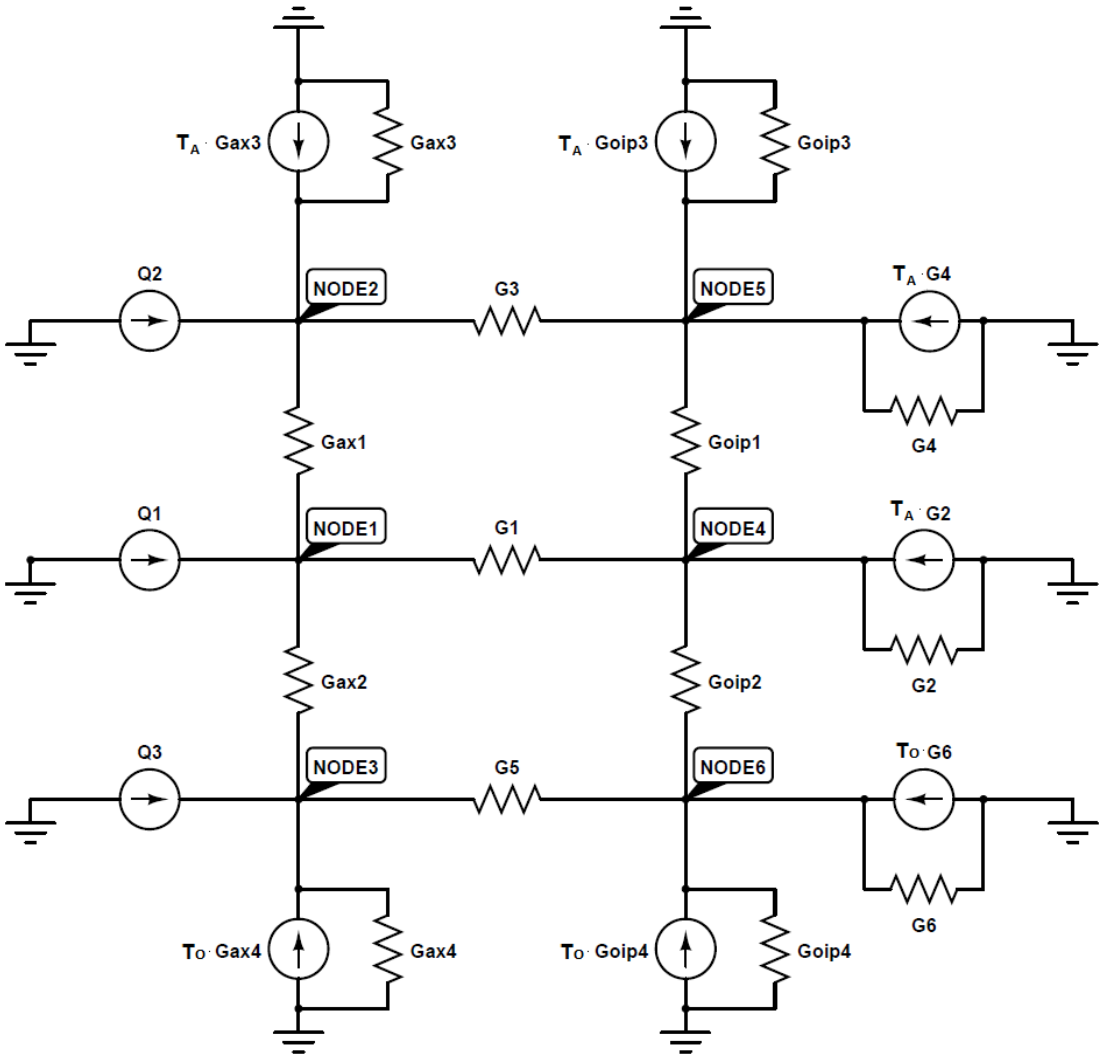

Figure 5.9 - Equivalent Thermal Circuit Modified to Can Apply the Nodal Analysis

$$I := \begin{pmatrix} -Q_1 \\ -Q_2 - T_A \cdot G_{ax3} \\ -Q_3 - T_O \cdot G_{ax4} \\ -T_A \cdot G_2 \\ -T_A \cdot G_4 - T_A \cdot G_{oip3} \\ -T_O \cdot G_6 - T_O \cdot G_{oip4} \end{pmatrix}$$

Figure 5.10 - Matrix of the current sources

DEFINITION OF A BUSHING EQUIVALENT THERMAL CIRCUIT

$$G := \begin{pmatrix} -G_{ax1} - G_{ax2} - G_1 & G_{ax1} & G_{ax2} & G_1 & 0 & 0 \\ G_{ax1} & -G_{ax1} - G_{ax3} - G_3 & 0 & 0 & G_3 & 0 \\ G_{ax2} & 0 & -G_{ax2} - G_{ax4} - G_5 & 0 & 0 & G_5 \\ G_1 & 0 & 0 & -G_1 - G_{oip1} - G_2 - G_{oip2} & G_{oip1} & G_{oip2} \\ 0 & G_3 & 0 & G_{oip1} & -G_3 - G_{oip3} - G_4 - G_{oip1} & 0 \\ 0 & 0 & G_5 & G_{oip2} & 0 & -G_5 - G_{oip2} - G_6 - G_{oip4} \end{pmatrix}$$

Figure 5.11 - Matrix of The Conductances of the Equivalent Thermal Circuits

$$V_n := G^{-1} \cdot I$$

Equation 5.6 - Nodal Voltages Calculation Formula

6 RESOLVING PROGRAM FOR THE BUSHING EQUIVALENT THERMAL CIRCUIT

6.1 Introduction

The developed calculation program to resolve the thermal equivalent circuit of a PNO bushing in order to find the temperature values reached, is reported here below. It has been make with the software "*Mathcad 15*" by PTC Company, so its implementation follows both the rules and the own syntax of this particular program. However, it is possible rewrite the resolving process with others calculation software (providing the necessaries adjustments) without losing any information.

The parameters highlights in green are the only input given by the user necessary at the calculation program to can solve the thermal circuit, all the remaining ones are or constants or auto-calculated parameters.

6.2 Constants of the Materials

The first operation is defining the constants used in the calculation program, which means the thermal conductivity and convection coefficients of the materials that could be employed as

bushing components. Their values has been taken from literature, from experimental evaluation and sometimes from a direct indication by the supplier of the material. Once they are defined, they remain the same for all the PNO bushings:

$\lambda_{aisi} := 16 \frac{W}{m \cdot K}$	Thermal conductivity coefficient of the AISi
$\lambda_{oip} := 0.4 \frac{W}{m \cdot K}$	Thermal conductivity coefficient of the oil impregnated paper
$\lambda_{SF6} := 0.013 \frac{W}{m \cdot K}$	Thermal conductivity coefficient of the SF6 gas
$\lambda_{cu} := 350 \frac{W}{m \cdot K}$	Thermal conductivity coefficient of the copper
$\lambda_{rip} := 0.25 \frac{W}{m \cdot K}$	Thermal conductivity coefficient of the resin impregnated paper
$\lambda_{epoxy} := 0.35 \frac{W}{m \cdot K}$	Thermal conductivity coefficient of the epoxi resin
$\lambda_{porc} := 1.5 \frac{W}{m \cdot K}$	Thermal conductivity coefficient of the porcelain
$\lambda_{flange} := 175 \frac{W}{m \cdot K}$	Thermal conductivity coefficient of the flange (average value, it isn't necessary modify it for every type of aluminium)
$\lambda_{tube} := 175 \frac{W}{m \cdot K}$	Thermal conductivity coefficient of the tube (average value, it isn't necessary modify it for every type of aluminium)
$\lambda_{al} := 270 \quad \frac{W}{m \cdot K}$	Thermal conductivity coefficient of the aluminium, used for the axial resistivity of the OIP
$\lambda_{p} := 0.17 \quad \frac{W}{m \cdot K}$	Thermal conductivity coefficient of the paper used for the axial resistivity of the OIP
$\lambda_{a} := 0.025 \quad \frac{W}{m \cdot K}$	Thermal conductivity coefficient of the air

Conductor type (CT)

1= copper-ETP - NT1300
2= aluminium AW-6060 - NT1390
3= aluminium AW-6082 - NT1388
4= aluminium AW-5083 - NT1381
5= aluminium AW-1050 - NT1460

Typical material used to make the conductor

$CT := 1$

Conductor material used, selecting a number between 1 to 5 the relative material properties are used into calculation

$$\lambda_{cond} := \begin{cases} 350 \cdot \frac{W}{m \cdot K} & \text{if } CT = 1 \\ 175 \cdot \frac{W}{m \cdot K} & \text{if } CT = 2 \\ 172 \cdot \frac{W}{m \cdot K} & \text{if } CT = 3 \\ 120 \cdot \frac{W}{m \cdot K} & \text{if } CT = 4 \\ 227 \cdot \frac{W}{m \cdot K} & \text{if } CT = 5 \end{cases}$$

Thermal conductivity coefficient of the materials

$$\lambda_{cond} = 350 \cdot \frac{W}{m \cdot K}$$

Thermal conductivity coefficient chosen for the conductor

$$h_{oil} := 80 \frac{W}{m^2 \cdot K}$$

Thermal convenction coefficient of the oil

$$h_{air} := 8 \frac{W}{m^2 \cdot K}$$

Thermal convenction coefficient of the ambient air

6.3 Geometrical Dimension of the Bushing

The geometrical values are the principal input given by the user to can resolve the circuit; they could be taken from the project drawings of the bushing itself.

6.3.1 Bushing radius and lengths

They are represent in the Figure 6.1, to can better understand which is the correspondence between geometrical dimensions and bushing model. The bushing model used has a rod conductor, but for a tube conductor there would be only few differences (for example, the inner radius of the conductor r_0 would have been different from zero).

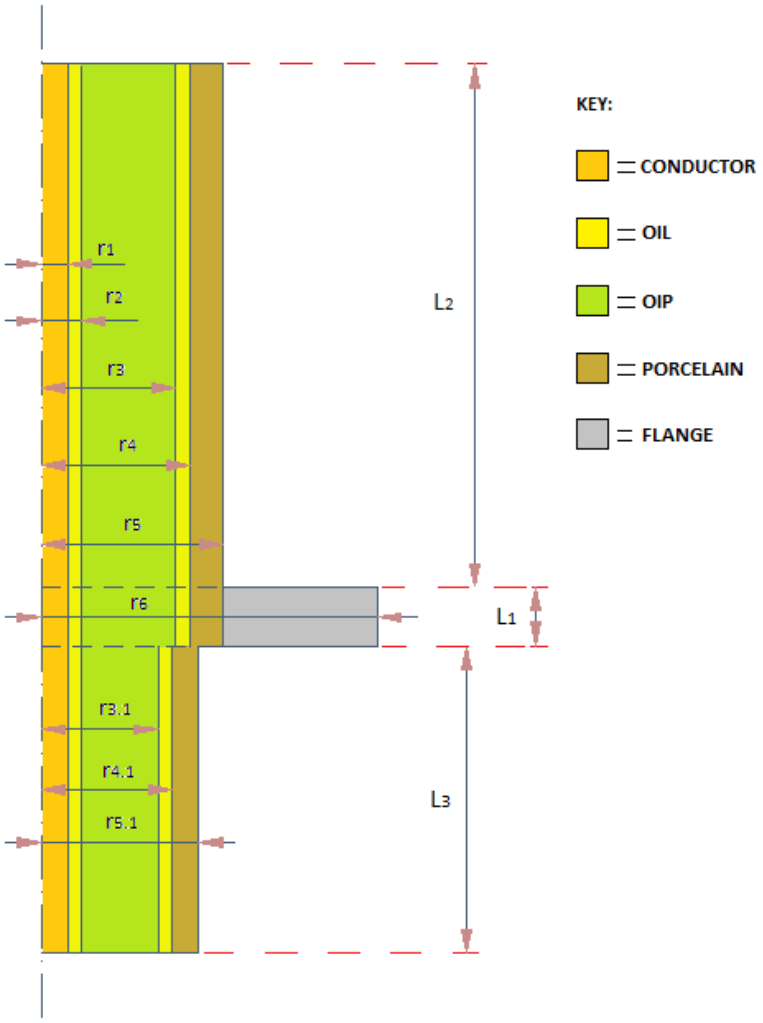

Figure 6.1 - Bushing Model with Radius and Length

$r_0 :=$ mm — Inner radius of the conductor, it's different to 0 only when the conductor is a tube

$r_1 :=$ mm — External radius of the conductor

$r_3 :=$ mm — Radius of the OIP at flange's height and in air side

$r_4 :=$ mm — Radius of the second duct of oil at flange's height and in air side

$r_5 :=$ mm	Radius of the external porcelain at flange's height and in air side
$r_6 :=$ mm	Maximum radius of the flange
$r_7 :=$ mm	Radius of the second duct of oil in the oil side
$r_8 :=$ mm	Radius of external porcelain in the oil side
$L_1 :=$ mm	Length of the flange's height
$L_2 :=$ mm	Length of the section between upper flange's surface and the top terminal
$L_3 :=$ mm	Length of the sectionbetween the uder flange's surface and the bottom terminal
$L_{tot} := L_1 + L_2 + L_3 =$ m	Total lenght of the bushing

6.3.2 Equivalent Cylindrical Section of the Bushing Oil Side

In order to can treat the oil side of the bushing as formed by only cylindrical components with the same radius for all the line 3, it is necessary make some modifications.

For the first, the bottom conic section is transformed in an equivalent one but with a cylindrical shape. After this passage, the bushing oil side results composed by two cylindrical sections but with different radiuses. The follows step is create a cylinder with an equivalent surface respect to the one given by the joint of the two cylindrical sections, obtaining a uniform radius along all the bushing oil side. The components affected by this process are the oil impregnated paper, the external porcelain and the duct of oil between them.

This passage is illustrated in the Figure 6.2, where are schematically reported the bushing oil side of the model (on the left) and how it results after the equivalent cylindrical calculation (on the right).

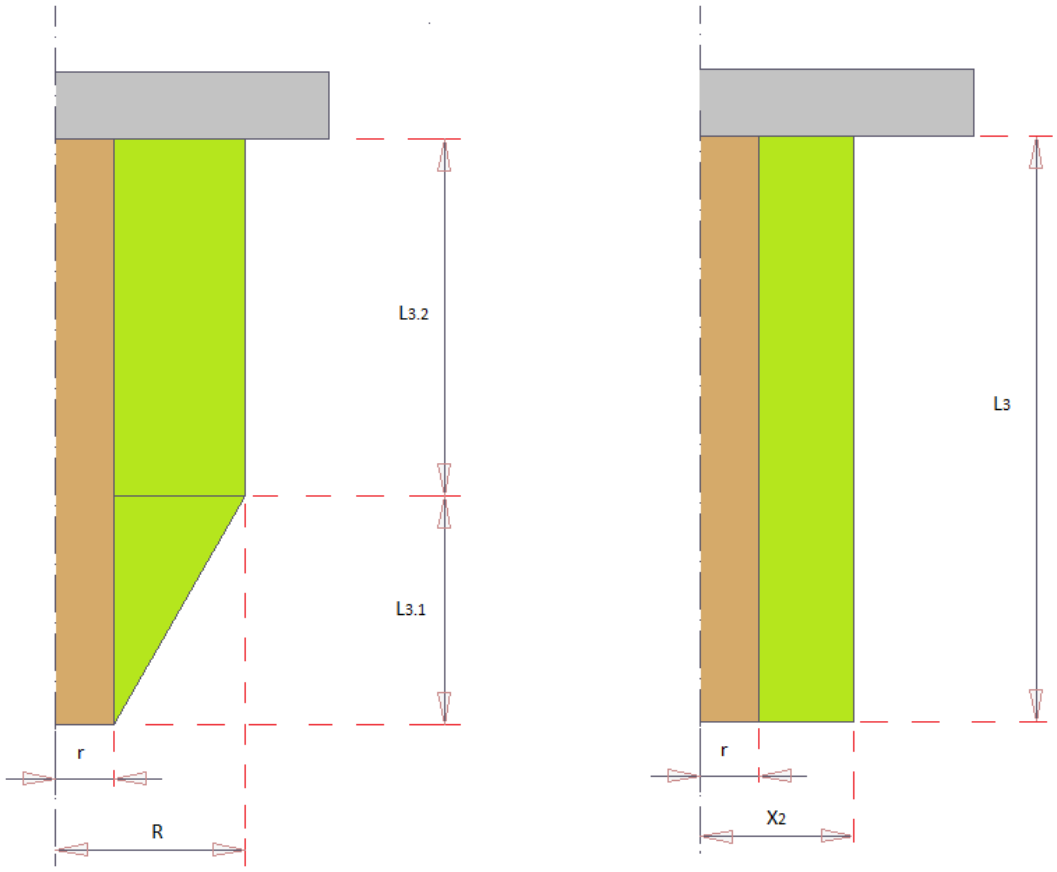

Figure 6.2 - Schematic Representation of the Equivalent Cylindrical Section of the Bushing Oil Side

$L_{3.1} :=$ mm — Length of the conic section of the bushing oil side

$L_{3.2} := L_3 - L_{3.1} =$ m — Length of the cilyndrical section of the bushing oil side

$h := L_{3.1} =$ m — Height of the conic surfaces

$R := \begin{pmatrix} r_3 \\ r_7 \\ r_8 \end{pmatrix} =$ m — External higher radius of the components involved, in the oil side

$r := r_2 =$ m — Radius of the inner surface, which remain constant

$Vol := \frac{\pi}{3} \cdot h \cdot \left(R^2 + r^2 + r \cdot R\right) - \pi \cdot r^2 \cdot h =$ m^3 — Conical volumes of the components

$X := \sqrt{\frac{Vol}{\pi \cdot h} + r^2} =$ m — Radius of the equivalent cylinders that have the same surface of the starting cones

$S := \frac{Vol}{h} =$ m^2 — Surfaces of the equivalents cylinders

$h_2 := L_{3.2} =$ m — Height of the natural cylindircal section of the bushing oil side

$Vol_b := \pi \cdot \left(R^2 - r^2\right) \cdot h_2 =$ m^3 — Volumes of the natural cylindircal components

$S_2 := \frac{Vol_b}{h_2} =$ m^2 — Surfaces of the natural cylindircal components

$S + S_2 =$ m^2 — Total surface given by the natural cylinders and the equivalent ones

$Vol_c := Vol + Vol_b =$ m^3 — Total volume

$X_2 := \sqrt{\frac{Vol_c}{\pi(h + h_2)} + r^2} =$ m — Radius of the finals equivalent cylinders

$r_{3.1} := X_{2_{0,0}} =$ m — Radius of the equivalent cylinder of the OIP, in the oil side

$r_{4.1} := X_{2_{1,0}} =$ m — Radius of the equivalent cylinder of the second duct of oil, in the oil side

$r_{5.1} := X_{2_{2,0}} =$ m — Radius of the equivalent cylinder of the porcelain, in the oil side

6.4 Definition of the Sources and Boundary Conditions

The user must insert here the last input to give at the calculation program for reaching the circuit solution.

The boundary conditions are chosen following the Standard IEC indications, so the ambient temperature is taken equal to 30 °C and the temperature of the oil in the tank is taken equal to 90 °C. These temperatures must be inserted in degrees Kelvin, then the ambient one becomes 303.15 K and the oil one becomes 363.15 K. They are the same for all the PNO bushings type.

The losses calculated with the following passages given the values of the heat flow due to the current flow in the conductor, therefore they define the current generator in the equivalent thermal circuit.

$f := 50Hz$ — Rated frequency

$ir :=$ A — Rated a.c. current

$T_c := 60\ °C$ — Avergae temperature of the conductor, is an estimate value

Conductor material

1 = copper-ETP - NT1300
2 = aluminium AW-6060 - NT1390
3 = aluminium AW-6082 - NT1388
4 = aluminium AW-5083 - NT1381
5 = aluminium AW-1050 - NT1460

Typical material used to make the conductor

$mat :=$ — Conductor material used, selecting a number between 1 to 5 and the relative material properties are used into calculation

$$\rho_{20} := \begin{cases} 1.71 \cdot 10^{-8}\,\Omega\cdot m & \text{if } mat = 1 \\ 3.25 \cdot 10^{-8}\,\Omega\cdot m & \text{if } mat = 2 \\ 3.85 \cdot 10^{-8}\,\Omega\cdot m & \text{if } mat = 3 \\ 5.90 \cdot 10^{-8}\,\Omega\cdot m & \text{if } mat = 4 \\ 2.82 \cdot 10^{-8}\,\Omega\cdot m & \text{if } mat = 5 \end{cases}$$

Material resistivity at the reference temparature of 20°C of the materials

$$\alpha_0 := \begin{cases} \frac{1}{234.5} & \text{if } mat = 1 \\ \frac{1}{232} & \text{if } mat = 2 \\ \frac{1}{232} & \text{if } mat = 3 \\ \frac{1}{232} & \text{if } mat = 4 \\ \frac{1}{228} & \text{if } mat = 5 \end{cases}$$

Temperature coefficient of resistivity of the materials

$\alpha_{20} := \frac{1}{20 + \frac{1}{\alpha_0}} =$ K^{-1} — Resultant temperature coefficient of resistivity

$\rho := \rho_{20} \cdot \left[1 + \alpha_{20} \cdot (T_c - 20)\right] =$ $\Omega \cdot m$ — Resultant resistivity

$CO\_din := 2r_0$ — Conductor inner diameter

$CO\_dout := 2 \cdot r_1$ — Conductor outer diameter

$CO\_sec := \pi \cdot \left(\frac{CO\_dout}{2}\right)^2 - \pi \cdot \left(\frac{CO\_din}{2}\right)^2 =$ $\cdot mm^2$ — Conductor section

$P_{sdc} := \frac{\rho \cdot \left(i_r^2\right)}{CO\_sec} =$ $\frac{W}{m}$ — Specific d.c. losses

$k_{add2}(r_{out}) :=$ — Coefficient of the total additional losses in the conductor, from tables

$P_{s50} := P_{sdc} \cdot k_{add2}(r_{out}) =$ $\cdot \frac{W}{m}$ — Specific linear a.c. losses

$Q_1 := P_{s50} \cdot L_1 =$ W — Heat flow from the conductor to Line 1

$Q_2 := P_{s50} \cdot L_2 =$ W — Heat flow from the conductor to Line 2

$Q_3 := P_{s50} \cdot L_3 =$ W — Heat flow from the conductor to Line 3

$Q := P_{s50} \cdot (L_1 + L_2 + L_3) =$ W — Total heat flow from the conductor

$T_A := 303.15K$ — Temperature of ambient air

$T_O := 363.15K$ — Temperature of the tank oil, where is immersed the bushing oil side

6.5 Radial Thermal Resistances

This phase of the program has been realized considering the various possibility of bushing construction. The user must not make anything to specify if the bushing has a rod or a tube as conductor, or else if between the conductor and the OIP there is a duct of oil or not. The program can recover this information from a confrontation among the radius inserted in the paragraph 6.3.1 and then calculate automatically the correct radial thermal resistances.

6.5.1 Line 1

Section of the bushing that corresponding to the height L_1, which is between the lower flange's face and the top flange's face.

$L_1 =$ m	Length of the flange's height
$\lambda_1 := \begin{cases} \lambda_{oil} & \text{if } r_0 = 0 \\ \lambda_{cond} & \text{otherwise} \end{cases}$	Thermal conductivity coefficient of the first thermal resistance of Line 1
$\lambda_2 := \lambda_{oip}$	Thermal conductivity coefficient of the second thermal resistance of Line 1
$\lambda_3 := \lambda_{oil}$	Thermal conductivity coefficient of the thrid thermal resistance of Line 1
$\lambda_4 := \lambda_{flange}$	Thermal conductivity coefficient of the fourth thermal resistance of Line 1
$h_1 := h_{oil}$	Thermal convenction coefficient of the first thermal resistance of Line 1
$h_3 := h_{oil}$	Thermal convenction coefficient of the second thermal resistance of Line 1
$h_a := h_{air}$	Thermal convenction coefficient of the last thermal resistance of Line 1

$$R_{1D} := \begin{cases} \dfrac{\ln\left(\frac{r_2}{r_1}\right)}{2\pi \cdot L_1 \cdot \lambda_1} & \text{if } r_0 = 0 \\ \dfrac{\ln\left(\frac{r_1}{r_0}\right)}{2\pi \cdot L_1 \cdot \lambda_1} & \text{otherwise} \end{cases}$$

Thermal resistance due to conduction in the first duct of oil

Thermal resistance due to conduction in the conductor

$$R_{1D} = \frac{K}{W}$$

First thermal resistance due to conduction

$$R_{1V} := \begin{cases} \text{if } r_1 = r_2 \\ \quad \begin{cases} R_{1V} \leftarrow \dfrac{1}{2\pi \cdot L_1 \cdot r_0 \cdot h_1} & \text{if } r_0 \neq 0 \\ R_{1V} \leftarrow 0 & \text{otherwise} \end{cases} \\ R_{1V} \leftarrow \dfrac{1}{2\pi \cdot L_1 \cdot r_1 \cdot h_1} & \text{otherwise} \end{cases}$$

Thermal resistance due to convection between conductor and oil

Thermal resistance due to convection between internal oil and conductor

Thermal resistance due to convection between conductor and oil

$$R_{1V} = \frac{K}{W}$$

First thermal resistance due to convection

$$R_{2D} := \frac{\ln\left(\frac{r_3}{r_2}\right)}{2\pi \cdot L_1 \cdot \lambda_2} = \frac{K}{W}$$

Thermal resistance due to conduction in the OIP section

$$R_{3D} := \frac{\ln\left(\frac{r_4}{r_3}\right)}{2\pi \cdot L_1 \cdot \lambda_3} = \frac{K}{W}$$

Thermal resistance due to concuction in the second duct of oil

$$R_{3V} := \frac{1}{2\pi \cdot L_1 \cdot r_3 \cdot h_3} = \frac{K}{W}$$

Thermal resistance due to convection between OIP and oil

$$R_{4D} := \frac{\ln\left(\frac{r_6}{r_4}\right)}{2\pi \cdot L_1 \cdot \lambda_4} = \frac{K}{W}$$

Thermal resistance due to conduction in the flange

$$R_{aV} := \frac{1}{2\pi \cdot L_1 \cdot r_6 \cdot h_a} = \frac{K}{W}$$

Thermal resistance due to convection between flange and the surroundings ambient

6.5.2 Line 2

Section of the bushing that corresponding to the height L_2, which is between upper flange's face and the bushing top connection.

$L_2 =$ m — Length of the section between upper flange surface and top terminal

$$\lambda_5 := \begin{cases} \lambda_{oil} & \text{if } r_0 = 0 \\ \lambda_{cond} & \text{otherwise} \end{cases}$$

Thermal conductivity coefficient of the first thermal resistance

$\lambda_6 := \lambda_{oip}$ — Thermal conductivity coefficient of the second thermal resistance of Line 2

$\lambda_7 := \lambda_{oil}$ — Thermal conductivity coefficient of the thrid thermal resistance of Line 2

$\lambda_8 := \lambda_{porc}$ — Thermal conductivity coefficient of the fourth thermal resistance of Line 2

$h_5 := h_{oil}$ — Thermal convenction coefficient of the first thermal resistance of Line 2

$h_7 := h_{oil}$ — Thermal convenction coefficient of the second thermal resistance of Line 2

$h_b := h_{air}$ — Thermal convenction coefficient of the last thermal resistance of Line 2

$$R_{5D} := \begin{cases} \dfrac{\ln\left(\frac{r_2}{r_1}\right)}{2\pi \cdot L_2 \cdot \lambda_5} & \text{if } r_0 = 0 \\ \dfrac{\ln\left(\frac{r_1}{r_0}\right)}{2\pi \cdot L_2 \cdot \lambda_5} & \text{otherwise} \end{cases}$$

Thermal resistance due to conduction in the first duct of oil

Thermal resistance due to conduction in the conductor

$R_{5D} =$ $\frac{K}{W}$ — First thermal resistance due to conduction

$$R_{5V} := \begin{cases} \text{if } r_1 = r_2 \\ \quad \begin{cases} R_{5V} \leftarrow \dfrac{1}{2\pi \cdot L_2 \cdot r_0 \cdot h_5} & \text{if } r_0 \neq 0 \\ R_{5V} \leftarrow 0 & \text{otherwise} \end{cases} \\ R_{5V} \leftarrow \dfrac{1}{2\pi \cdot L_2 \cdot r_1 \cdot h_5} & \text{otherwise} \end{cases}$$

Thermal resistance due to convection between conductor and oil

Thermal resistance due to convection between internal oil and conductor

Thermal resistance due to convection between conductor and oil

$R_{5V} = \quad \frac{K}{W}$

First thermal resistance due to convection

$R_{6D} := \frac{\ln\left(\frac{r_3}{r_2}\right)}{2\pi \cdot L_2 \cdot \lambda_6} = \quad \frac{K}{W}$

Thermal resistance due to conduction in OIP

$R_{7D} := \frac{\ln\left(\frac{r_4}{r_3}\right)}{2\pi \cdot L_2 \cdot \lambda_7} = \quad \frac{K}{W}$

Thermal resistance due to concuction in the second duct of oil

$R_{7V} := \frac{1}{2\pi \cdot L_2 \cdot r_3 \cdot h_7} = \quad \frac{K}{W}$

Thermal resistance due to convection between OIP and oil

$R_{8D} := \frac{\ln\left(\frac{r_5}{r_4}\right)}{2\pi \cdot L_2 \cdot \lambda_8} = \quad \frac{K}{W}$

Thermal resistance due to conduction in the porcelain

$R_{bV} := \frac{1}{2\pi \cdot L_2 \cdot r_5 \cdot h_b} = \quad \frac{K}{W}$

Thermal resistance due to convection between porcelain and the surrounding ambient

6.5.3 Line 3

Section of the bushing that corresponding to the height L_3, which is between lower flange's face and the bushing bottom connection.

$L_3 = \quad m$

Length between the uder flange's surface and bottom terminal

$$\lambda_9 := \begin{cases} \lambda_{oil} & \text{if } r_0 = 0 \\ \lambda_{cond} & \text{otherwise} \end{cases}$$

Thermal conductivity coefficient of the first thermal resistance of Line 3

$$\lambda_{10} := \lambda_{oip}$$

Thermal conductivity coefficient of the second thermal resistance of Line 3

$$\lambda_{11} := \lambda_{oil}$$

Thermal conductivity coefficient of the thrid thermal resistance of Line 3

$$\lambda_{12} := \lambda_{porc}$$

Thermal conductivity coefficient of the fourth thermal resistance of Line 3

$$h_9 := h_{oil}$$

Thermal convenction coefficient of the first thermal resistance of Line 3

$$h_{11} := h_{oil}$$

Thermal convenction coefficient of the second thermal resistance of Line 3

$$h_c := h_{oil}$$

Thermal convenction coefficient of the last thermal resistance of Line 3

$$R_{9D} := \begin{cases} \dfrac{\ln\left(\dfrac{r_2}{r_1}\right)}{2\pi \cdot L_3 \cdot \lambda_9} & \text{if } r_0 = 0 \\ \dfrac{\ln\left(\dfrac{r_1}{r_0}\right)}{2\pi \cdot L_3 \cdot \lambda_9} & \text{otherwise} \end{cases}$$

Thermal resistance due to conduction in the first duct of oil

Thermal resistance due to conduction in the conductor

$$R_{9D} = \frac{K}{W}$$

First thermal resistance due to conduction

$$R_{9V} := \begin{cases} \text{if } r_1 = r_2 \\ \quad \begin{cases} R_{59V} \leftarrow \dfrac{1}{2\pi \cdot L_3 \cdot r_0 \cdot h_9} & \text{if } r_0 \neq 0 \\ R_{9V} \leftarrow 0 & \text{otherwise} \end{cases} \\ R_{9V} \leftarrow \dfrac{1}{2\pi \cdot L_3 \cdot r_1 \cdot h_9} & \text{otherwise} \end{cases}$$

Thermal resistance due to convection between conductor and oil

Thermal resistance due to convection between internal oil and conductor

Thermal resistance due to convection between conductor and oil

$$R_{9V} = \frac{K}{W}$$

First thermal resistance due to convection

$$R_{10D} := \frac{\ln\left(\frac{r_{3.1}}{r_2}\right)}{2\pi \cdot L_3 \cdot \lambda_{10}} = \quad \frac{K}{W}$$

Thermal resistance due to conduction in OIP

$$R_{11D} := \frac{\ln\left(\frac{r_{4.1}}{r_{3.1}}\right)}{2\pi \cdot L_3 \cdot \lambda_{11}} = \quad \frac{K}{W}$$

Thermal resistance due to concuction in the second duct of oil

$$R_{11V} := \frac{1}{2\pi \cdot L_3 \cdot r_{3.1} \cdot h_{11}} = \quad \frac{K}{W}$$

Thermal resistance due to convection between OIP and oil

$$R_{12D} := \frac{\ln\left(\frac{r_{5.1}}{r_{4.1}}\right)}{2\pi \cdot L_3 \cdot \lambda_{12}} = \quad \frac{K}{W}$$

Thermal resistance due to concuction in the porcelain

$$R_{cV} := \frac{1}{2\pi \cdot L_3 \cdot r_{5.1} \cdot h_c} = \quad \frac{K}{W}$$

Thermal resistance due to convection between porcelain and transformer oil

6.6 Axial Thermal Resistances

6.6.1 Axial Thermal Resistances of the Conductor

The axial thermal resistances along the conductor are calculated taking as height of the sections the distance between the middle points of the three sections, besides with the ends.

$$L_{ax1} := \frac{L_1}{2} + \frac{L_2}{2} = \quad mm$$

Length of the axial section between middle point of the flange and middle point of porcelain air side

$$L_{ax2} := \frac{L_1}{2} + \frac{L_3}{2} = \quad mm$$

Length of the axial section between middle point of the flange and middle point of porcelain oil side

$$L_{ax3} := \frac{L_2}{2} = \quad mm$$

Length of the axial section between middle point of porcelain air side and top terminal

$$L_{ax4} := \frac{L_3}{2} = \quad mm$$

Length of the axial section between middle point of porcelain oil side and bottom terminal

$$\lambda_{ax1} := \lambda_{cond}$$

Thermal conductivity coefficient of the conductor

$\lambda_{ax2} := \lambda_{cond}$ Thermal conductivity coefficient of the conductor

$\lambda_{ax3} := \lambda_{cond}$ Thermal conductivity coefficient of the conductor

$\lambda_{ax4} := \lambda_{cond}$ Thermal conductivity coefficient of the conductor

$$R_{ax1} := \frac{L_{ax1}}{\pi \cdot \lambda_{ax1} \cdot \left(r_1^{\,2} - r_0^{\,2}\right)} = \quad \frac{K}{W}$$

Thermal resistance of the conductor axial section between middle point of the flange and middle point of porcelain air side

$$R_{ax2} := \frac{L_{ax2}}{\pi \cdot \lambda_{ax2} \cdot \left(r_1^{\,2} - r_0^{\,2}\right)} = \quad \frac{K}{W}$$

Thermal resistance of the conductor axial section between middle point of the flange and middle point of porcelain oil side

$$R_{ax3} := \frac{L_{ax3}}{\pi \cdot \lambda_{ax3} \cdot \left(r_1^{\,2} - r_0^{\,2}\right)} = \quad \frac{K}{W}$$

Thermal resistance of the conductor axial section between middle point of porcelain air side and top terminal

$$R_{ax4} := \frac{L_{ax4}}{\pi \cdot \lambda_{ax4} \cdot \left(r_1^{\,2} - r_0^{\,2}\right)} = \quad \frac{K}{W}$$

Thermal resistance of the conductor axial section between middle point of porcelain oil side and bottom terminal

6.6.2 Axial Thermal Resistances of the OIP

The OIP presents a non-negligible axial thermal resistance, since it is formed by paper and aluminium foils alternately winding, and is the presence of these last ones that allows a certain heat transfer.

$$L := \begin{pmatrix} L_{ax1} \\ L_{ax2} \\ L_{ax3} \\ L_{ax4} \end{pmatrix} = \quad m$$

Lenght of the bushing axial sections

$$d_{out} := \begin{pmatrix} 2 \cdot r_3 \\ 2 \cdot r_{3.1} \\ 2 \cdot r_3 \\ 2 \cdot r_{3.1} \end{pmatrix} = \quad mm$$

External paper diameters of the OIP

$$d_{in} := \begin{pmatrix} 2 \cdot r_2 \\ 2 \cdot r_2 \\ 2 \cdot r_2 \\ 2 \cdot r_2 \end{pmatrix} = \quad mm$$

Internal paper diameter of the OIP

$s_{rad} := 1.5 \quad mm$

Distance between foils

$s_{el} := 14 \times 10^{-3} \quad mm$

Electrode thickness

$$N_a := round\left[\frac{(d_{out} - d_{in})}{2 \cdot s_{rad}}\right] =$$

Number of the aluminum foils wounded around the conductor in the OIP

$tk_{el} := N_a \cdot s_{el} = \quad mm$

Total electrodes thickness

$$d_{av} := \frac{(d_{out} - d_{in})}{2} = \quad mm$$

Average diameters

$$S_{elr} := \left[\pi \cdot \left[\left(\frac{d_{av}}{2}\right) + tk_{el}\right]^2\right] - \left[\pi \cdot \left(\frac{d_{av}}{2}\right)^2\right] = \quad mm^2$$

Rought estimation of electrodes sections

$$S_{el0} := \sum_{n=1}^{N_{a_{0,0}}} \left[\left[\pi \cdot \left[\left[\frac{d_{in} + 2 \cdot (s_{rad} \cdot n)}{2}\right] + s_{el}\right]^2\right] - \left[\pi \cdot \left[\frac{d_{in} + 2 \cdot (s_{rad} \cdot n)}{2}\right]^2\right]\right] = \quad mm^2$$

$$S_{el1} := \sum_{n=1}^{N_{a_{1,0}}} \left[\left[\pi \cdot \left[\left[\frac{d_{in} + 2 \cdot (s_{rad} \cdot n)}{2}\right] + s_{el}\right]^2\right] - \left[\pi \cdot \left[\frac{d_{in} + 2 \cdot (s_{rad} \cdot n)}{2}\right]^2\right]\right] = \quad mm^2$$

$$S_{el2} := \sum_{n=1}^{N_{a_{2,0}}} \left[\left[\pi \cdot \left[\left[\frac{d_{in} + 2 \cdot (s_{rad} \cdot n)}{2}\right] + s_{el}\right]^2\right] - \left[\pi \cdot \left[\frac{d_{in} + 2 \cdot (s_{rad} \cdot n)}{2}\right]^2\right]\right] = \quad mm^2$$

$$S_{el3} := \sum_{n=1}^{N_{a_{3,0}}} \left[\left[\pi \cdot \left[\left[\frac{d_{in} + 2 \cdot (s_{rad} \cdot n)}{2} \right] + s_{el} \right]^2 \right] - \left[\pi \cdot \left[\frac{d_{in} + 2 \cdot (s_{rad} \cdot n)}{2} \right]^2 \right] \right] = \quad mm^2$$

$$S_{el} := \begin{pmatrix} S_{el0_{1,0}} \\ S_{el1_{1,0}} \\ S_{el2_{1,0}} \\ S_{el3_{1,0}} \end{pmatrix} = \quad mm^2$$

Total axial ectrode sections

$$S_p := \overrightarrow{\left[\left[\pi \cdot \left(\left(\frac{d_{out}}{2} \right) \right)^2 \right] - \left[\pi \cdot \left(\frac{d_{in}}{2} \right)^2 \right] \right]} = \quad mm^2$$

Sections of the paper

$$R_{ael} := \frac{\overrightarrow{L}}{\lambda_{al} \cdot S_{el} \cdot 10^{-6}} = \quad \frac{K}{W}$$

Thermal resistances due to the aluminium foils

$$R_{ap} := \frac{\overrightarrow{L}}{\lambda_p \cdot S_p \cdot 10^{-6}} = \quad \frac{K}{W}$$

Thermal resistances due to the the paper

$$R_{eq} := \frac{\overrightarrow{(R_{ael} \cdot R_{ap})}}{R_{ael} + R_{ap}} = \quad \frac{K}{W}$$

Equivalent axial thermal resistances

$$R_{oip1} := R_{eq_{0,0}} \cdot \frac{K}{W} = \quad \frac{K}{W}$$

Thermal resistance of the oip axial section between middle point of the flange and middle point of porcelain air side

$$R_{oip2} := R_{eq_{1,0}} \frac{K}{W} = \quad \frac{K}{W}$$

Thermal resistance of the oip axial section between middle point of the flange and middle point of porcelain oil side

$$R_{oip3} := R_{eq_{2,0}} \frac{K}{W} = \quad \frac{K}{W}$$

Thermal resistance of the oip axial section between middle point of porcelain air side and top terminal

$$R_{oip4} := R_{eq_{3,0}} \frac{K}{W} = \quad \frac{K}{W}$$

Thermal resistance of the oip axial section between middle point of porcelain oil side and bottom terminal

6.7 Equivalent Thermal Conductances

As already explained in the lasts paragraphs of the Chapter 5 of this thesis, the resolving method used is the nodal analysis. Here below are reported the passages to can calculate both

the equivalent series resistances of the thermal circuit lines and the equivalent conductances with which find the nodal voltages.

$R_1 := R_{1D} + R_{1V} + R_{2D} = \frac{K}{W}$ First equivalent series thermal resistance of the Line 1

$R_2 := R_{3D} + R_{3V} + R_{4D} + R_{aV} = \frac{K}{W}$ Second equivalent series thermal resistance of the Line 1

$R_3 := R_{5D} + R_{5V} + R_{6D} = \frac{K}{W}$ First equivalent series thermal resistance of the Line 2

$R_4 := R_{7D} + R_{7V} + R_{8D} + R_{bV} = \frac{K}{W}$ Second equivalent series thermal resistance of the Line 2

$R_5 := R_{9D} + R_{9V} + R_{10D} = \frac{K}{W}$ First equivalent series thermal resistance of the Line 3

$R_6 := R_{11D} + R_{11V} + R_{12D} + R_{cV} = \frac{K}{W}$ Second equivalent series thermal resistance of the Line 3

$G_1 := \frac{1}{R_1} = \frac{W}{K}$ Equivalent Thermal Conductance of R_1

$G_2 := \frac{1}{R_2} = \frac{W}{K}$ Equivalent Thermal Conductance of R_2

$G_3 := \frac{1}{R_3} = \frac{W}{K}$ Equivalent Thermal Conductance of R_3

$G_4 := \frac{1}{R_4} = \frac{W}{K}$ Equivalent Thermal Conductance of R_4

$G_5 := \frac{1}{R_5} = \frac{W}{K}$ Equivalent Thermal Conductance of R_5

$G_6 := \frac{1}{R_6} = \frac{W}{K}$ Equivalent Thermal Conductance of R_6

$G_{ax1} := \frac{1}{R_{ax1}} = \frac{W}{K}$ Equivalent Thermal Conductance of R_{ax1}

$G_{ax2} := \frac{1}{R_{ax2}} = \frac{W}{K}$ Equivalent Thermal Conductance of R_{ax2}

$G_{ax3} := \frac{1}{R_{ax3}} = \frac{W}{K}$ Equivalent Thermal Conductance of R_{ax3}

$G_{ax4} := \frac{1}{R_{ax4}} = \frac{W}{K}$ Equivalent Thermal Conductance of R_{ax4}

$G_{oip1} := \frac{1}{R_{oip1}} = \frac{W}{K}$ Equivalent Thermal Conductance of R_{oip1}

$G_{oip2} := \frac{1}{R_{oip2}} = \frac{W}{K}$ Equivalent Thermal Conductance of R_{oip2}

$G_{oip3} := \frac{1}{R_{oip3}} = \frac{W}{K}$ Equivalent Thermal Conductance of R_{oip3}

$G_{oip4} := \frac{1}{R_{oip4}} = \frac{W}{K}$ Equivalent Thermal Conductance of R_{oip4}

6.8 Resolution of the Thermal Circuit

The matrix of the thermal conductances has built through the inspection process, as explained in the Chapter 5. The final temperatures are reported automatically in degrees Celsius, to have more clearly values.

$$G := \begin{pmatrix} -G_{ax1} - G_{ax2} - G_1 & G_{ax1} & G_{ax2} & G_1 & 0 & 0 \\ G_{ax1} & -G_{ax1} - G_{ax3} - G_3 & 0 & 0 & G_3 & 0 \\ G_{ax2} & 0 & -G_{ax2} - G_{ax4} - G_5 & 0 & 0 & G_5 \\ G_1 & 0 & 0 & -G_1 - G_{oip1} - G_2 - G_{oip2} & G_{oip1} & G_{oip2} \\ 0 & G_3 & 0 & G_{oip1} & -G_3 - G_{oip3} - G_4 - G_{oip1} & 0 \\ 0 & 0 & G_5 & G_{oip2} & 0 & -G_5 - G_{oip2} - G_6 - G_{oip4} \end{pmatrix}$$

$$I := \begin{pmatrix} -Q_1 \\ -Q_2 - T_A \cdot G_{ax3} \\ -Q_3 - T_O \cdot G_{ax4} \\ -T_A \cdot G_2 \\ -T_A \cdot G_4 - T_A \cdot G_{oip3} \\ -T_O \cdot G_6 - T_O \cdot G_{oip4} \end{pmatrix} = \quad W$$

Matrix of the current given by current sources that converge on the nodes

$V_{nk} := G^{-1} \cdot I = \quad K$

Matrix of the voltages at the nodes, in degrees Kelvin

$V_n := V_{nk} \cdot \frac{1}{K} - 273.15 = \quad °C$

Matrix of the voltages at the nodes, in degrees Celsius

$T_1 := V_{n_{0,0}} = \quad °C$

Temperature in the node 1 of the thermal network

$T_2 := V_{n_{1,0}} = \quad °C$

Temperature in the node 2 of the thermal network

$T_3 := V_{n_{2,0}} = \quad °C$

Temperature in the node 3 of the thermal network

$T_4 := V_{n_{3,0}} = \quad °C$

Temperature in the node 4 of the thermal network

$T_5 := V_{n_{4,0}} = \quad °C$

Temperature in the node 5 of the thermal network

$T_6 := V_{n_{5,0}} = \quad °C$

Temperature in the node 6 of the thermal network

Particularly interesting are the values of T_1, T_2, and T_3, which represent the temperature along the conductor body. Since they are the evaluation points nearest at the heat source, the maximum temperature of the bushing should be given by these terms with high probability.

7 COMPARISON AND ANALYSIS OF THE CIRCUITAL METHOD RESULTS

7.1 Introduction

To can have a proper evaluation about the effective reliability of the hottest temperatures and maximum temperatures rise obtained by applying the developed equivalent thermal circuit method, it is necessary realize a confrontation between its results and the ones obtained by tests and thermal simulations.

With this comparison, is possible make some observations about the method developed, even analyzing the weak points of this circuital approach and the possible improvements for it.

7.2 Results Comparison: Bushing with Removable Conductor

For the bushing with removable conductor the confrontation between the hottest spot found with the three methods is very meaning, since for these cases the tests temperatures are obtained through direct measures (as already explained in the Chapter 3) with an high accuracy (the measuring error on the final result is about 1%), giving then some good reference values.

7.2.1 Report of the Obtained Results

The maximum temperature and temperature rise are inserted in two tables: in the Table 7.1 there are the values found with tests, with simulations and with the circuital method, while in the Table 7.2 there are the calculated discrepancies between the three previous methods results, both as simply differences (absolute values) and as percentages (relative values).

It has been pretty difficult find cases of bushing on which were realized temperature rise test and thermal simulation at the same time, probably because making both is considering unnecessary due the good accuracy e relative simplicity of the measuring method. This is unfortunate, because even the analysis of the discrepancies with the simulations is important for appreciate the circuital calculation accuracy.

In order to can have a higher number of data to compare, it has been realized a few thermal simulations expressly to improve the confrontation process in this thesis.

It is very important to specify that all the temperatures present in the following tables are reported at the same reference ambient temperature, which is taken equal to 30 °C.

This solution is applied to can have a most immediately and clearly confrontation among the maximum temperature values, but at the same time it makes less important the analysis of the temperatures rise found, since all the increments are referred at the same value.

		TEST		SIMULATION		CALCULATION	
PNO Bushing Name	Test Current [A]	Tmax [°C]	ΔTmax [K]	Tmax [°C]	ΔTmax [K]	Tmax [°C]	ΔTmax [K]
PNO 145.650.1250	1250	104,9	74,9			97,01	67,01
PNO 170.170.1250	1250	103,6	76,6			97,4	67,4
PNO 245.1050.800	812,202	92,8	62,8	94,9	64,9	89,65	59,65
PNO 245.1050.1250	1250	92	62			88,89	58,89
PNO 420.1425.1250	1250	93,2	63,2			88,76	58,76
PNO 420.1425.1600	1000			90,89	60,89	91,33	61,33
PNO 420.1425.1600	1600	103,2	73,2	104,11	74,11	102,87	72,87
PNO 420.1425.1600	2000			120	90	113,53	83,53
PNO 550.1800.1250	1250	101,8	71,8			100,57	70,57

Table 7.1 - Maximum Temperatures and Temperatures Rise Obtained, Removable Conductor Cases

		TEST vs. SIMULATION				CALCULATION vs.TEST				CALCULATION vs. SIMULATION			
PNO Bushing Name	Test Current [A]	dTmax [°C]	dTmax [%]	dΔTmax [K]	dΔTmax [%]	dTmax [°C]	dTmax [%]	dΔTmax [K]	dΔTmax [%]	dTmax [°C]	dTmax [%]	dΔTmax [K]	dΔTmax [%]
PNO 145.650.1250	1250					-7,89	-7,52%	-7,89	-10,53%				
PNO 170.170.1250	1250					-6,2	-5,98%	-9,2	-12,01%				
PNO 245.1050.800	812,202	2,1	2,26%	2,1	3,34%	-3,15	-3,39%	-3,15	-5,02%	-5,25	-5,53%	-5,25	-8,09%
PNO 245.1050.1250	1250					-3,11	-3,38%	-3,11	-5,02%				
PNO 420.1425.1250	1250					-4,44	-4,76%	-4,44	-7,03%				
PNO 420.1425.1600	1000									0,44	0,48%	0,44	0,72%
PNO 420.1425.1600	1600	0,91	0,88%	0,91	1,24%	-0,33	-0,32%	-0,33	-0,45%	-1,24	-1,19%	-1,24	-1,67%
PNO 420.1425.1600	2000									-6,47	-5,39%	-6,47	-7,19%
PNO 550.1800.1250	1250					-1,23	-1,21%	-1,23	-1,71%				

Table 7.2- Comparison Between Results Obtained with the Three Methods, Removable Conductor Cases

The voices in the previous tables mean:

- Test Current= Feeding current of the bushing during the test, the simulation and the calculation, in [A];
- Tmax= Hottest temperature value found, in [°C];
- ΔTmax= Maximum temperature rise value found, in [K];
- dTmax= Discrepancy between both relative and absolute values of the maximum temperature found, in [°C] and [%];
- dΔTmax= Discrepancy between both relative and absolute values of the maximum temperatures rise found, in [°C] and [%].

The confrontation parameter dTmax is calculated for the three cases in the following way:

- For Test vs. Simulation case:

$$Tmax_{test} - Tmax_{simul} \quad [°C] \qquad \frac{Tmax_{test} - Tmax_{simul}}{Tmax_{test}} 100 \quad [\%]$$

Equation 7.1 - dTmax Formulas in Test vs. Simulation Cases

- For Calculation vs. Test case:

$$Tmax_{test} - Tmax_{calc} \quad [°C] \qquad \frac{Tmax_{test} - Tmax_{calc}}{Tmax_{test}} 100 \quad [\%]$$

Equation 7.2- dTmax Formulas in Calculation vs. Test Cases

- For Calculation vs. Simulation case:

$$Tmax_{simul} - Tmax_{calc} \quad [°C] \qquad \frac{Tmax_{simul} - Tmax_{calc}}{Tmax_{simul}} \; 100 \quad [\%]$$

Equation 7.3 - dTmax Formulas in Calculation vs. Simulation Cases

Even the confrontation parameter ΔTmax has different formulations for the three cases, they are defined calculated as follow:

- For Test vs. Simulation case:

$$\Delta Tmax_{test} - \Delta Tmax_{simul} \quad [°C] \qquad \frac{\Delta Tmax_{test} - \Delta Tmax_{simul}}{\Delta Tmax_{test}} \; 100 \quad [\%]$$

Equation 7.4 - ΔTmax Formulas in Test vs. Simulation Cases

- For Calculation vs. Test case:

$$\Delta Tmax_{test} - \Delta Tmax_{calc} \quad [°C] \qquad \frac{\Delta Tmax_{test} - \Delta Tmax_{calc}}{\Delta Tmax_{test}} \; 100 \quad [\%]$$

Equation 7.5 - ΔTmax Formulas in Calculation vs. Test Cases

- For Calculation vs. Simulation case:

$$\Delta Tmax_{simul} - \Delta Tmax_{calc} \quad [°C] \qquad \frac{\Delta Tmax_{simul} - \Delta Tmax_{calc}}{\Delta Tmax_{simul}} \; 100 \quad [\%]$$

Equation 7.6 - ΔTmax Formulas in Calculation vs. Simulation Cases

7.2.2 Analysis of the Results Comparison

In order to can have a clearer confrontation between the most significant results of Table 7.1 and Table 7.2, two bar graphs have been made: in the first one (Figure 7.1) are represented for each bushing the values of the highest temperatures obtained with the three methods, while their discrepancies, express as relative values, are represented in the second graph (Figure 7.2).

Observing the Figure 7.1, it can be see immediately how the maximum temperatures found by applying the circuital calculation (which are represent by the central purple bar) at the removable conductor cases have surely a contained gap with both tests and simulations results, but this gap is a negative value in almost every case.

Therefore, it can be said that the application of the circuital calculation gives results not very different respect the others two methods, but it is present the risk to underestimated the temperature hottest spot.

Even with these few cases analyzed, it is possible make some consideration about the possible gap of the calculated highest temperatures respect the ones measured by the tests.

The difference between them ranges from -1.21% to -7.52 %, remaining always less than 10%, and with an average gap equal to -3.80%. Speaking in degrees Celsius, the difference ranges from -1.23 °C to -7.89 °C, with the average gap equal to -3.76 °C.

Therefore, it can be said that the circuital calculating method developed gives a response of the bushing maximum temperature that differs respect the measured one by an average gap less than 5%.

Respect the simulations results, the discrepancies with the calculating method are a little more contained: they range from 0.48% to -5.53%, with an average gap equal to -2.91%. These values are in line with the ones founds in the comparison with the tests results, but since the very low number of simulations reported in tables, it is better considering this data more as an indication.

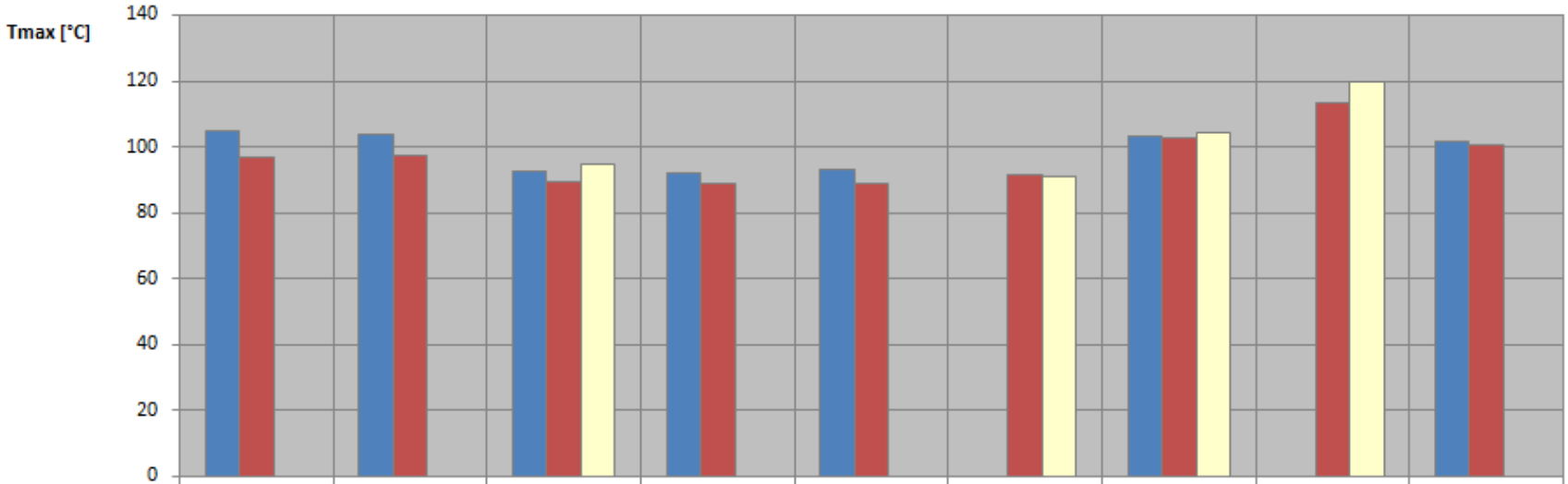

	PNO 145.650.1250	PNO 170.170.1250	PNO 245.1050.800	PNO 245.1050.1250	PNO 420.1425.1250	PNO 420.1425.1600	PNO 420.1425.1600	PNO 420.1425.1600	PNO 550.1800.1250
Test Current	1250 A	1250 A	812,202 A	1250 A	1250 A	1000 A	1600 A	2000 A	1250 A
TEST	104,9	103,6	92,8	92	93,2		103,2		101,8
CALCULATION	97,01	97,4	89,65	88,89	88,76	91,33	102,87	113,53	100,57
SIMULATION			94,9			90,89	104,11	120	

Figure 7.1 - Comparison Between the Maximum Temperatures Values, Removable Conductor Cases

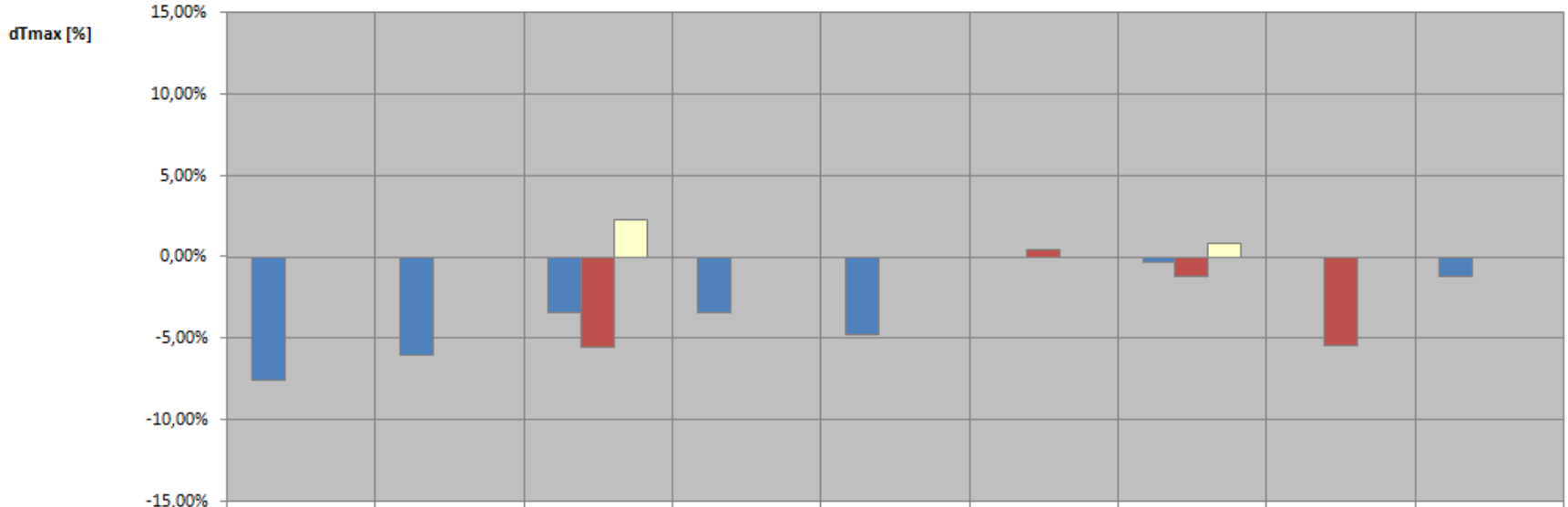

	PNO 145.650.1250	PNO 170.170.1250	PNO 245.1050.800	PNO 245.1050.1250	PNO 420.1425.1250	PNO 420.1425.1600	PNO 420.1425.1600	PNO 420.1425.1600	PNO 550.1800.1250
Test Current	1250 A	1250 A	812,202 A	1250 A	1250 A	1000 A	1600 A	2000 A	1250 A
CALCULATION vs.TEST	-7,52%	-5,98%	-3,39%	-3,38%	-4,76%		-0,32%		-1,21%
CALCULATION vs. SIMULATION			-5,53%			0,48%	-1,19%	-5,39%	
TEST vs. SIMULATION			2,26%				0,88%		

Figure 7.2 - Discrepancies Between the Maximum Temperatures Values, Removable Conductor Cases

It is worth observing that there is a leak of accuracy on the bushing with lower voltage, the gaps in these cases has an increment. This means that the equivalent thermal circuit presents some difficulties to can evaluate correctly the temperature of PNO bushings with the lower voltage and, therefore, the smaller dimensions.

For the PNO.145.650.1250 case, it is a good thing highlight the zone where has been measured the temperature: at 1/3 of the bushing height, near to the bushing head.

Passing to observe the temperature rise discrepancies, it can be noticed that the gaps, if they are express as absolute values, remain the same of the corresponding maximum temperature ones. Instead, if they are express as relative values the differences between results increase respect the previous analysis, but this is logical: when the percentages are calculated the numerator remain the same, but the denominator decrease of 30 degrees (which is the value of the ambient temperature). Therefore, the results increase for sure.

7.3 Resulting Comparison: Bushing with Non-Removable Conductor

Due to the loss of reliability of the temperatures measured by tests with these bushing types, for the following analysis the most interesting comparison for the thermal equivalent circuit method results is for sure with the ones obtained by the thermal simulations.

7.3.1 Report of the Obtained Results

Just like in the paragraph 7.2.1, the data are separated in two tables: in the Table 7.3 are reported the values of the maximum temperatures and the maximum temperatures rise obtained by applying the three methods while in the Table 7.4 are inserted the discrepancies between the results.

All the voices in the following two tables have the same mean of the correspondents ones already explained in the paragraph 7.2.1.

Even for this analysis, all the values are reported at the same reference ambient temperature equal to 30 °C.

			TEST		SIMULATION		CALCULATION	
PNO Bushing Name	connection	Test Current [A]	Tmax [°C]	ΔTmax [K]	Tmax [°C]	ΔTmax [K]	Tmax [°C]	ΔTmax [K]
PNO.420.1425.2000	bottom connection	2000	104,3	74,3			108,97	78,97
PNO.550.1675.3000	bottom connection	2000			97,67	67,67	101,41	71,41
PNO.550.1675.3000	bottom connection	2500			106,9	76,9	111,52	81,52
PNO.550.1675.3000	bottom connection	3000			119,53	89,53	123,88	93,88
PNO.550.1675.3000	bottom connection	3500			135,8	105,8	138,48	108,48
PNO.800.2550.2500	fix rod	2500	90	60	102	72	106,96	76,96
PNO.800.2550.2500	fix rod	2000	89,8	59,8			99,28	69,28
PNO.1100.2400.2500	bottom connection	1500	87,4	57,4	92	62	95,8	65,8
PNO.1100.2400.2500	bottom connection	2000	92,1	62,1	97	67	102,42	72,42
PNO.1100.2400.2500	bottom connection	2500	90,5	60,5	105	75	111,86	81,86
PNO.1100.2400.2500	bottom connection	3150			119	89	127,28	97,28

Table 7.3 - Maximum Temperatures and Temperatures Rise, Non-Removable Conductor Case

			TEST vs. SIMULATION				TEST vs. CALCULATION				SIMULATION vs. CALCULATION			
PNO Bushing Name	connection	Test Current [A]	dTmax [°C]	dTmax [%]	dΔTmax [K]	dΔTmax [%]	dTmax [°C]	dTmax [%]	dΔTmax [K]	dΔTmax [%]	dTmax [°C]	dTmax [%]	dΔTmax [K]	dΔTmax [%]
PNO.420.1425.2000	bottom connection	2000					4,67	4,48%	4,67	6,29%				
PNO.550.1675.3000	bottom connection	2000									3,74	3,83%	3,74	5,53%
PNO.550.1675.3000	bottom connection	2500									4,62	4,32%	4,62	6,01%
PNO.550.1675.3000	bottom connection	3000									4,35	3,64%	4,35	4,86%
PNO.550.1675.3000	bottom connection	3500									2,68	1,97%	2,68	2,53%
PNO.800.2550.2500	fix rod	2500	12	13,33%	12	20,00%	16,96	18,84%	16,96	28,27%	4,96	4,86%	4,96	6,89%
PNO.800.2550.2500	fix rod	2000					9,48	10,56%	9,48	15,85%				
PNO.1100.2400.2500	bottom connection	1500	4,6	5,26%	4,6	8,01%	8,4	9,61%	8,4	14,63%	3,8	4,13%	3,8	6,13%
PNO.1100.2400.2500	bottom connection	2000	4,9	5,32%	4,9	7,89%	10,32	11,21%	10,32	16,62%	5,42	5,59%	5,42	8,09%
PNO.1100.2400.2500	bottom connection	2500	14,5	16,02%	14,5	23,97%	21,36	23,60%	21,36	35,31%	6,86	6,53%	6,86	9,15%
PNO.1100.2400.2500	bottom connection	3150									8,28	6,96%	8,28	9,30%

Table 7.4 - Comparison Between Results Obtained with the Three Methods, Non-Removable Conductor Cases

7.3.2 Analysis of the Results Comparison

In the previous tables is possible observing immediately a difference about the typology analyzed respect the removable conductor cases: the number of reported bushing is minor, but on every bushing has been make more tests and simulations with different current values. There are also more thermal simulation cases, because once the simulation settings are done, it is a rapid process changing the input current value and launch the simulation again.

There are more cases of study where a feeding current higher than the rated one is given at the bushing, for this reason some hottest temperatures reach such a high values.

In order to have a clearer confrontation, two bar graphs have been made with the most interesting data, just like the ones in the paragraph 7.2.2: in Figure 7.3 is realized a confrontation between the maximum temperature obtained whit the three methods, in Figure 7.4 is realized a confrontation between the differences of these maximum temperature, calculated as relative values.

Even in this analysis it possible found the problems of unreliability for the tests made by following the Standard IEC indications. In particular, are reported two significant cases: for the PNO.800.2550.2500 with a test current of 2000 A the resulting hottest spot by test should be equal to 49.9 °C, and for the PNO.1100.2400.2500 with a test current of 2500 A the resulting hottest spot by test should be equal to 12.3 °C. For both these cases is taken as maximum temperature the ones measured by the thermocouples, which correspond at the bottom connection ones, then respectively 89.8 °C and 90.5 °C .

For this reason the comparison between the results obtained by the calculation program and by the tests is not considerable a very reliable indication.

Observing the graphs, respect at the bushings with non-removable conductor case, this time the results obtained with the equivalent thermal circuit method are often greater of the others, reducing the risk to underestimate the maximum temperature .

Confronting the maximum temperatures calculated with the circuital method and the ones calculated through thermal simulations, it must noticed that the differences between the values are limited in a range from 1.97 % to 6.96 %, with an average value of 4.65 %. Speaking in degrees Celsius, this mean a difference that ranges from 2.68 °C to 8.28 °C, with the average gap equal to 4.96 °C.

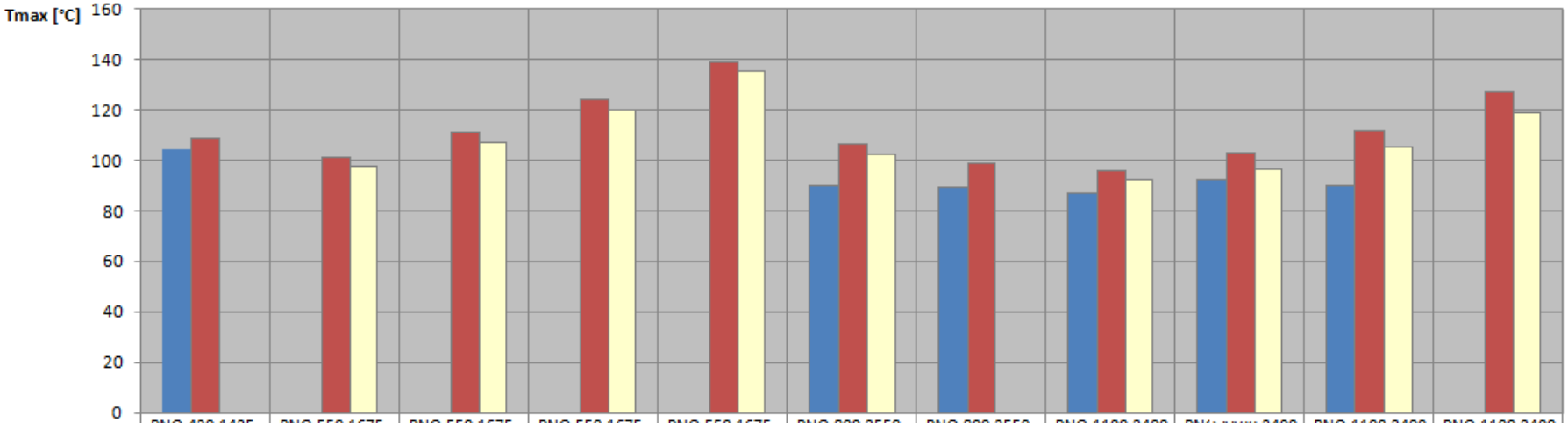

	PNO.420.1425.2000	PNO.550.1675.3000	PNO.550.1675.3000	PNO.550.1675.3000	PNO.550.1675.3000	PNO.800.2550.2500	PNO.800.2550.2500	PNO.1100.2400.2500	PNO.1100.2400.2500	PNO.1100.2400.2500	PNO.1100.2400.2500
Test Current	2000 A	2000 A	2500 A	3000 A	3500 A	2500 A	2000 A	1500 A	2000 A	2500 A	3150 A
TEST	104,3					90	89,8	87,4	92,1	90,5	
CALCULATION	108,97	101,41	111,52	123,88	138,48	106,96	99,28	95,8	102,42	111,86	127,28
SIMULATION		97,67	106,9	119,53	135,8	102		92	97	105	119

Figure 7.3 - Comparison Between the Maximum Temperatures Values, Non-Removable Conductor Cases

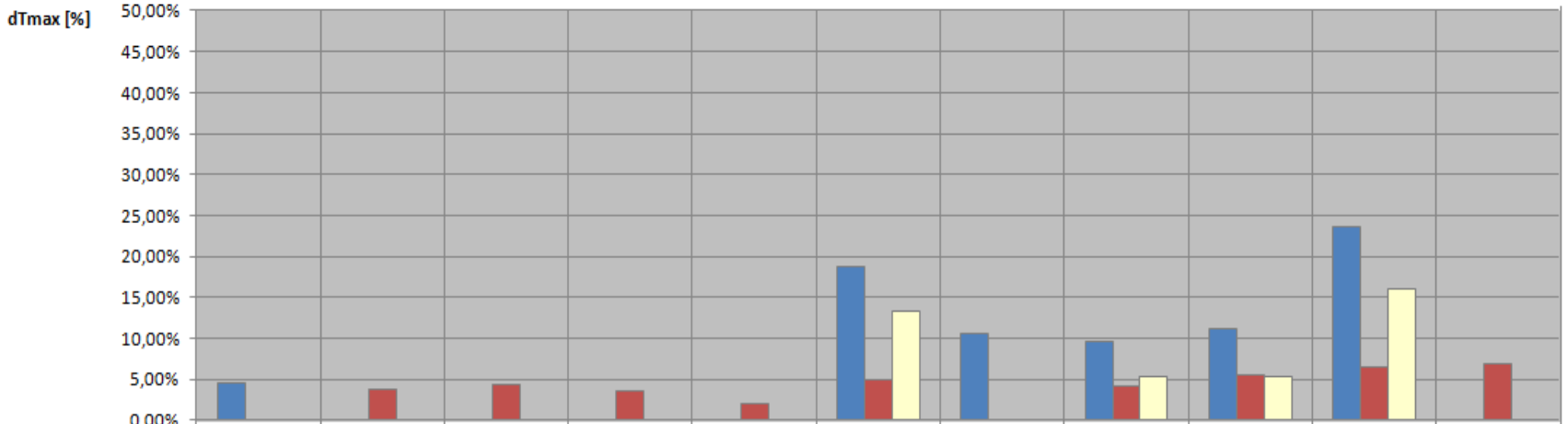

	PNO.420.142 5.2000	PNO.550.167 5.3000	PNO.550.167 5.3000	PNO.550.167 5.3000	PNO.550.167 5.3000	PNO.800.255 0.2500	PNO.800.255 0.2500	PNO.1100.24 00.2500	PNO.1100.24 00.2500	PNO.1100.24 00.2500	PNO.1100.24 00.2500
Test Current	2000 A	2000 A	2500 A	3000 A	3500 A	2500 A	2000 A	1500 A	2000 A	2500 A	3150 A
TEST vs. CALCULATION	4,48%					18,84%	10,56%	9,61%	11,21%	23,60%	
SIMULATION vs. CALCULATION		3,83%	4,32%	3,64%	1,97%	4,86%		4,13%	5,59%	6,53%	6,96%
TEST vs. SIMULATION						13,33%		5,26%	5,32%	16,02%	

Figure 7.4 - Discrepancies Between the Maximum Temperatures Values, Non-Removable Conductor Cases

The results in percentage and in absolute values are pretty similar at the ones found during the analysis in the paragraph 7.2.2, with the difference that this time they are positive gap.

This mean that with the developed method is possible obtaining maximum temperature that are similar to the ones obtained with the realization of a surely more laborious finite element analysis.

7.4 General Observations and Future Possible Improvements

7.4.1 Accuracy of the Circuital Method

Observing the results and the discrepancies of the analyzed data, it can be affirmed that the alternative circuital method developed in this thesis permits to have an estimation of the maximum temperature reached in a PNO bushing with a good accuracy grade.

For the bushing types with removable conductor the highest and average discrepancies are respectively -7.52% and -3.80% respect the tests results, while they are -5.53% and -2.91% respect the results of the simulations.

For the bushing with non-removable conductor the highest and average discrepancies are respectively +6.96% and +4.65% respect the simulations.

The modulus of the gaps are very similar, but for the bushing with removable conductor the difference is almost always negative while for the bushing with non-removable conductor is almost always positive.

The result of the analytical method can not reach the precision and reliability of a thermo-magnetic simulation realized by an expert (even if in there are cases where the difference is practically negligible). However, the circuital calculation can be useful to have a rapid evaluation of the highest temperature in an acceptable range, since to launch it are necessary only few and easily definable parameters and a limited employment of time.

7.4.2 Influence of the Boundary Conditions

During the analysis of the results in paragraph 7.2.2, one of the facts seen was about the losses of accuracy of the calculation method when the voltages of the bushing treated are lows.

This happens because these bushings have reduced dimension, therefore all the boundaries conditions imposed on the external bushing surfaces are so much closer to the central conductor, giving an increase influence on the calculation. In an ideal case, in fact, the boundary conditions would be imposed at some point placed to the infinity, giving no influence on the results.

The boundaries imposed on the model are an approximation of the reality, they are reasonable values but they are not always true (for example, the ambient air around the bushing air side is not all equal to 30 °C, in the zone near to the flange increases it until 60 °C due to the heat coming from the tank oil).

With bushings of small dimensions, is less probable that the hottest spot is placed in a zone around the flange or at the bottom connection (and in fact for the PNO.145.650.1250 is placed near the head). Therefore, some of the model simplifications as, for example, having neglected the head at all and the terminal components also, resulting less justified since even they are much closer to core of the problem, giving an higher influence on final results.

It can be affirmed that the thermal equivalent circuit method become more inaccurate if applied on bushings with rated voltages low than 200 kV, since they have small dimensions.

7.4.3 Influence of the Conductor Reference Temperature

In the calculating program a lot of parameters are depending from the temperature of the conductor as, for example, the conductor resistivity used to define many thermal resistances and the losses values. However, the conductor temperature is even the incognita of the problem.

In order to resolve this issue, a reference temperature is assigned at the conductor, and it is chosen equal to 60 °C. This value represents an expected average temperature value along the entire conductor.

It is reasonable wonder how this arbitrary temperature influences the final result of the calculation program, and if would not be better realize an interactive cycle that applies again the resolving program once an average temperature along the conductor is defined with the first iteration, replacing the reference value with the calculated one.

To can have an answer at this question, on the bushing PNO.550.1800.1250 and PNO.550.1675.3000 have been realized several calculations, applying each time a different reference conductor temperatures, with every step equal to 20 °C. The two graphs reported in Figure 7.5 and in Figure 7.6 show the response at these variations given by the conductor resistivity, by the total losses and by the maximum temperatures calculated (which are the final target of the method).

In this way is possible well appreciate the weight of the reference temperature variations on these parameters.

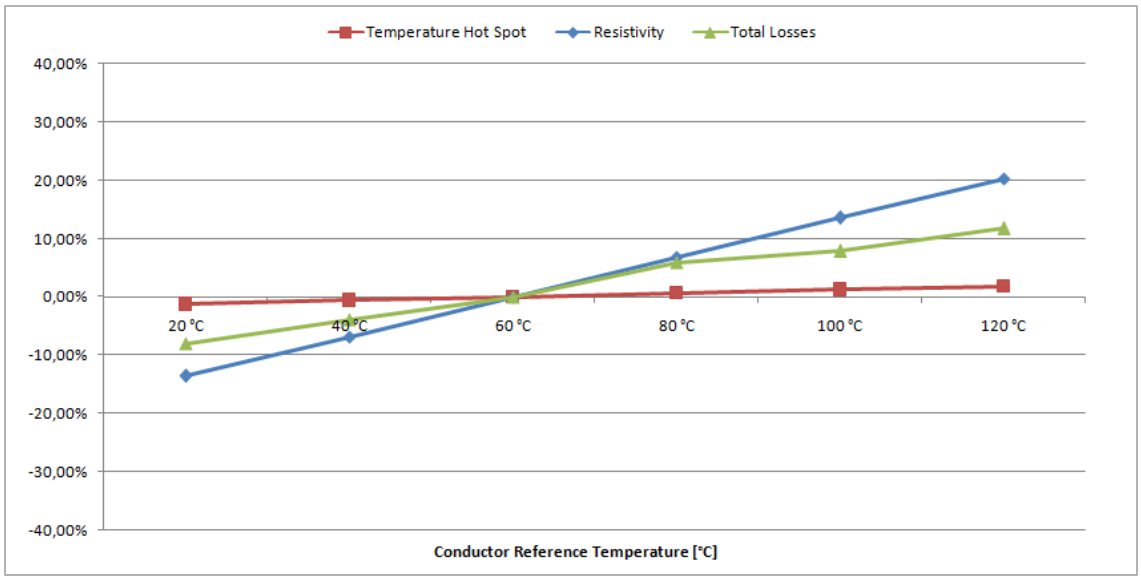

Figure 7.5 - Influence of the Conductor Reference Temperature for PNO.550.1675.3000

How it is possible observe in both the two graphs, changing the reference conductor temperature has a certain effect on the both resistivity and losses values. However, the influence on the maximum temperatures calculated by the program is very limited: even in front of a taken reference conductor temperature equal to 120 °C (which represent a +100% increase), the respective variation of the calculated temperature is about +1.82% for PNO.550.1800.1250 and +3.61% for PNO.550.1675.3000.

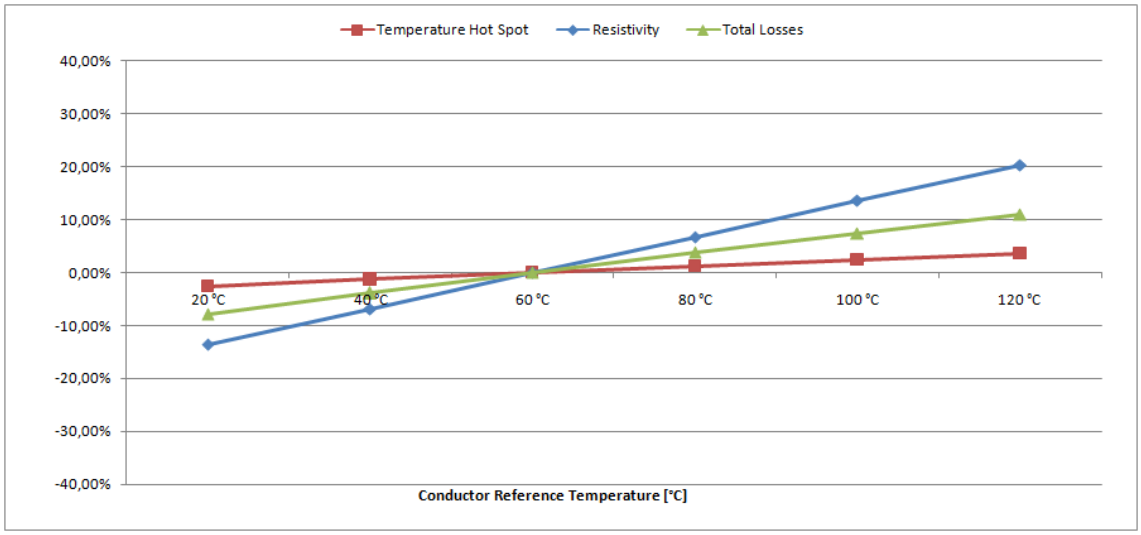

Figure 7.6 - Influence of the Conductor Reference Temperature for PNO.550.1675.3000

Every steps of 20 °C gives a maximum temperature variation pair about at 0.6% in the first case and 1.25% in the second case.

In conclusion, this parameter has a limited effect on the final hottest spot calculated, especially considering that the real average temperature of a bushing conductor is with high probability in a range of about 60 °C ÷ 80 °C, giving a possible variation on the temperature hottest spot around at 1%.

7.4.4 Position on Where is Individuated the Hot Spot

It has been seen how the equivalent thermal circuit method can calculate temperature values similar to the ones obtained by test and simulation. However, there are often discrepancies with the others two methods about the effective position where these temperatures are individuated.

Using the calculation program, the maximum temperature is always found at the node 3 of the equivalent circuit, which represent the conductor in the bushing oil side, but from test and simulation this value it sometimes positioned at the flange height, or even above it.

The low accuracy in to detecting the right hot spot position is probably due at the choice to split the bushing in only three sections. Increasing them (and therefore increasing the number

of radial lines) probably the position individuated through analytic evaluation it will be much closer to the reality.

7.4.5 Possible Future Improvements of the Circuital Method

The equivalent circuital method developed in this thesis has for sure the possibility to can be improved under various aspects.

Increasing the number of the sections into which is divided the bushing model gives geometrical dimensions of the materials (especially the radius) closer to the reality, in this way the thermal resistances calculated and the temperature distribution obtained are more accurate. Obviously, a higher number of section means a higher number of radial lines present in the equivalent circuit, therefore it is necessary heavily modify the resolving calculation program to can find the temperature values.

The ideal solution would be making a program capable to define the parameters and the resolving matrices in function of the number of the lines imposed, without losing its usage simplicity for the user.

Whit these modifications, it can be expected an increase accuracy about both the maximum temperature values calculate and for the bushing position where they are individuated.

Another addition could be the implementation of a cycle that replace the reference conductor temperature with an average calculated one after the first iteration, as explained in the paragraph 7.4.3. This can give a little increase of the accuracy of the maximum temperatures calculated (as already said, about 1%) and the iterative cycle should not make too heavy the calculation program.

It would be good improving the comparison with the results of the others methods making new tests and simulations, to can have a more accurate prediction about the reliability grade of the temperatures calculate.

The equivalent circuital method has been developed in order to be applied to the PNO bushings, but remain the possibility to adapt it for the others bushing types. Obviously, there are necessaries various modifies at all the method passages: on the bushing model definition, on the parameter calculations and on the structure of the resolving program.

For same bushing families the process should not be too complicated while for others families should be necessaries heavy modifications.

For the RIP bushings, for examples, good results are expected making only few differences at the developed circuital method, since the pretty similar both structure and thermal phenomena respect the PNO bushings.

Instead, for bushing insulted in gas (like PHI) are expected a lot of changes and the introduction of some phenomena negligible in the PNO bushing, like the heat thermal radiation and the circulation movements of the inner fluids.

CONCLUSIONS

At the end of this thesis work, the initial objective to define a simplified methodology for the calculation and prediction of the thermal behaviour of the transformer bushing can be considered partially satisfied.

After having spent the early months of the stage duration to can understand what a bushing is, the various difficulties to can make a good thermal simulation, the problems with the temperature rise tests realizations and the uncertainties about this test given by the reference Standard IEC for the bushing itself, the chosen approach to can achieve the initial focus has been the development of an analytic resolving method.

It has been realized a simplified model for the bushing body, from which it is possible obtaining a thermal equivalent circuit thankfully the property of the heat flow to can be modelled with electrical components.

A calculation program it has been made in order to can define the unknowns parameters (as the thermal resistance, the losses, etc.) of the equivalent circuit and then resolve it. This program has been developed to have only few necessaries inputs given by the user, with all of them easily definable (they are almost all geometrical values).

At the end of the resolving pattern, the program gives directly as results the temperature values calculated on the bushing body, whence is possible define the maximum temperature value and the temperature rise reached.

It has been made a comparison between the results of the circuital method with the ones obtained by tests and by thermomagnetic simulations in order to can evaluate its accuracy. After this analysis, it can be affirmed that the alternative method developed during this thesis permits to calculate the temperature hottest spot in a bushing with an acceptable grade of accuracy, since the average discrepancy with the others methods is less than 5% and the maximum one is always less than 10%.

This method has not been thought to substitute the thermomagnetic simulations during the design phases, but it represents a useful tool to can obtain a quickly first evaluation of the final temperature hottest spot.

The advantages of the equivalent thermal circuit method are mainly two: the facility of the usage, since are necessaries only few easily definable parameters to can achieve the final values, and the great saving of time respect the several hours of work necessaries to can define the thermal behaviour with a good make thermal simulation.

The thesis objective must be considered only partially satisfied because the circuital method developed has not been designed to be applied equally at all the bushings types, but it is limited to the only PNO family.

However, the analytics method maintains the possibility to be improved in future, both for what concerns the level of accuracy of the final temperatures calculated and even for the adaptability at the various families of bushing. The having to make modifications expected to reach good results with some types (as like RIP bushings) are few and light, while for some others families (like PHI bushings) are many and heavy.

BIBLIOGRAPHY

[1] "*Power transformers volume 2 - Expertise*", written by Various Authors, published by Ligaris L'Agence, August 2008, pages: 114 ÷ 124.

[2] "*Isolatori passanti per trasformatori*", written by Filippo Coppadoro, Emilio Warnots, published by CESI, April 1989.

[3] "*High voltage engineering and testing*"- Second Edition, written by Hugh M. Ryan, published by Institution Electrical Engineers, December 2001, pages: 405 ÷ 433.

[4] International Standard IEC 60137- Edition 06, "*Insulated bushings for alternating voltages above 1000 V*", written by Various Authors, published by CEI, June 2008.

[5] International Standard IEC 62199 - Edition 01, "*Bushings for d.c. application*", written by Various Authors, published by CEI, March 2005.

[6] IEEE Standard C57.19.100-1995, "*IEEE guide for application of power apparatus bushing*", written by Various Authors , August 1995, pages: 4 ÷ 10.

[7] Technical paper "*Mathematical Modelling - A Basis for Bushing Loading Guides"*, written by W.J. McNutt, J.K.Easley, published on "IEEE Transactions on Power Apparatus and System", November 1978, pages: 2393 ÷ 2404.

[8] Technical paper "*An improved method for estimating temperature rise of a bushing loaded above nameplate rating*", written by Daxiong Zeng, published on "IEEE Transactions on Power Delivery", July 1999, pages: 986 ÷ 995.

[9] Technical paper "*Temperature rise characteristics on OIP bushing with circular fluid convection*", written by H. Katsukawa, H. Sakai and Y. Fukami, published on "NGK Review - Overseas Edition" n°32, December 2009, pages: 14 ÷ 19.

[10] Technical paper "*99/1964 - Sviluppi nella progettazione e nella fabbricazione di isolatori passanti per alte ed altissime tensioni*", written by G. Villa, extract from "Rendiconti della LXV riunione annuale dell'AEI", 1964.

[11] Encyclopedia online " *www.wikipedia.org*"

ACKNOWLEDGES

The realization of this graduation thesis would not be possible without the contribution and the assistance of various people.

In the first place, I would thank the division Passoni&Villa of the Alstom Grid S.p.A. for given me the opportunity to can develop the thesis in its working ambient.

In particular, special thanks must be done to ing. Giovanni Testin for having made possible my introduction in the R&D department, and also for the support given in these months with its knowledge and precious advises.

I'm grateful also to professor Antonino Claudio Di Gerlando, always available for a confrontation and whose suggestions have been helpful to overtake several problems during the thesis development.

An heartfelt thank to ing. Luca Perego, his preparation and his willingness to transmit his experience in the various working fields have been fundamentals, without its contribution would not be possible realizing this thesis.

It cannot miss a mention to ing. Paolo Cardano, an example for the professional point of view, and to ing. Stefano Pellegrino, for having shared its knowledge of the testing chamber and measurement methods.

A general thank to all the rest of R&D group, for how they have warmly welcomed in their ambient and for having taught me various aspects of the world of work.

This thesis represents the conclusion of my university experience, so it is mandatory for me express here my gratitude to my parents, whose have always support me in these years but also letting the total freedom and responsibility of my choices.

Lastly, I want to make a general thank also to all my classmates and friends that have accompanied and assisted me in these years, giving the motivations to get through the difficult moments.